APPLICATIONS OF ACTIVE COMPENSATORS TO MAGNET POWER SUPPLIES

Ying Wang

A Thesis
in
the Department
of
Electrical & Computer Engineering

Presented in Partial Fulfillment of the Requirements
for the Degree of Master of Applied Science at
Concordia University
Montreal, Quebec, Canada

February 1995

ISBN 0-612-01352-9

ABSTRACT

APPLICATIONS OF ACTIVE COMPENSATORS TO MAGNET POWER SUPPLIES

Ying Wang

This thesis presents the analysis and design of high-current magnet power supply systems. These power supplies are intended for magnet load applications where low-ripple and fast response load regulation are required. They can be used in application areas where the conventional magnet power supplies are inadequate.

The hybrid structures proposed in this work are based on the combination of a conventional phase-controlled rectifier structure and a series or a shunt connected switch-mode PWM compensator. The operating principles of the hybrid power supplies are presented. By using this hybrid structure, phase-controlled rectifiers can be effectively designed to handle the large power required by the load. The switch-mode PWM compensators are required to provide only a small portion of output power for harmonic cancellation and tracking error compensation.

The phase-controlled rectifier utilizes a feedforward control technique to provide the desired power sharing during steady state and transient operating conditions. Design considerations of the power circuits and control schemes are developed and examples are presented. Computer simulation and experiments on prototypes are conducted to verify the theoretical analysis. Results confirm the validity of the proposed concepts.

ACKNOWLEGEMENTS

I would like to express my sincere appreciation to my supervisors Dr. Hua Jin and Dr. Geza Joos for their invaluable guidance and expert advice throughout the preparation of this thesis. Deep gratitude is given to my former supervisor, late Dr. Phoivos D. Ziogas, for his encouragement.

To all the staff and students in the Power Electronics Group, I wish to thank them for their friendship, help, cooperation, many useful discussions and suggestions. I will never forget the wonderful memory of working in the Power Electronics Lab. Special thanks are due to Mr. Donato Vincenti for his laboratory assistance, and to Mr. José Espinoza for his valuable assistance in word processing.

I would also like to thank Ms. Bonnie Weppler for her helpful suggestions in reading and correcting of this manuscript.

Special appreciation goes to my husband, Zhisong Chen, for his love and wholehearted support, and to my parents for their patience and encouragement.

Financial support from the Government of Quebec through the FCAR grants, and from the Government of Canada through the NSERC grants is gratefully acknowledged.

TABLE OF CONTENTS

List of Figures x

List of Tables xiv

List of Symbols xv

CHAPTER 1. Introduction 1

1.1 Background 1

1.2 Review of Magnet Power Supply Configurations 3

1.2.1 Linear Power Supplies 3

1.2.2 Rectifier Power Supplies 5

1.2.3 Switching Power Supplies 6

1.2.4 Hybrid Structures 8

1.2.4.1 Series Topologies 9

1.2.4.2 Shunt Topologies 12

1.3 Proposed Approach 15

1.3.1 Proposed Power Circuit 15

1.3.2 Hybrid Structure with Feedforward Control 15

1.4 Thesis Objectives and Contributions 17

1.5 Thesis Outline 17

CHAPTER 2. Phase-Controlled Rectifier Modelling and Feedforward Control Technique 19

2.1 Introduction 19

2.2 Steady State Characteristics 20

2.3 Dynamic Characteristics 24

2.3.1 Feedforward Control Technique 27

2.3.2 Feedforward Control Principles 27

2.3.3 Implementation and Experimental Results 28

2.4 Summary 30

CHAPTER 3. Series Topology - Principle 32

3.1 Introduction 32

3.2 Principle of Harmonic Cancellation 33

3.3 System Configuration 34

3.3.1 Rectifier Power Circuit 35

3.3.2 PWM Converter 36

3.4 Control Scheme 39

3.4.1 Rectifier Control 40

3.4.2 PWM Converter Control 41

3.4.2.1 Voltage Loop 42

3.4.2.2 Current Feedback Loop 44

3.5 Summary 45

CHAPTER 4. Series Topology - Design and Implementation 46

4.1 Introduction 46

4.2 Design Procedures 47

4.3 Design Example 48

4.3.1 Power Circuit Design 50

4.3.1.1 Rectifier 50

4.3.1.2 PWM Converter 52

4.3.2 Power Ratings 54

4.3.2.1 Rectifier Power Rating 54

4.3.2.2 PWM Converter Power Rating 55

4.3.3 Control Design 56

4.3.3.1 Rectifier Control 56

4.3.3.2 PWM Converter Control 56

4.4 Results 58

4.5 Summary 58

CHAPTER 5. Shunt Topology - Principle 60

5.1 Introduction 60

5.2 Principle of Harmonic Cancellation. 61

5.3 System Configuration 63

5.3.1 Rectifier Power Circuit 64

5.3.2 PWM Converter Power Circuit 64

5.4 Control Scheme 65

5.4.1 Rectifier Control 67

5.4.1.1 Feedforward/Feedback Control 68

5.4.1.2 α Correction Loop 69

5.4.2 PWM Converter Control 69

5.5 Summary 70

CHAPTER 6. Shunt Topology - Design and Implementation 72

6.1 Introduction 72

6.2 Design Procedures 73

6.3 Design Example. 74

6.3.1 Power Circuits Design 76

6.3.1.1 Smoothing Reactor 76

6.3.1.2 Rectifier 78

6.3.1.3 PWM Converter 79

6.3.2 Power Ratings of the Rectifier and the Compensator 80

6.3.2.1 Rectifier Power Rating 80

6.3.2.2 PWM Converter Power Rating 81

6.3.3 Relationship of the Passive Filter and the Compensator 82

6.3.4 Control Circuit Design 84

6.3.4.1 Rectifier Control 84

6.3.4.1.1 Feedforward/Feedback Control 84

6.3.4.1.2 α Correction Control 89

6.3.4.2 PWM Converter Control 90

6.4 Results 91

6.5 Summary 96

CHAPTER 7. Conclusion 97

7.1 Summary 97

7.2 Contributions and Conclusions 98

7.3 Future Work 103

REFERENCES 104

LIST OF FIGURES

Figure 1.1: Current profile of the magnet power supplies. 2

Figure 1.2: (a) Block diagram of a series-pass regulated linear power supply; (b) Basic circuit of a linear regulator. 4

Figure 1.3: Configuration of the phase-controlled rectifier power supply. 6

Figure 1.4: Block diagram of the switchmode dc power supply. 7

Figure 1.5: Equivalent circuits of series topologies. (a) using voltage-type converters as active filters; (b) using current-type converters as active filters. 10

Figure 1.6: Transformer-decoupled magnet power supplies using a series topology. 11

Figure 1.7: Equivalent circuit for shunt topologies. (a) using voltage-type converters as active filters; (b) using current-type converters as active filters. 13

Figure 1.8: Block diagram of a shunt active filter using transformer-decoupling. 14

Figure 1.9: A proposed magnet power supply using series topologies. 16

Figure 1.10: A proposed magnet power supply using shunt topologies. 16

Figure 2.1: Power circuit of the phase-controlled rectifier of Figure 1.9. 20

Figure 2.2: Rectifier output voltage at firing angle α=60°. (a) Waveform; (b) Harmonic spectrum. 21

Figure 2.3: Passive filter output voltage at firing angle α=60°, ξ = 0.7 and f_c = 160 Hz. (a) Voltage waveform; (b) Harmonic spectrum. 25

Figure 2.4: Bode plot of the rectifier voltage transfer function. 26

Figure 2.5: The load current and voltage profiles. 28

Figure 2.6: Phase-controlled rectifier power supplies using proposed feedforward control technique. 29

Figure 2.7: Experimental results of Figure 2.6. a) Load voltage and voltage reference; b) Load current and current reference; c) Expanded load current at i_o = 2A; d) Harmonic spectrum of the waveform of (c). 31

Figure 3.1: Series topology. (a) Power circuit; (b) Equivalent circuit. 33

Figure 3.2: Power circuit configuration of the proposed magnet power supply system using series topology. 35

Figure 3.3: (a) Carrier waveform with two opposite modulation waveforms; (b) Gating signal for switch Q_1; (c) Gating signal for switch Q_2; (d) Output voltage waveform $v_j(t)$; (e)Harmonic spectrum of $v_j(t)$. 38

Figure 3.4: Proposed control scheme. 39

Figure 3.5: Block diagram of the voltage control to PWM converter. 43

Figure 3.6: (a) and (b) Filter output voltage waveform and harmonic spectrum;

(c) and (d) Error signal waveform and harmonic spectrum. 43

Figure 3.7: Block diagram of the PWM converter current feedback loop. 45

Figure 4.1: Proposed magnet power supply with hybrid structure using series topology. 49

Figure 4.2: Bode plot of the PWM converter current feedback loop. 57

Figure 4.3: Experimental results. (a) Load voltage and voltage reference; (b) Load current and current reference; (c) Expanded load current at 2A; (d) Harmonic spectrum of the load current at 2A. 59

Figure 5.1: Shunt topology. (a) Power circuit; (b) Equivalent circuit. 62

Figure 5.2: Proposed power circuit configuration. 63

Figure 5.3: Block diagram of the proposed control scheme. 66

Figure 5.4: Small-signal block diagram of the rectifier control scheme.. 67

Figure 5.5: Small-signal block of the inverter current feedback loop. 70

Figure 6.1: Proposed magnet power supply using shunt topology. 75

Figure 6.2: Equivalent power circuit for harmonic calculation. 77

Figure 6.3: Harmonic current of the active compensator vs. impedance of the smoothing inductor ("*" is the selected operating point). 77

Figure 6.4: Peak voltage rating of the PWM converter. 83

Figure 6.5: Simplified small-signal block diagram of Figure 5.4. 85

Figure 6.6: Simplified block diagram of the phase-controlled rectifier of Figure 6.5. 85

Figure 6.7: Bode plot of the rectifier current feedback loop transfer function. . 88

Figure 6.8: Bode plot of the converter current loop transfer function.. 90

Figure 6.9: Experimental waveforms of the system with only the rectifier. (a) Load current and current reference; (b) Expanded ac portion of the load current at 2A; (c) Harmonic spectrum of the load current at $\alpha = 80^0$ (i_o=2A).. 93

Figure 6.10: Experimental waveforms of the proposed system. (a) Load current and current reference; (b) Expanded ac portion of load current at 2A; (c) Harmonic spectrum of load current at $\alpha = 80^o$. 94

Figure 6.11: Experimental inverter current waveforms. (a) Current reference; (b) Without α correction loop (Figure 5.3, loop #3); (c) Including α correction loop.. 95

LIST OF TABLES

Table 7.1 : Steady state performance of using the series topology

($I_{base} = i_o(t) = 2A$). 99

Table 7.2 : Steady state performance of using the shunt topology

($I_{base} = i_o(t) = 2A$). 100

Table 7.3 : Series topology (Base: Load rated quantity). 101

Table 7.4 : Shunt topology (Base: Load rated quantity) 102

LIST OF PRINCIPAL SYMBOLS

1. Voltage:

v_{ce}	Transistor collector-emitter voltage
$v_r(t)$	Rectifier output voltage
$v_{rf}(t)$	Passive filter output voltage
v_{ref}	Voltage reference
$v_f(t)$	Feedback voltage
$v_o(:)$	Load voltage
$v_j(t)$	Injected (PWM converter output) voltage
$v_{rn}(t)$	Rectifier output harmonic voltage
V_{rn}	Rectifier harmonic voltage amplitude
V_{rd}	Rectifier output DC voltage
V_{ll}	Rectifier input line-to-line rms voltage
$V_{ll,min}$	Minimum rectifier input line-to-line rms voltage
$V_{s,ll}$	Line-to-line rms source voltage
$V_{r,6peak}$	Maximum amplitude of 6^{th} harmonic
V_{fd}	Passive filter output DC voltage
V_{rfn}	Passive filter output harmonic amplitude

$v_{err}(t)$	Error voltage
$V_{o,max}$	Maximum load voltage
$V_{r,rated}$	Rectifier rated voltage
$V_{j,rated}$	PWM converter rated voltage
V_{dc}	PWM converter DC bus voltage
$V_{dc,min}$	Minimum PWM converter DC bus voltage
$V_{ll,diode}$	Diode rectifier line-to-line rms voltage
V_{ro}	Resistance voltage
Δv_{lo}	Inductance voltage - during ramp
Δv_l	Load voltage - during ramp
ΔV_{rd}	Additional rectifier output voltage
ΔI_{rd}	Additional rectifier output current
V_{base}	Base voltage

2. Current:

$i_o(t)$	Load current
i_{ref}	Load current reference
$i_r(t)$	Rectifier output current
$i_{rn}(t)$	Rectifier harmonic current
I_{rd}	Rectifier output DC current
$i_{err}(t)$	Current error

$i_{sn}(t)$	Smoothing reactor's current
$i_j(t)$	Injected (PWM converter output) current
$I_{o,max}$	Maximum load current
$I_{r,rated}$	Rectifier rated current
$I_{j,rated}$	PWM converter rated current
I_{base}	Base current

3. Power Rating:

$S_{r,rated}$	Rectifier rated apparent power
$S_{j,rated}$	PWM converter rated apparent power
$P_{o,rated}$	Load rated real power
S_{base}	Base apparent power

4. Frequency:

ω_c, f_c	Resonant (cut-off) frequency
ω_s, f_s	Source frequency
ω_{sw}, f_{sw}	Switching frequency
f_r	Ripple frequency

5. Transformer:

T_1, T_2	Transformers
a_{T1}, a_{T2}	Transformer turns ratio

6. Load Parameters:

R_o	Load resistance
L_o	Load inductance
τ_o	Magnet load time constant

7. Passive Filter Parameters:

L_s	Smoothing reactor
L	Filter inductance
C	Filter capacitance
R_f	Filter damping resistance
C_f	Filter damping capacitance
X_s	Impedance of smoothing reactor
ξ	Damping ratio

8. Control Parameters:

$G_r(s)$	Rectifier voltage transfer function
$G_{co}(s)$	PWM converter voltage transfer function
K_r	Rectifier gain
K_{re}	Proportional controller of rectifier control loop
K_{co}	Proportional controller of PWM converter control loop
$G_{rf}(s)$	Rectifier feedforward controller

K_{rf}	Gain of $G_{rf}(s)$
T_{rf}	Time constant of $G_{rf}(s)$
$G_{rc}(s)$	Rectifier α correction controller
K_{rc}	Gain of $G_{rc}(s)$
T_{rc}	Time constant of $G_{rc}(s)$
$G_{ri}(s)$	Rectifier current feedback loop controller
K_{ri}	Gain of $G_{ri}(s)$
T_{ri}	Time constant of $G_{ri}(s)$
$G_{pi}(s)$	PWM converter current feedback controller
K_{pi}	Gain of $G_{pi}(s)$
T_{pi}	Time constant of $G_{pi}(s)$
K_j	PWM converter gain
$G_{rl}(s)$	Rectifier loop transfer function
$G_{pl}(s)$	PWM converter loop transfer function

9. Miscellaneous

Q_1, Q_2, Q_3, Q_4	Switches
T_d	Average rectifier dead time delay
T_s	Source time period
α	Rectifier phase delay angle
Z_{base}	Base impedance

Chapter 1

Introduction

1.1 Background

In particle accelerators, there is one (or more) particle beam path, which usually takes the shape of a circle, called the acceleration ring. Numerous magnets are installed at various locations along the ring. A magnet is essentially a set of coils fixed securely in the metal assembly. Electric current flows through the coils to create the magnetic field which steers the particles whirling around the ring. There are several types of magnets. Bending magnets (dipoles) bend the particle beam in a small angle so that the beam is guided along the ring. Quadrupoles focus the beam and prevent the particles from straying off their narrow path. Correction magnets rectify any small imperfections in the bending magnets and quadrupoles and compensate for a small misalignment. There are other special magnets at the interaction region. The excitation currents, such as the bending magnets, require power supplies with larger current ratings [1].

The quality of the magnet field is the key to precise particle beam control. Moreover, in the geometric position and in the mechanical design of the magnets, accurate control of the magnet current is the most important factor of accelerator performance. The

more accurate the magnet current, the more precise the particle beam position. In some applications, focus precision up to 10 "ppm" may be required [1][2][3]. Since the magnet current is provided and controlled by the magnet power supplies, two stringent requirements are placed on magnet power supplies: fast dynamic response and low current ripple [1-8].

A typical profile of the magnet current is shown in Figure 1.1. An operational cycle involves four stages: flat-bottom, ramp-up, flat-top and ramp-down. During the flat-bottom and the flat-top stages, the current has to be very steady and the current ripple has to be within the tolerance. In the ramp-up stage, the current should be able to track the ramp and at the flat-top, reach the steady state quickly. The function of the ramp-down period is to reset the current for next cycle of operation. During the ramp-down interval, the dynamics of the current are not of concern.

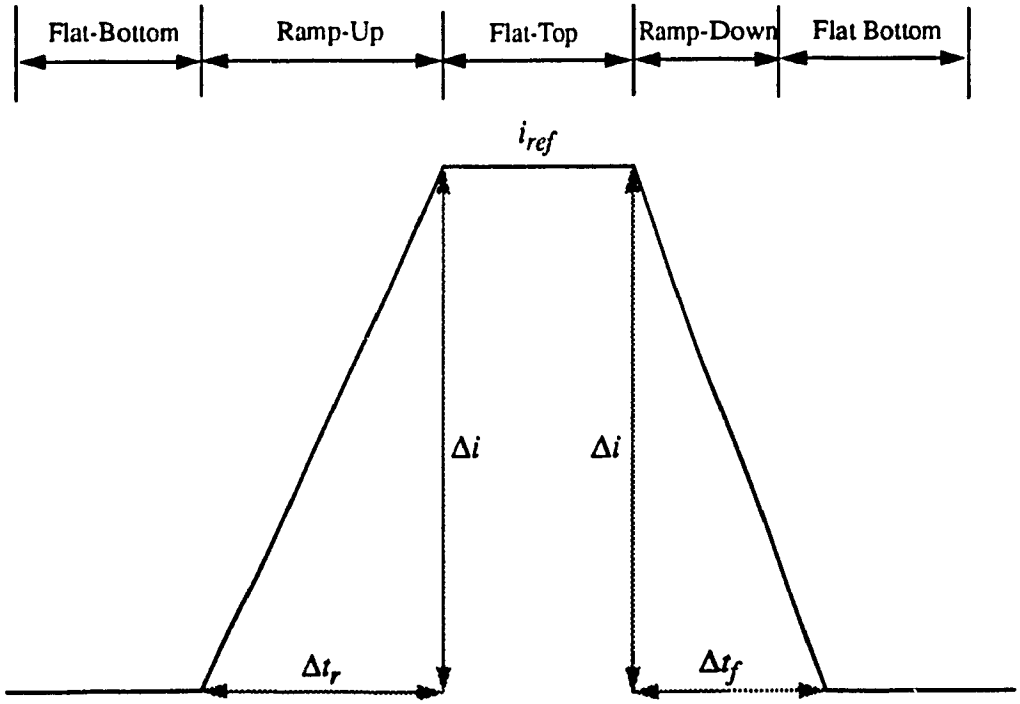

Figure 1.1: Current profile of the magnet power supplies.

In conventional phase-controlled rectifier power supplies for accelerator magnets, the specifications of power supplies are more concerned with stability and ripple under constant current operation[3]. The dynamic requirements, however, are difficult to meet with conventional phase-controlled rectifier power supplies, particularly if $\Delta i/\Delta t$ is large. This is largely due to the inherent large dead times and delays existing in conventional thyristor rectifiers.

To design magnet power supplies which can simultaneously meet both the steady state and dynamic requirements is a challenge because the fast pace of research in high energy physics and the increasing applications of particle accelerators constantly demand better magnet power supplies [1].

1.2 Review of Magnet Power Supply Configurations

Linear power supplies and thyristor power supplies have been traditionally used in magnet load applications. With the advantage of switching devices, switching power supplies have been increasingly used. In this sections, these three types of power supplies are briefly reviewed.

1.2.1 Linear Power Supplies

Figure 1.2 (a) shows the block diagram of a linear power supply. In this configuration, a 60-Hz transformer is used for isolation or voltage adjustment. The secondary voltage is rectified and filtered, and the resulting dc is fed into a series-pass active element. The transistor operates in the active region (linear region) and works as a "variable resistor" to control the output voltage. The collector-emitter voltage drop v_{ce} of the transistor

shown in Figure 1.2 (b) is controlled in such a way that the ripple content in the output voltage is eliminated. Thus, the voltage waveform across the magnet load is smooth and the harmonic current in the magnet load is very low.

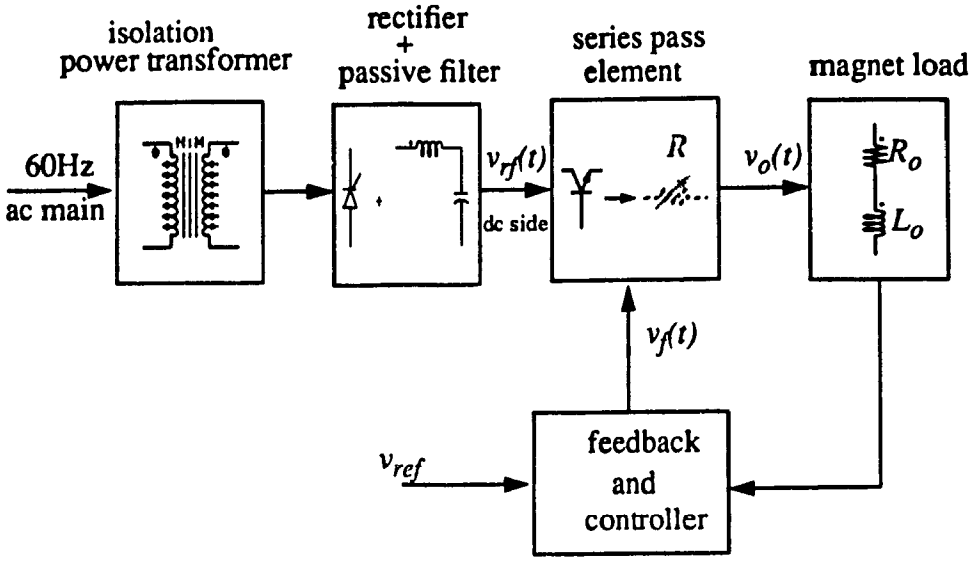

(a)

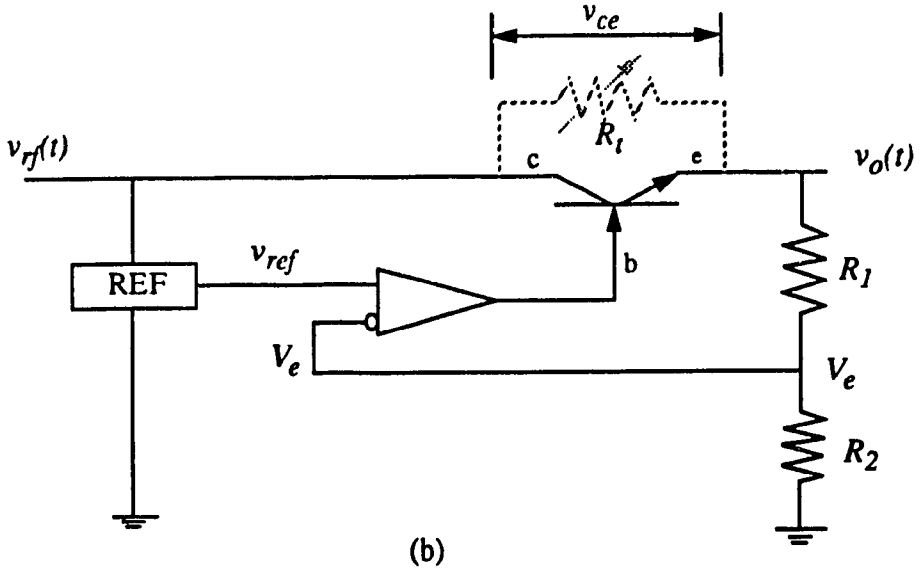

(b)

Figure 1.2: (a) Block diagram of a series-pass regulated linear power supply; (b) Basic circuit of a linear regulator.

Linear regulators are particularly suited for compensating low frequency harmonics. Therefore, the passive filter can be designed with a high cut-off frequency. Consequently, fast dynamic response of the entire magnet power supply system can be obtained.

Although linear power supplies in general have a tight regulation together with a very low output noise and ripple, the disadvantage is the low efficiency. As the transistor bank constantly carries the full magnet current, and at the same time a positive collector-emitter voltage drop v_{ce} must simultaneously be maintained, a large amount of power is dissipated as heat, resulting in substantial power losses and a very low efficiency (40% ~ 50%) [9]. Moreover, it is difficult to protect the linear regulator when large current variations exist. As a result, this type of power supply is not easily applicable in high current applications such as bending magnet power supplies.

1.2.2 Rectifier Power Supplies

Currently, most magnet power supplies use phase-controlled rectifiers [2-4] [7][8][10-13]. This is due to several advantages, such as high power capacity, simple converter structure, simple control scheme, and low cost switching devices (thyristors). Figure 1.3 shows the system configuration. It consists of a phase-controlled rectifier, a passive filter and a magnet load represented by a resistor and an inductor.

However, this configuration gives high harmonic ripples in the rectifier output. In addition, it may contain non-characteristic harmonics which are generated by the imperfection of practical systems [1][3][11]. These non-characteristic harmonics, i.e. 120-Hz, are not easy to filter out by a passive filter without reducing the system dynamic response. The larger the harmonic attenuation by the passive filter, the lower the cut-off frequency, and hence the slower the dynamic response. Moreover, only limited improvement of the

system dynamic response can be achieved since there is a delay in the rectifier. Therefore, by using the conventional magnet rectifier power supply, it is difficult to meet the ever strict requirements of fast dynamic response and low harmonic content simultaneously.

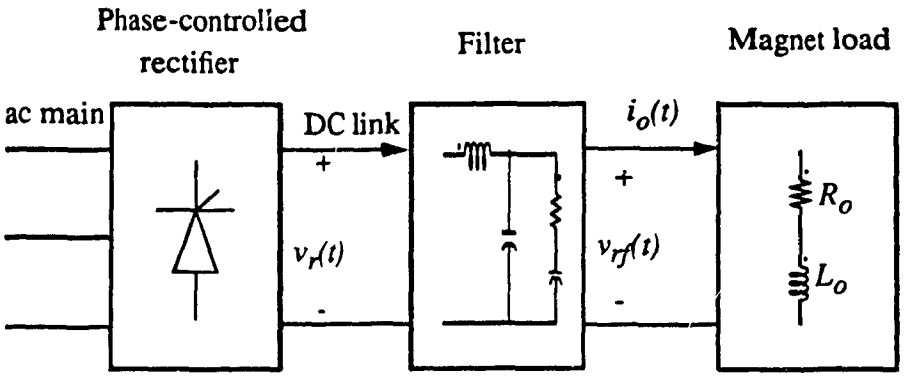

Figure 1.3: Configuration of the phase-controlled rectifier power supply.

1.2.3 Switching Power Supplies

Since the end of the 1970's, switchmode power supplies operating at high switching frequencies have been increasingly used in magnet load applications [3-5][10][14-16]. They offer substantial advantages such as very low harmonic contents and fast system response in the accelerator environment. The general system configuration is shown in Figure 1.4. In this configuration, the solid-state devices (IGBT, MOSFETS, etc.) operate as switches, either completely off or completely on. By avoiding operation in the active region, significant reduction of the power losses is achieved. This results in a high overall power supply efficiency of about 70% ~ 90% [9]. Moreover, a transistor operating in on/

off mode has a much larger power handing capability compared to linear power supplies. Another advantage of using the switchmode power supply is that the power transformer size can be very small due to the very high operating frequency. However, because of the limited current switching capacities of self-commutated switches available today, switch-mode magnet power supplies have been, so far, limited largely to low and medium power ranges.

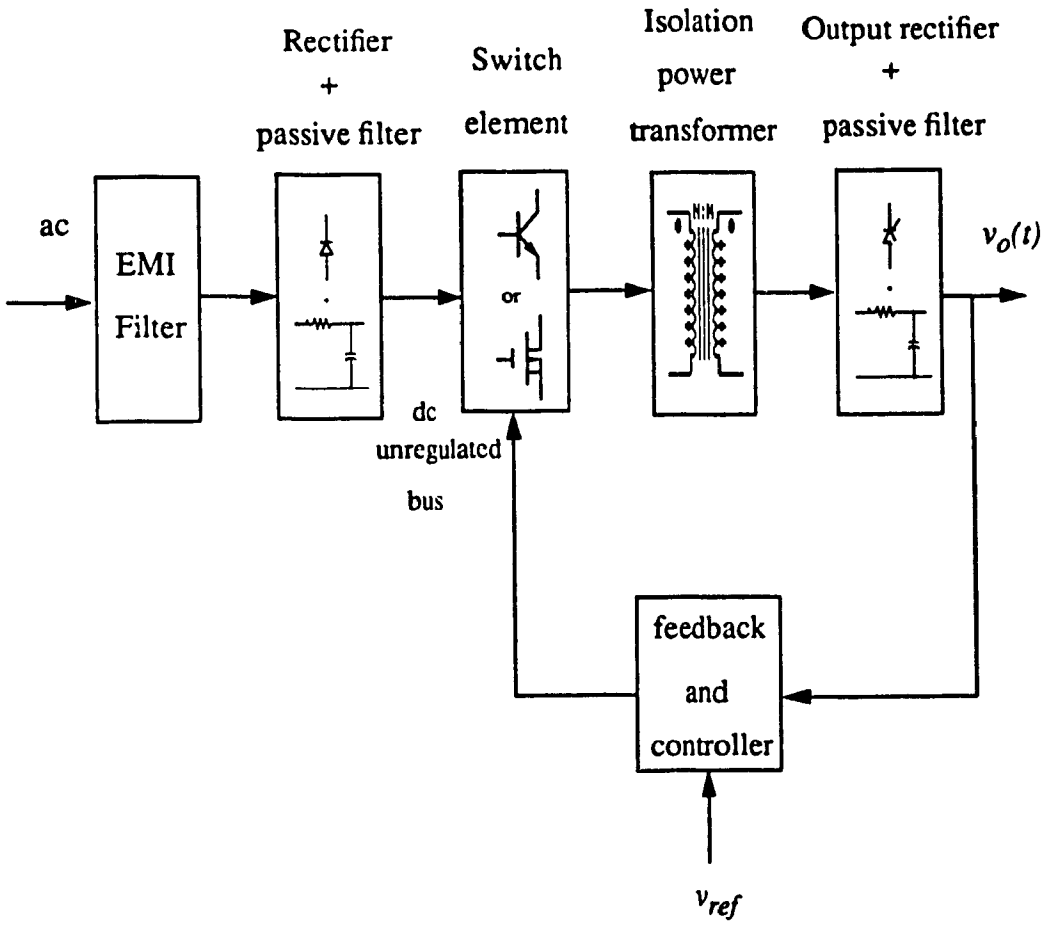

Figure 1.4: Block diagram of the switchmode dc power supply.

1.2.4 Hybrid Structures

As shown in the previous sections, the phase-controlled rectifier is still a preferred choice in high power applications. However, the main difficulty to use the phase-controlled rectifier as a magnet power supply is the large harmonics at the output. A possible solution to cancel these harmonics is to use a second-order passive filter. There are, however, several limitations in this approach:

1) Filtering is incomplete because the cut-off frequency of the passive filter can not be designed to zero. Consequently, the filtering requirements may not be satisfied.

2) Passive filters tend to be bulky and expensive when high attenuation is required.

3) The system dynamic response is significantly reduced if low order harmonics need to be filtered.

4) The filtering result is sensitive to the change of the system parameters.

In order to reduce the large voltage harmonics at the rectifier output without reducing the system dynamic response, a hybrid structure has been proposed in magnet power supply systems in recent years. It is based on the combination of the phase-controlled rectifier and the high-frequency switch-mode power converter which acts as an active filter. The basic idea of this hybrid structure is that high power can be provided by the phase-controlled rectifier and the high-frequency converter (active filter) is only used for harmonic cancellation.

In active filter, harmonics are reduced or cancelled based on the principle of harmonic injection [1][8][17][18]. In contrast to passive filters, active filters have several obvious advantages:

1) Filtering is, in theory, complete. The active filter acts as a harmonic isolator not

as a harmonic attenuator.

2) Active filters are cheaper and smaller than passive filters when very high attenuation is required [19][20][21].

3) When active filters are applied, they do not slow down the system dynamic response, since they operate at a high frequency.

4) Active filters are not sensitive to system parameters change, since feedback control loop can be applied to control the active filter.

The principle of the harmonic cancellation using active power filter is similar to that used in AC or DC active power filters [17-26]. Active filters can be connected either in series or in parallel with a load. Also, the active compensator topology can be either of a voltage type or of a current type.

1.2.4.1 Series Topologies

In this structure, the active power filter (injection source) is connected between the rectifier and the magnet load in order to remove the harmonic voltage at the magnet load. Either voltage-type converters or current-type converters can be used.

Figure 1.5 (a) shows the equivalent circuit using a voltage type converter which is controlled to inject a harmonic voltage equal but opposite to that generated by the rectifier; that is, to make $v_f(t) = -v_{rn}(t)$, where $v_f(t)$ is the injection voltage at the output of the voltage-type converter, $v_{rn}(t)$ is the harmonic voltage produced by the main source, and V_{rd} is the fundamental voltage of the rectifier. In this way, the load voltage becomes ripple-free as expected, that is, $v_o(t) = V_{rd}$.

Figure 1.5 (b) shows the equivalent circuit using a current-type converter as an injection source. In this configuration, the output voltage of the current-type converter,

$v_j(t)$, is controlled to produce an equal-but-opposite value with the rectifier harmonic voltage, $v_{rn}(t)$, by controlling the converter current $i_j(t)$. Thus, the harmonic voltage in the magnet load can be cancelled.

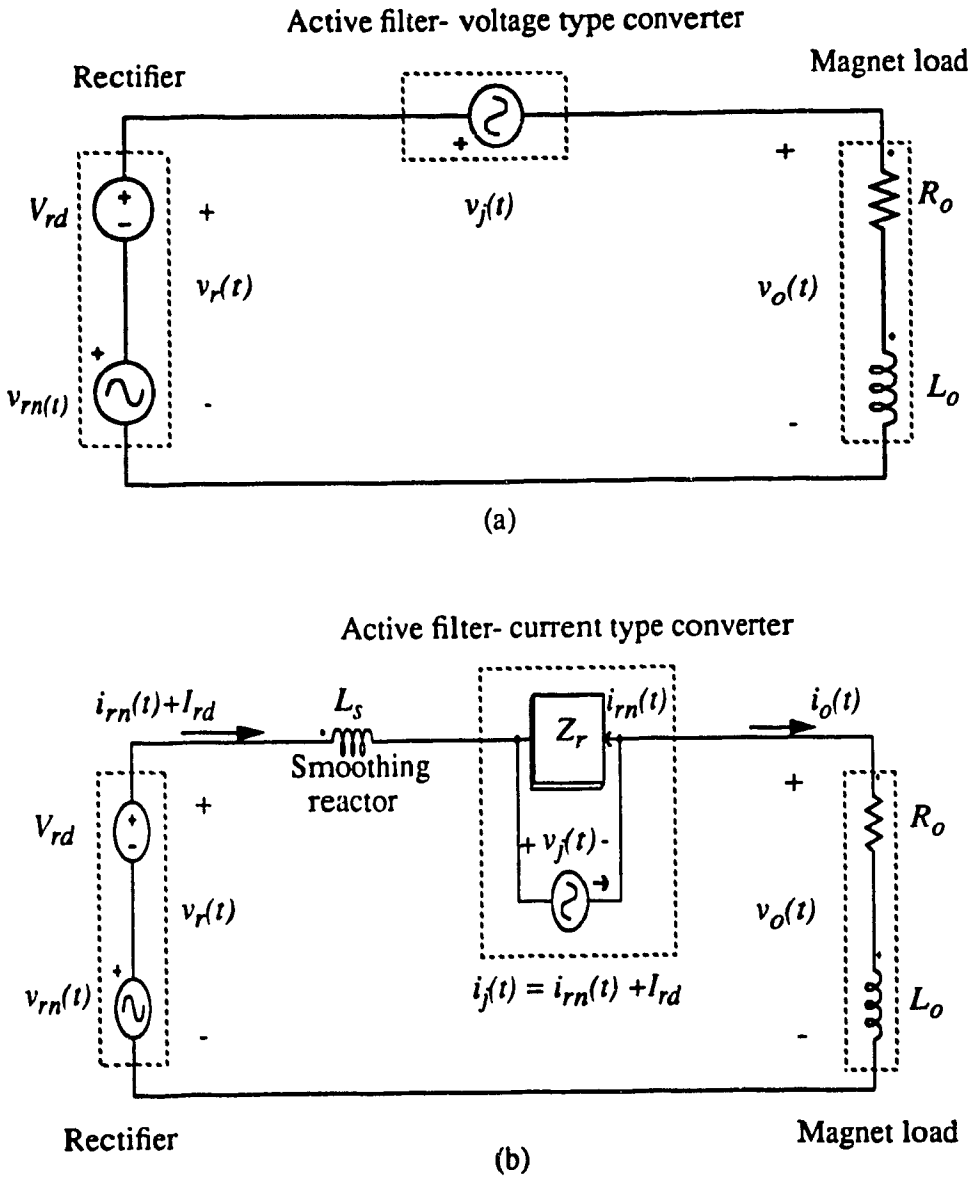

Figure 1.5: Equivalent circuits of series topologies.

(a) using voltage-type converters as active filters;

(b) using current-type converters as active filters.

The major difference between active power filters and passive filters is that active filters act as harmonic eliminators and not as harmonic attenuators. At fundamental frequency, active filters behavior as a short circuit. In series topologies, voltage-type converters are commonly used because they are lighter, less expensive and easier to control than current-type converters [14-18].

Due to the switching capacities of devices, the power rating of active filters is a major concern for researchers. Recently, some techniques, such as transformer-decoupled active filters have been evaluated [14][27]. The system configuration is shown in Figure 1.6 [27]. Transformer-decoupled power supplies have certain advantages such as a higher system efficiency, and a low power rating of the active filter compared with linear power supplies [27]. In addition, this type of power supplies give very good performance at the steady state operation. However, it does not improve the system dynamic response.

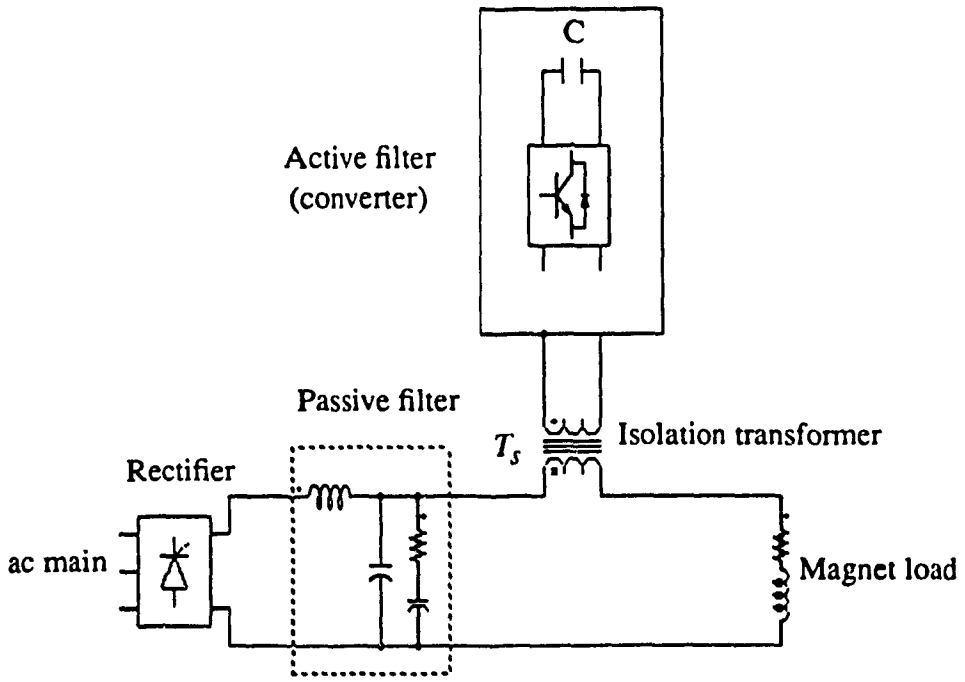

Figure 1.6: Transformer-decoupled magnet power supplies using a series topology.

1.2.4.2 Shunt Topologies

In this structure, the converter is connected in parallel with the magnet load to provide a bypass for the harmonic currents, thereby reducing or cancelling harmonic current at the load. The converter can be implemented either by the current-type converter or voltage-type converter.

Figure 1.7(a) shows the equivalent circuit using a voltage-type converter as an active filter. In this configuration, the injection current, $i_j(t)$, passing through the voltage-type converter is controlled to have an equal-but-opposite value as the rectifier harmonic current, $i_{rn}(t)$, thereby cancelling the harmonic current in the magnet load. By using the current control technique, the injected voltage-type converter acts as a current source.

Figure 1.7 (b) shows the equivalent circuit using a current-type converter as an active filter. In this configuration, the current of the current-source converter, $i_j(t)$, is controlled to produce an equal-but-opposite current as the rectifier harmonic current, $i_{rn}(t)$. Thus, it cancels the harmonic current in the load.

Again, in shunt topologies, active filters act as harmonics eliminators and not as harmonic attenuators. They work as open circuits at the fundamental frequency, where the converters are controlled as a current source. Therefore, they do not affect the fundamental component when the unexpected harmonics are filtered.

In some applications, such as HVDC stations, active filters are used to reduce the harmonics in the dc side [20][21]. Voltage-source converters are recommended in these applications. Because the voltage-type converters behave like a zero impedance when the output voltage is zero. In particular, when the system uses a combination of passive and active filters harmonic currents can pass through the passive filters without any difficulty. Therefore, the performance of the existing passive filter is not affected [20][21].

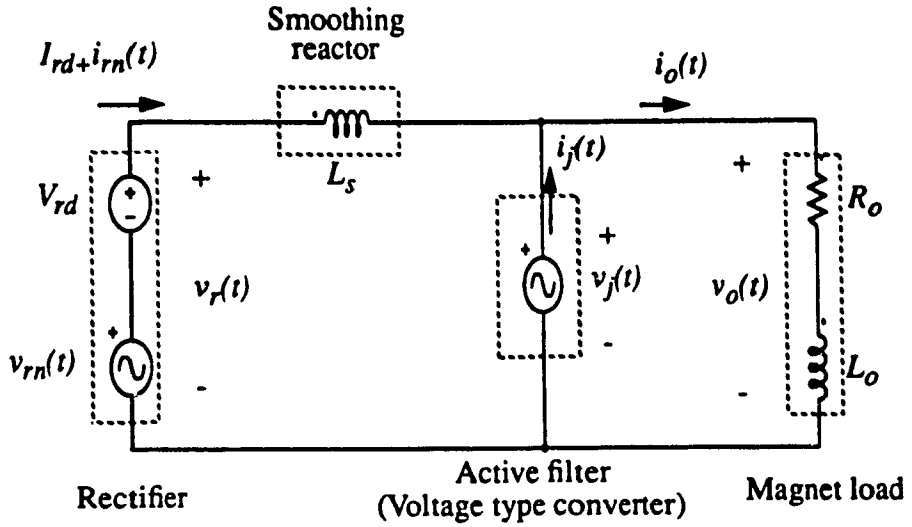

(a)

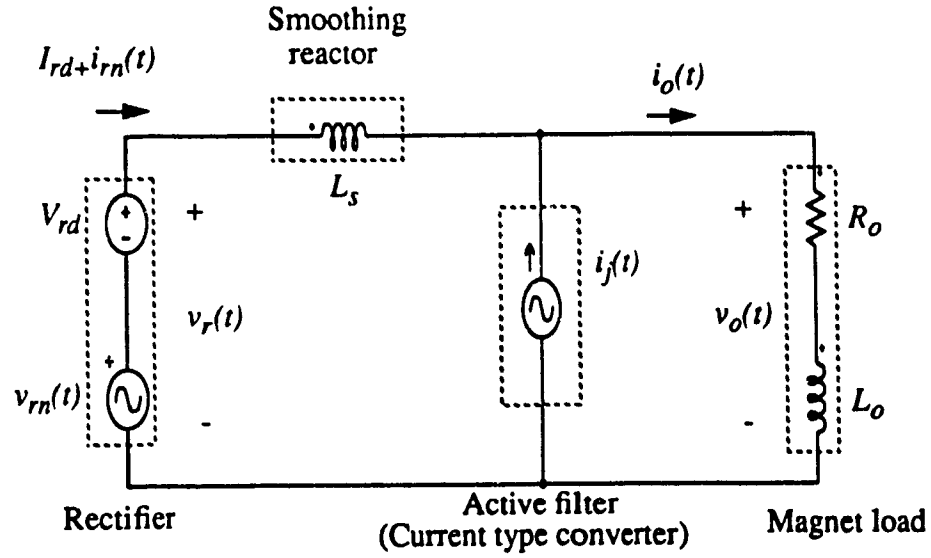

(b)

Figure 1.7: Equivalent circuit for shunt topologies.

(a) using voltage-type converters as active filters;

(b) using current-type converters as active filters.

Recent works on shunt topologies use transformer-decoupled converters instead of linear power supplies in order to improve the efficiency of the system and minimize the power rating of the active filter [20][21]. The system configuration is shown in Figure 1.8. In this configuration, the capacitor C_s and the isolation transformer T_s guarantee that the active filter compensates only for small ripples, therefore, the power rating of the active filter is minimum. Again, this configuration does not improve the system dynamic response.

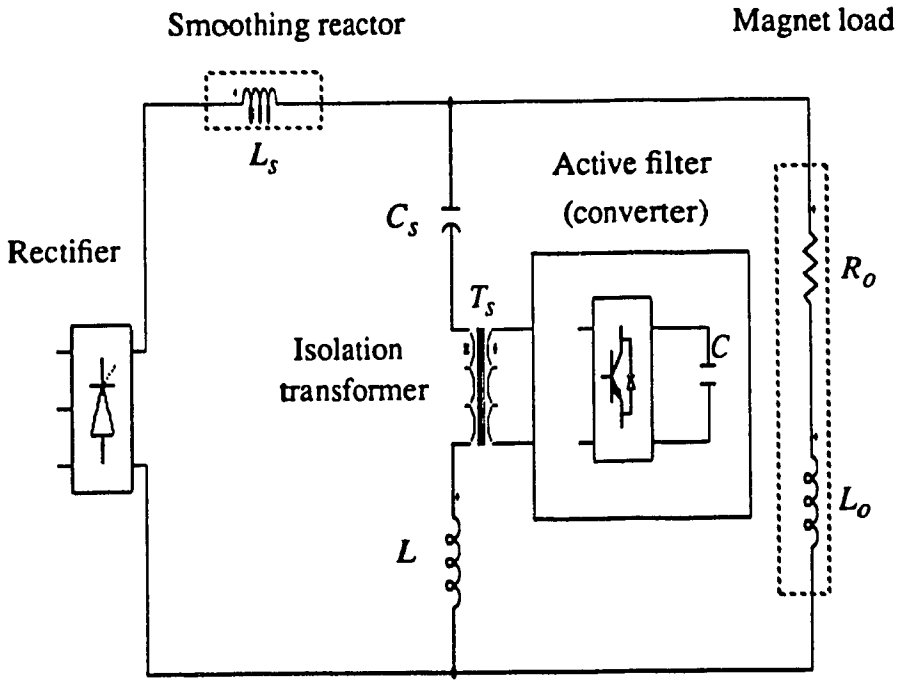

Figure 1.8: Block diagram of a shunt active filter using transformer-decoupling.

1.3 Proposed Approach

1.3.1 Proposed Power Circuit

As discussed in the previous sections, by using the hybrid structures shown in Figure 1.6 and Figure 1.8, high power rating and low harmonic contents can be simultaneously achieved. However, it is still difficult to meet the stringent dynamic requirement since the system dynamic response has not been improved compared to that of the conventional rectifier power supply.

In order to solve this problem, alternate system structures are proposed in this thesis. The idea is that a small portion of the dc power is provided by switch-mode active power filters during the ramp transient period in order to compensate for tracking errors. Therefore, the system dynamic response can be improved.

Two configurations, the series topology shown in Figure 1.9 and the shunt topology shown in Figure 1.10, are proposed.

1.3.2 Hybrid Structure with Feedforward Control

A major problem in the proposed hybrid structures shown in Figure 1.9 and Figure 1.10 is the power sharing between the slow phase-controlled rectifier and the fast compensator. The compensators are directly coupled to the magnet load. During the transient period, the PWM compensator tends to take over the main power required by the load from the phase-controlled rectifier. To overcome this problem, a feedforward or predictive control scheme is proposed to control the rectifier. It forces the phase-controlled rectifier

to provide the desired output power during the whole operation period. In other words, this feedforward technique guarantees that the main power is provided by the phase-controlled rectifier in the whole operation cycle. Details will be discussed in the following chapters.

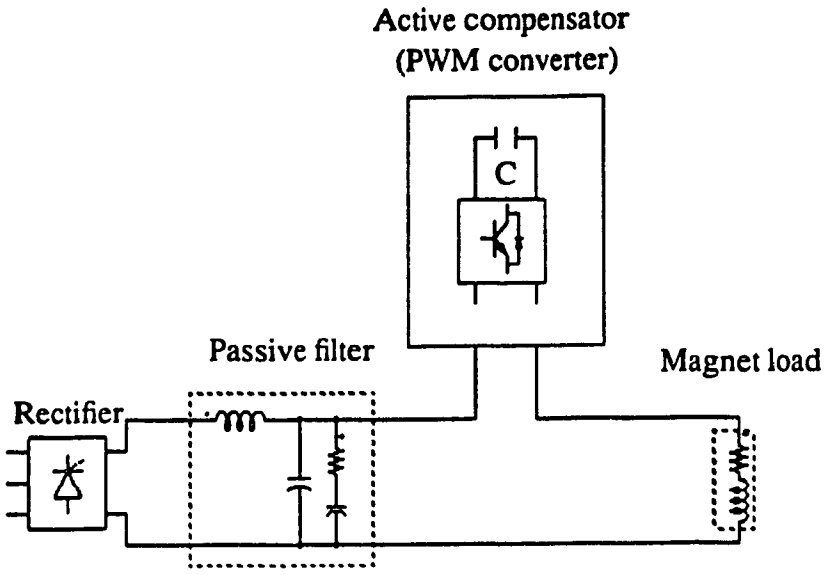

Figure 1.9: A proposed magnet power supply using series topologies.

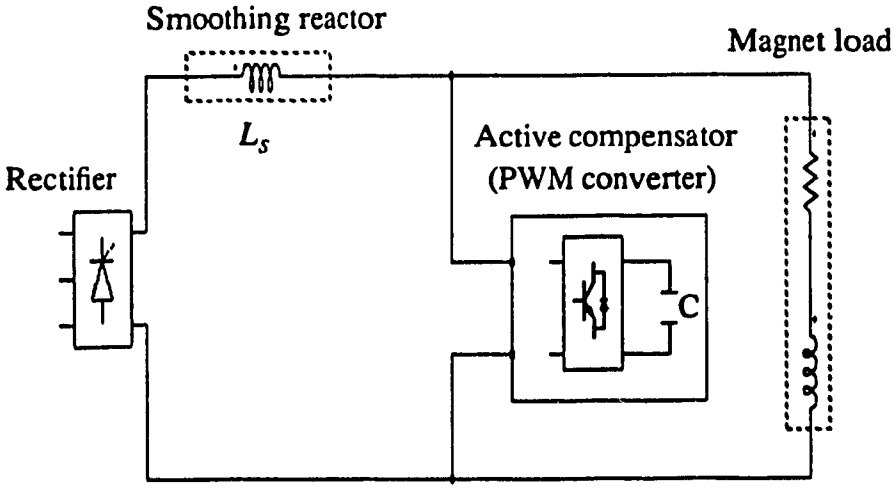

Figure 1.10: A proposed magnet power supply using shunt topologies.

1.4 Thesis Objectives and Contributions

The main objective of this thesis is to improve the harmonic and dynamic performance of phase-controlled rectifiers used as magnet power supplies. Contributions of this work include:

(a) Demonstrating the feasibility of using low-power, high-frequency series or shunt connected power converters as active compensators for high-performance magnet power supplies.

(b) Developing the appropriate control loops for the PWM converters used as compensators.

(c) Applying a feedforward control scheme to the phase-controlled rectifier to solve the power sharing problem in the hybrid structure.

1.5 Thesis Outline

The contents of this thesis are as follows:

In Chapter 2, the power circuit configuration and the characteristics of the conventional phase-controlled rectifier power supply are discussed. The concept of the feedforward control technique is explained. Experimental results are provided to verify the concept.

In Chapter 3, the hybrid magnet power supply with series topology is proposed. The principle of harmonic cancellation is explained. Control schemes for the phase-controlled rectifier and PWM converter (active compensator) are presented.

In Chapter 4, the design and implementation of the proposed magnet power supply using series topology are presented. Design procedures are given in details through a design example. The power ratings of the phase-controlled rectifier and PWM converter (active compensator) are calculated, and experimental results are presented.

In Chapter 5, the hybrid magnet power supply with shunt topology is proposed. The power circuit configuration and the control schemes are presented. The principle of harmonic cancellation is explained.

In Chapter 6, the design and implementation of the proposed magnet power supply using shunt topology are presented. Design procedures are explained in details through a design example. The power ratings of the phase-controlled rectifier and PWM converter (active compensator) are calculated. The relationship between the passive filter (smoothing reactor) and the active compensator is discussed. Experimental results are presented.

In Chapter 7, conclusions are given along with contributions of this thesis and suggestions for future work.

Chapter 2

Phase-Controlled Rectifier Modelling and Feedforward Control Technique

2.1 Introduction

The proposed magnet power supplies use the hybrid structure which consists of a conventional phase-controlled rectifier power supply and a high-frequency switchmode converter. For a proper design of the proposed magnet power supply system, the understanding and analysis of the phase-controlled rectifier are important.

In this chapter, the model of the phase-controlled rectifier is established by using the heuristic model [28]. Fourier analysis is applied to investigate the system's steady state harmonic contents. The controller of the conventional rectifier is designed in the frequency-domain by using MATLAB control tool box. The characteristics of the phase-controlled rectifier, both in the steady state and dynamic state, are studied. The output passive filter is designed to cancel the large amounts of the rectifier harmonic contents. Also, the feedforward (predicative) control technique is introduced to the conventional rectifier power supply. The results of the theoretical analysis are verified by computer simulation and experimental set-up.

2.2 Steady State Characteristics

The power circuit of the phase-controlled rectifier power supply, which is shown in Figure 1.9, is redrawn in Figure 2.1.

In analyzing the circuit of Figure 2.1, the following assumptions are made:

1) Switching devices in the power circuit are ideal.

2) The reactances between the three-phase ac voltage source and the rectifier input are considered to be zero.

3) The ac voltage source is symmetrical, unperturbed and sinusoidal.

4) The rectifier operates in a continuous current mode considering the fact that the magnet load is highly inductive.

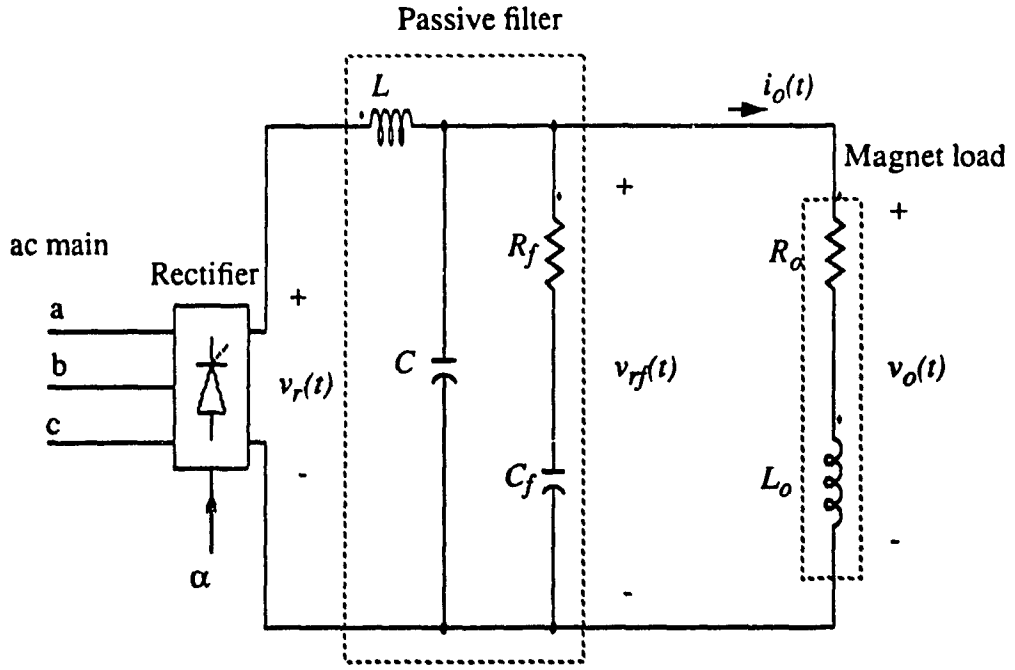

Figure 2.1: Power circuit of the phase-controlled rectifier of Figure 1.9.

Under the above assumptions, the rectifier power supply system operates in ideal operating conditions and the firing angle α determines the voltage values of the dc component and amplitude of the harmonic contents at the rectifier output. Figure 2.2 (a) shows the voltage waveform $v_r(t)$ in the rectifier output at firing angle $\alpha = 60^0$. Figure 2.2(b) shows the harmonic spectrum of $v_r(t)$. The line-to-line rectifier input voltage is chosen as the base in this simulation.

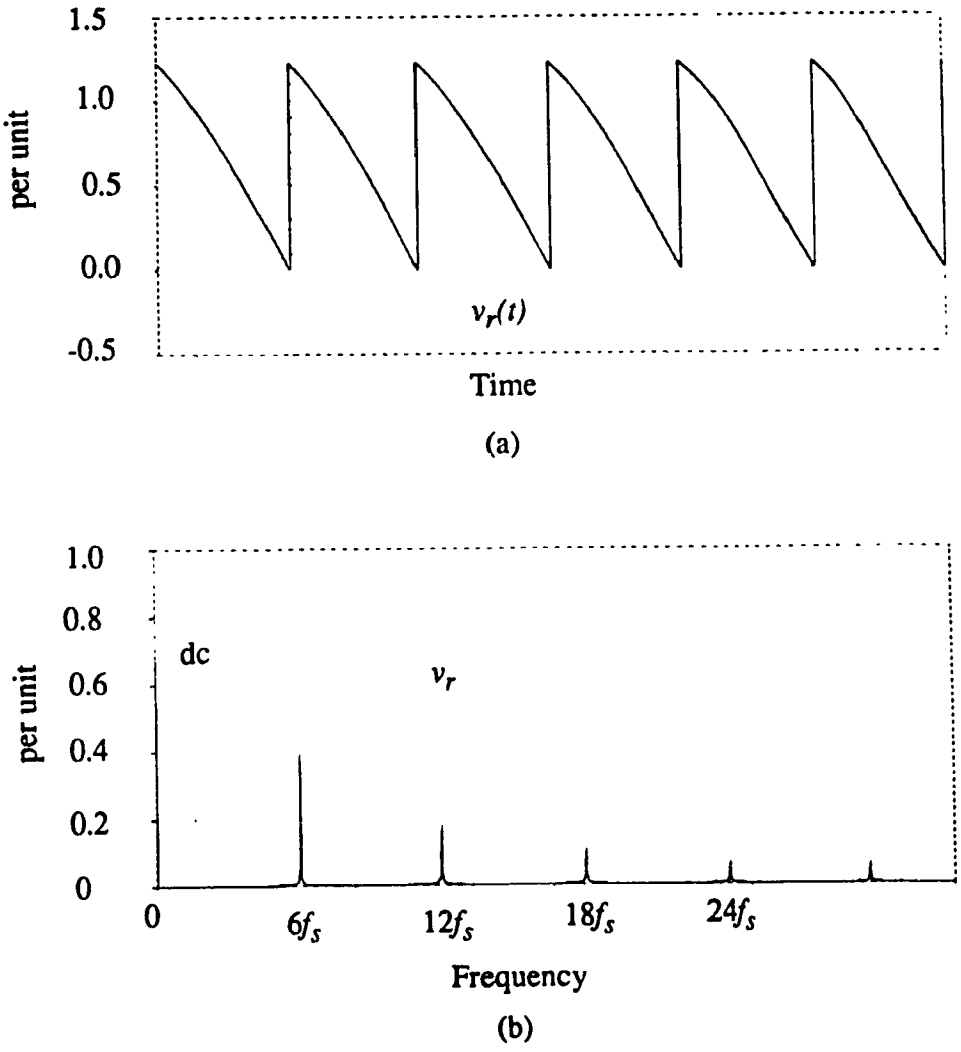

Figure 2.2: Rectifier output voltage at firing angle $\alpha=60^0$.
(a) Waveform; (b) Harmonic spectrum.

In steady state operation, the output voltage of the controlled rectifier, $v_r(t)$, can be expressed by a Fourier series:

$$v_r(t) = V_{rd} + \sum_{n=1}^{\infty} V_{rn} \times \sin(n\omega_s t + \theta_n) \tag{2.1}$$

where V_{rd} is the dc component of the rectifier output voltage, V_{rn} is the amplitude of the n^{th} order harmonic, ω_s is the ac main source frequency, and θ_n is the angle of the n^{th} order harmonic voltage.

There are six identical pulses in every cycle and each pulse lasts one-sixth of the cycle. Therefore, all of the harmonics in the waveform of $v_r(t)$ are of the order $n = 6m$ (m=1,2,3,4,...). The dc component is given by:

$$V_{rd} = \frac{3\sqrt{2}}{\pi} \times V_{ll} \times \cos\alpha \tag{2.2}$$

where V_{ll} is the line-to-line rms voltage of the rectifier input, and α is the rectifier firing angle.

The amplitudes of harmonics are given by:

$$V_{rn} = \frac{6V_{ll}}{\pi\sqrt{n^2-1}}\sqrt{(1-\cos 2\alpha + \frac{2}{n^2-1})} \approx \frac{6V_{ll}}{n\pi}\sqrt{1-\cos 2\alpha} \tag{2.3}$$

Equation (2.3) shows that the highest amplitude and the lowest frequency harmonic is the sixth order harmonic and it appears at α=90°; that is:

$$V_{r,6peak} = \frac{V_{ll}}{\pi}\sqrt{2} \approx 0.45V_{ll} \tag{2.4}$$

A second order L-C filter is usually used at the rectifier output for harmonic attenuation. Since the magnet load is highly inductive, it provides little damping to the L-C filter. In order to provide damping in the filter, an R-C branch is connected in parallel with the filter capacitor, as shown in Figure 2.1.

In Figure 2.1, if $C_f >> C$, the attenuation of the filter to the voltage harmonic at the rectifier output is given by:

$$|H(jn\omega_s)| = \left| \frac{1}{-\left(\frac{n\omega_s}{\omega_c}\right)^2 + 2j\xi \times \frac{n\omega_s}{\omega_c} + 1} \right| \tag{2.5}$$

where the resonant frequency is:

$$\omega_c = \frac{1}{\sqrt{LC}} \tag{2.6}$$

and the damping ratio is:

$$\xi = \frac{1}{2R_f}\sqrt{\frac{L}{C}} \tag{2.7}$$

It is common to choose a cut-off frequency of the passive filter ω_c below the frequency of the dominant harmonic component in the voltage $v_r(t)$. In this case, the dominant harmonic frequency is 6 ω_s. Therefore, the cut-off frequency of the passive filter can be chosen such that $\omega_c < 6\omega_s$. The approximation of (2.5) yields:

$$|H(jn\omega_s)| = \left(\frac{\omega_c}{n\omega_s}\right)^2 \tag{2.8}$$

The voltage waveform at the output of the passive filter can be expressed as:

$$v_{rf}(t) = V_{fd} + \sum_{n=6,12,\ldots}^{\infty} V_{rfn} \times \sin(n\omega_s t + \theta_n) \tag{2.9}$$

where the dc component of the output of passive filter is given by:

$$V_{fd} = V_{rd} \tag{2.10}$$

and the harmonic amplitudes are:

$$V_{rfn} = V_{rn}|H(jn\omega_s)| \approx \frac{6V_{s,ll}}{n\pi}\left(\frac{\omega_c}{n\omega_s}\right)^2 \sqrt{1-\cos 2\alpha} \tag{2.11}$$

Figure 2.3 shows the voltage waveform and the harmonic spectrum of the output of the passive filter. Comparison of Figure 2.2(b) and Figure 2.3(b) shows that the amplitude of harmonics at the passive filter output is much lower than it is at the rectifier output.

2.3 Dynamic Characteristics

The firing angle of the phase-controlled rectifier is discrete and the steady state and dynamic behavior of the controlled rectifier are highly nonlinear. Detailed analysis of dynamic processes in the line commutated rectifier is rather complex. Fortunately, the converter is usually followed by an inductive load having low-pass transfer characteristics. Therefore, the converter dynamic may be approximated by simple models [28]. This condition is well met in the magnet load.

In practice, a 'heuristic model' has often been used which is based on the observation that the firing of thyristors is sequential and the delay angle α may not be immediately

used until a certain period of time [28]. In three-phase-controlled rectifiers, the firing signal interval of each thyristor is 60^{o}. This means that the waiting interval is between 0 and $T_s/6$. The average delay time is then $T_d = T_s/12$. For a 60 Hz power supply, T_d = 1.38ms.

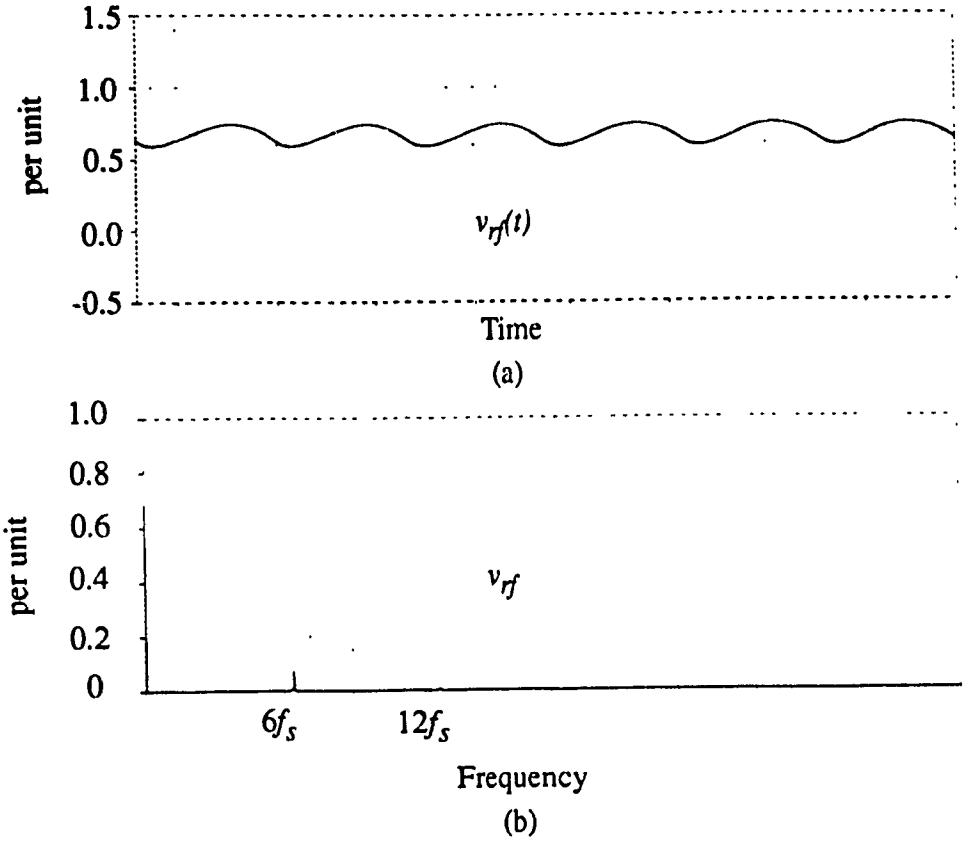

Figure 2.3: Passive filter output voltage at firing angle $\alpha=60^{o}$, ξ = 0.7 and f_c = 160 Hz. (a) Voltage waveform; (b) Harmonic spectrum.

By including an arc-cos function block at the α control input, the relationship between the rectifier dc output and the control variable can be linearized. The transfer function of the rectifier can, therefore, be expressed as:

$$G_r(s) = K_r e^{-sT_d} \tag{2.12}$$

where K_r is the gain of the rectifier, defined as $K_r = 1.35\ V_{ll}$ and T_d is the average dead time delay, as defined $T_d = T_s/12$.

By using (2.12), and assuming that T_s = 1/60 = 16.67 ms, the frequency response of the phase-controlled rectifier is drawn in Figure 2.4.

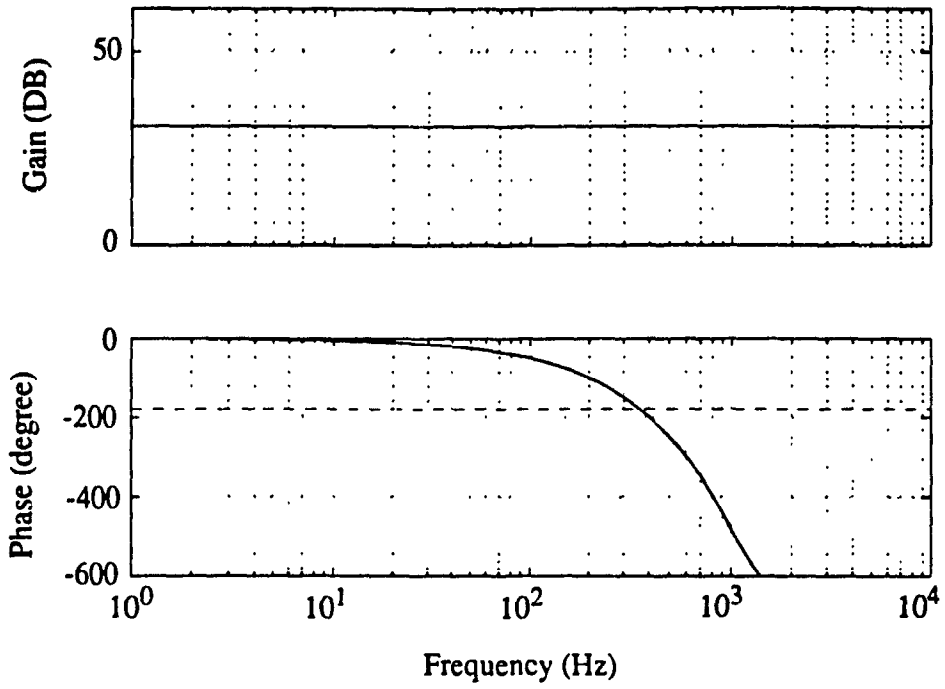

Figure 2.4: Bode plot of the rectifier voltage transfer function.

Figure 2.4 shows that the phase angle of the rectifier decreases linearly as the frequency increases. This makes the design of the conventional feedback rectifier control very difficult, when a larger bandwidth is required. This is because the maximum system cut-off frequency must be less than 360-Hz.

2.3.1 Feedforward Control Technique

As mentioned in Chapter 1, the main problem with the proposed hybrid magnet power supply is the power sharing between the slow rectifier and the fast active compensator. Conventional feedback control is difficult to improve the rectifier system dynamic response because of the rectifier dead-time delay. To overcome this problem, a feedforward control technique is introduced to control the rectifier.

2.3.2 Feedforward Control Principles

The feedforward control proposed is of the pre-regulation (predicative) control type. It is based on the known load parameters. It pre-calculates the rectifier output voltage needed, then adjusts the rectifier firing angle α accordingly. With this control technique, the system has faster dynamic response than with conventional feedback control because the firing angle α is pre-calculated. Moreover, the feedforward loop is independent of the control loop of the PWM converter. This guarantees that the necessary load voltage is always provided by the rectifier during the whole operation period.

In this thesis, the feedforward controller is designed based on the load parameters and current reference. The feedforward control technique works well both in steady state and transient operations. However, this technique is sensitive to system parameters changes.

By knowing the load resistance R_o, load inductance L_o, the filter inductance L, and the current profile, the corresponding voltage profile v_{ref} can be calculated as follows.

$$v_{ref} = R_o i_{ref} + (L_o + L)\frac{di_{ref}}{dt} \tag{2.13}$$

If only the flat-bottom, the ramp-up, and the flat-top operation period are concerned, the current and voltage profiles are illustrated in Figure 2.5.

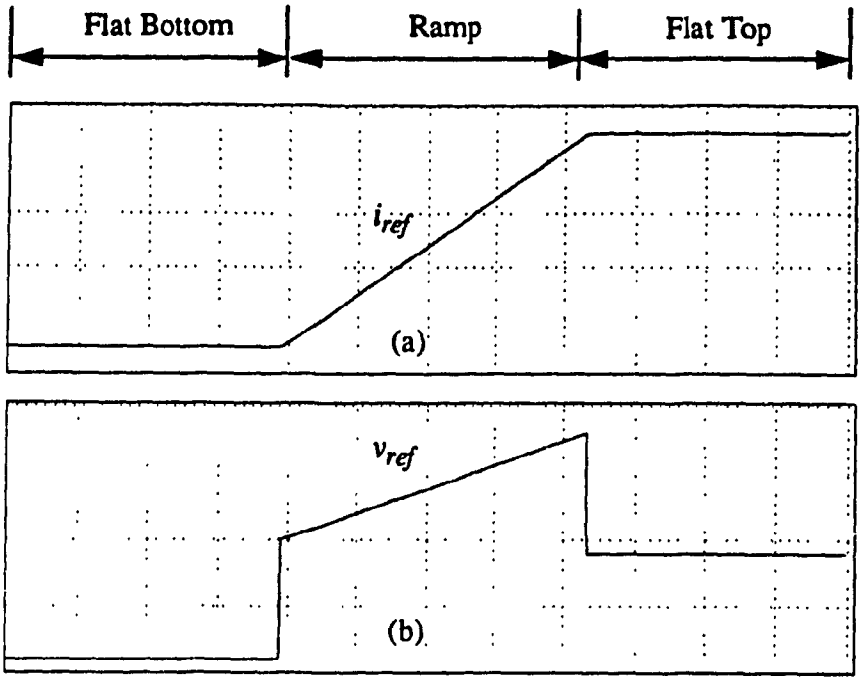

Figure 2.5: The load current and voltage profiles.

Therefore, the feedforward controller can be designed such as:

$$G_{ff}(s) = R_o + s\,(L_o + L) \tag{2.14}$$

By applying this feedforward control technique to the rectifier, the system only relates to the rectifier dead-time.

2.3.3 Implementation and Experimental Results

To illustrate the effectiveness of the feedforward control, the behavior of the rectifier power supply system is studied through an experimental setup. The schematic circuit

of the phase-controlled rectifier power supply with the proposed feedforward control is shown in Figure 2.6.

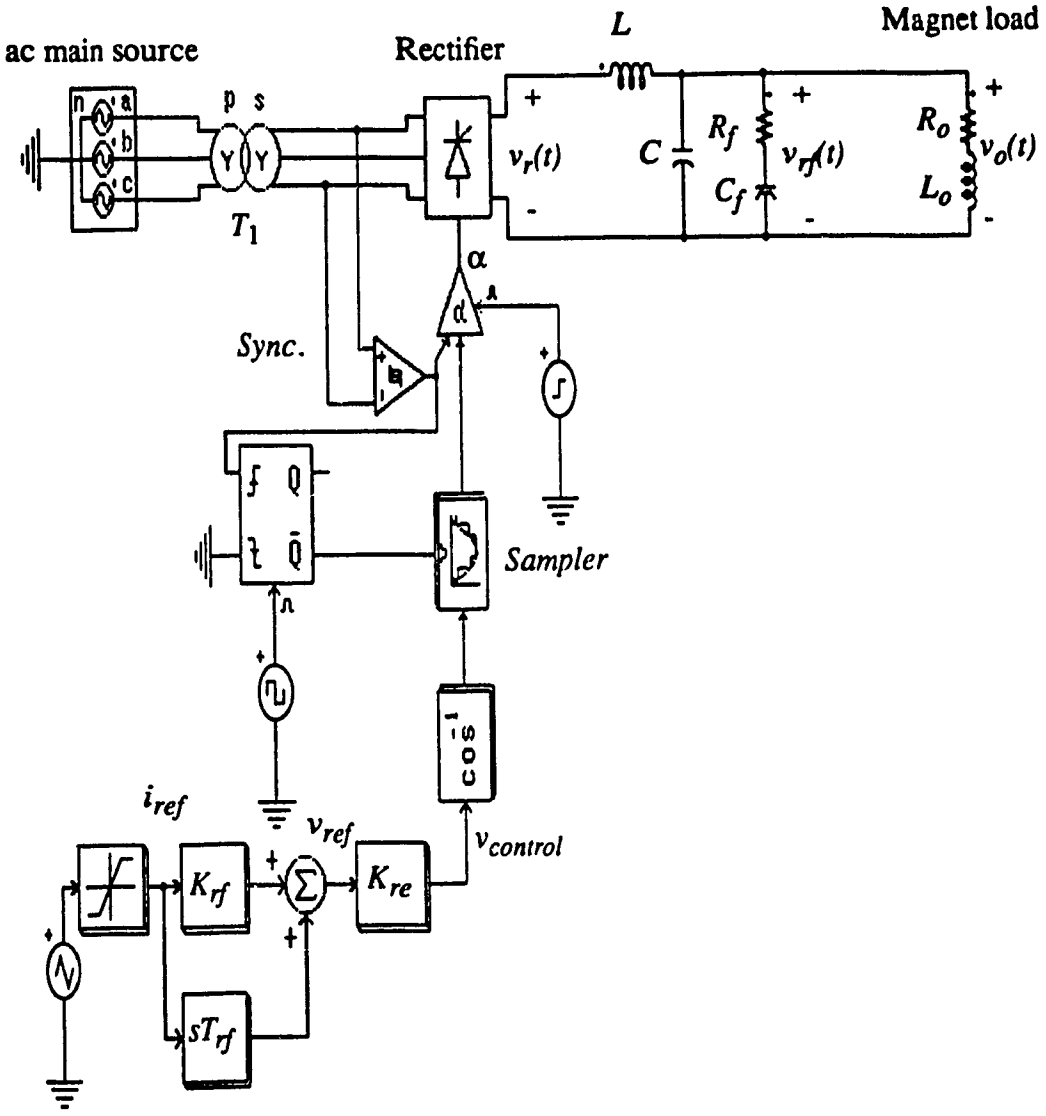

Figure 2.6: Phase-controlled rectifier power supplies using proposed feedforward control technique.

The system parameters are chosen to be as follows:

- ac source: 3-phase, 60 Hz, 207.8V;
- Magnet load: $P_{o,\,rated}$ = 200 w, $V_{o,\,rated}$ = 25V, and τ_o = 25.6ms;
- Load current: 2A to 10A; ramp period = 0.1s;
- Second order filter: ω_c = 160 Hz, ξ =0.7;
- Turn ratio of the rectifier input transformer: a_{T1} = 8.3.

Results of this experimental setup are shown in Figure 2.7. Figure 2.7 (a) shows that, with the rectifier using the feedforward control alone, the output voltage is capable of following the voltage reference very closely. This forces the current to track the reference, as shown in Figure 2.7 (b). Since the feedforward control is a type of open-loop control, there exists a steady state error during the flat bottom and flat top. Moreover, without the compensation from the active compensator, the load current contains a large amount of 360-Hz ripple, as can be seen in Figure 2.7(c) and Figure 2.7(d). The errors and the harmonics will be compensated by the active compensators discussed in Chapters 3 through 6.

2.4 Summary

There is a dead-time delay existing in the rectifier gating signal. Due to the delay of the gating signal, the speed of using the conventional current feedback control (i.e. PI controller) is limited. The feedforward technique or the predictive control technique, which is based on the actual system parameters, is introduced to the rectifier control system. It guarantees that the rectifier provides the desired output power during the whole operation period. Experimental results verify the basic concept presented in this chapter.

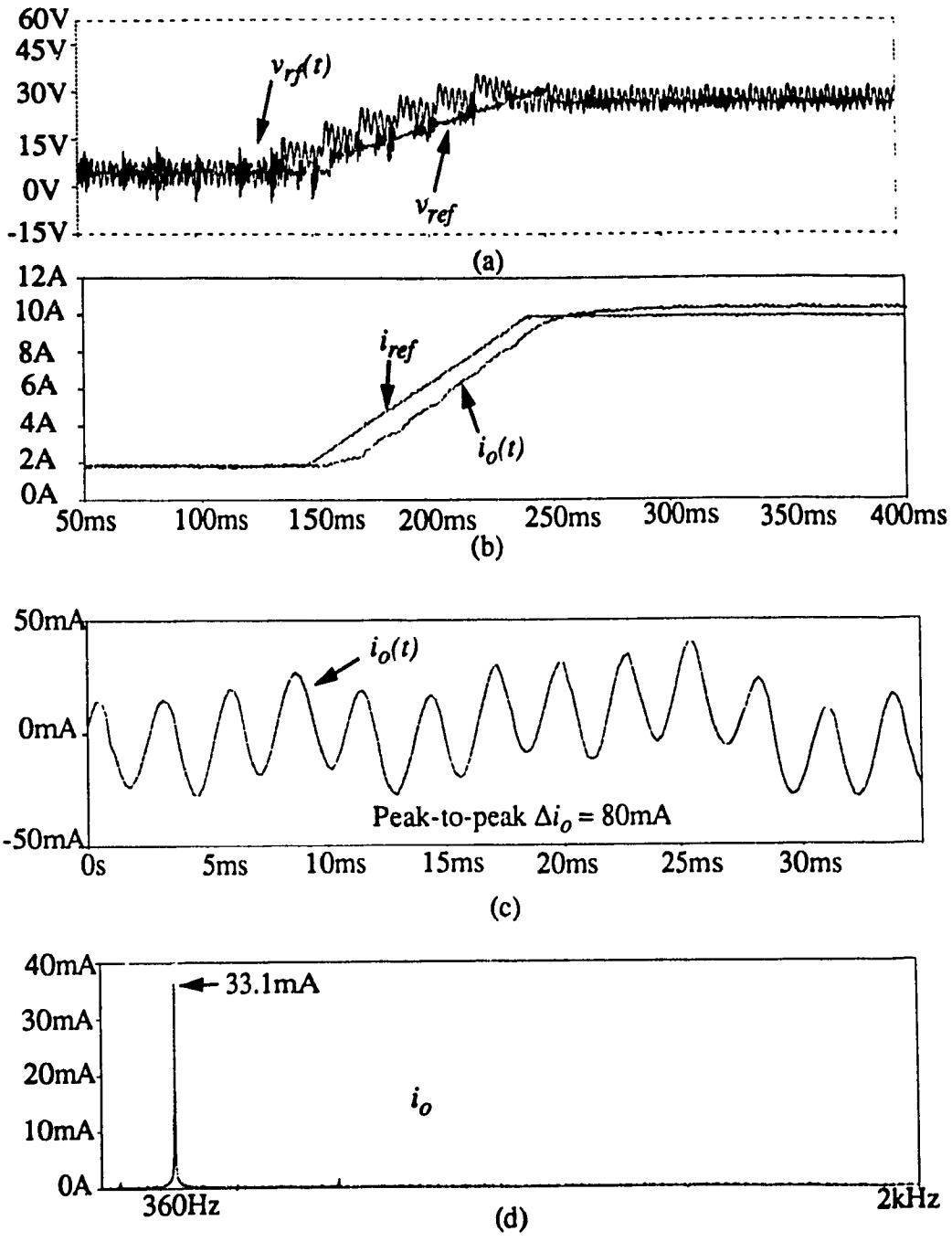

Figure 2.7: Experimental results of Figure 2.6. a) Load voltage and voltage reference; b) Load current and current reference; c) Expanded load current at i_o = 2A; d) Harmonic spectrum of the waveform of (c).

Chapter 3

Series Topology - Principle

3.1 Introduction

The proposed series topology uses a hybrid structure. It consists of a phase-controlled rectifier and a switch-mode PWM converter. In this structure, the large power handling capability of the controlled rectifier and the fast response characteristic of the PWM converter are fully utilized in a complementary way. The intention of this chapter is to provide a detailed overall picture and understanding of the proposed system.

In this chapter, the principle of harmonic cancellation and basic operation of the magnet power supply systems are explained. The mode of the PWM converter is established and the gating method is discussed. The power circuit configuration, including the phase-controlled rectifier and the switch-mode PWM converter, is presented. The idea of designing the control scheme both for the phase-controlled rectifier and the PWM converter is given. The feedforward control is designed to control the rectifier in order to solve the power sharing problem between the slow rectifier and the fast PWM converter. A combined voltage and current feedback loop is used to control the PWM converter for harmonic cancellation and error compensation.

3.2 Principle of Harmonic Cancellation

To explain the basic concept of harmonic cancellations, an equivalent circuit of the series topology, shown in Figure 3.1(a), is drawn in Figure 3.1 (b). For simplification, the rectifier output passive filter is not considered.

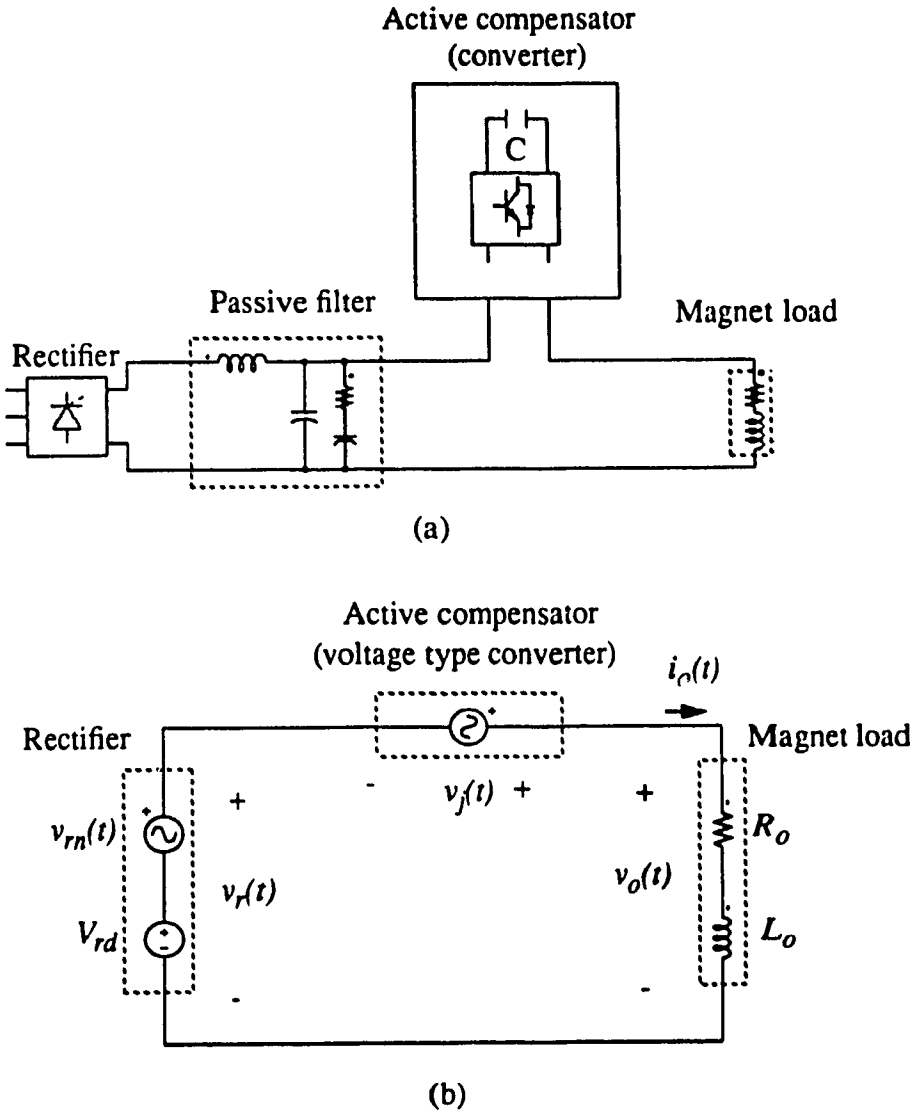

Figure 3.1: Series topology. (a) Power circuit; (b) Equivalent circuit.

The rectifier output voltage, $v_r(t)$, includes a dc component, V_{rd}, and harmonic components, $v_{rn}(t)$. To compensate for the harmonics $v_{rn}(t)$, a voltage $v_j(t)$, is generated from the active compensator. Based on KVL, the output voltage $v_o(t)$ is:

$$v_o(t) = V_{rd} + v_{rn}(t) + v_j(t) \tag{3.1}$$

Equation (3.1) reveals that the rectifier harmonics can be completely cancelled if an equal but opposite harmonic voltage is generated by the active compensator, i.e., if $v_j(t) = -v_{rn}(t)$, then $v_o(t) = V_{rd}$. In the proposed magnet power supply system, a voltage-type PWM converter is used as an active compensator. The voltage-type PWM converter acts as a power amplifier, the harmonic cancellation can be achieved by supplying the harmonics as the reference signal to the converter. This is the principle concept of harmonic cancellation using a series topology.

3.3 System Configuration

The magnet power supply system with the series topology is shown in Figure 3.2. In this configuration, a phase-controlled rectifier is connected in series with a voltage-type PWM converter. In order to compensate for any errors during transient operation or in abnormal operating conditions which result in low uncharacteristic harmonics in the rectifier output, the PWM converter is directly coupled to the magnet load. The PWM converter then works not only as an active filter for the harmonic cancellation, but also as a compensator for the errors compensation.

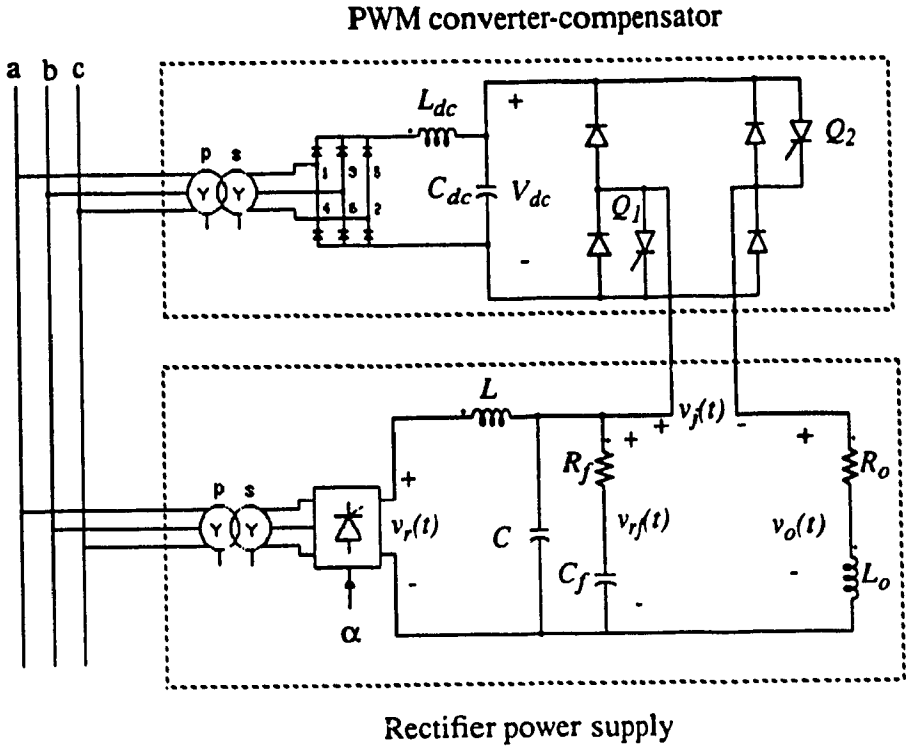

Figure 3.2: Power circuit configuration of the proposed magnet power supply system using series topology.

3.3.1 Rectifier Power Circuit

The rectifier power supply consists of a six-pulse phase-controlled rectifier and a second order passive filter.

The reason for using a second-order passive filter at the rectifier output is to reduce the power rating of the PWM converter. Passive filter is utilized as the first step in reducing output harmonics. After the passive filter, the harmonics level will be small and can be further reduced by the compensator with a small power rating.

Figure 3.1(b) shows that, in order to compensate for harmonics $v_{rh}(t)$ produced by

the rectifier, the output voltage of the PWM converter, $v_f(t)$, should be able to generate the same amplitude as $v_{rn}(t)$. The largest harmonic produced by the rectifier is the 6^{th} order harmonic and it occurs at $\alpha=90^0$. The amplitude is $V_{r,6peak} = 0.45V_{ll}$, which is given by (2.4). Since the PWM converter needs to compensate for all of the rectifier harmonics and any errors during steady state and transient operations, the voltage rating of the PWM converter must be larger than $V_{r,6peak}$. In other words, without a passive filter at the rectifier output, the voltage rating of the PWM converter will be comparable to the phase-controlled rectifier.

3.3.2 PWM Converter

The PWM power converter is directly coupled in series with the magnet load. The current direction does not change since the load current is always positive (seen from Figure 1.1). Therefore, a single phase two-quadrant chopper is chosen as an active compensator. The power circuit configuration of the active compensator is shown in Figure 3.2. This two-quadrant chopper is controlled by using a PWM technique and by operating in high frequency ranges.

There are two force-commutation switches, Q_1 and Q_2, in the two-quadrant chopper and they can be controlled independently of each other. Therefore, various gating signal patterns can be used. Different combinations of the two gating signals generate different voltage waveforms at the output of the two-quadrant chopper.

The gating method used in the proposed system for generating the gating signal is the triangular-carrier-wave modulation. This technique compares the two opposite reference signals with the triangular carrier waves in order to determine the state of the gating signal. The proposed gating method is illustrated with the waveforms shown in Figure 3.3.

This type of PWM scheme is called the pulse-width modulation with unipolar voltage switching.

For a modulation waveform $v_m(t)$ of a given frequency f_r, the same frequency amplitude of the output voltage of the chopper, $v_j(t)$, can be expressed as:

$$v_j(t) = \frac{V_{dc}}{V_{ca}} \cdot v_m(t) \tag{3.2}$$

where V_{dc} is the dc bus voltage of the two-quadrant chopper, V_{ca} is the amplitude of the carrier waveform.

It should be noted that the PWM chopper will proportionally amplify a combination of modulation signals of different frequencies (superposition applies), theoretically up to 1/2 of the switching frequency. In practice, to produce a quality compensation voltage, its frequency should not be exceed 1/3 of the switching frequency. This can be proved from the simulation waveforms shown in Figure 3.3. The simulation is done under the following system parameters:

- $V_{base} = V_{ca} = 1$ p.u.;
- $V_{dc} = 1$ p.u.;
- $v_m(t) = 0.4\ sin(6\omega_s t) + 0.4\ sin(12\omega_s t)$ (p.u.);
- $f_{s\omega} = 5$kHz.

In Figure 3.3 (a), two opposite modulation waveforms contain 6^{th} and 12^{th} harmonic components which have 0.4 p.u. amplitude. The load is considered to have a high inductance. Figure 3.3 (b) and Figure 3.3 (c) show the gating signals for the switches Q_1 and Q_2 using the PWM unipolar method. Figure 3.3 (e) shows that the output voltage of the two-quadrant chopper contains the same order components as the modulation wave-

forms, i.e., 6^{th} and 12^{th}, plus some higher order harmonics around $2f_{Sw}$ and so on. Figure 3.3 (e) also shows that PWM chopper proportionally amplifies all of the modulation signals, i.e., $V_{j,6}$ = 0.4 p.u., and $V_{j,12}$ = 0.4 p.u., as the gain of the two-quadrant chopper equals 1.

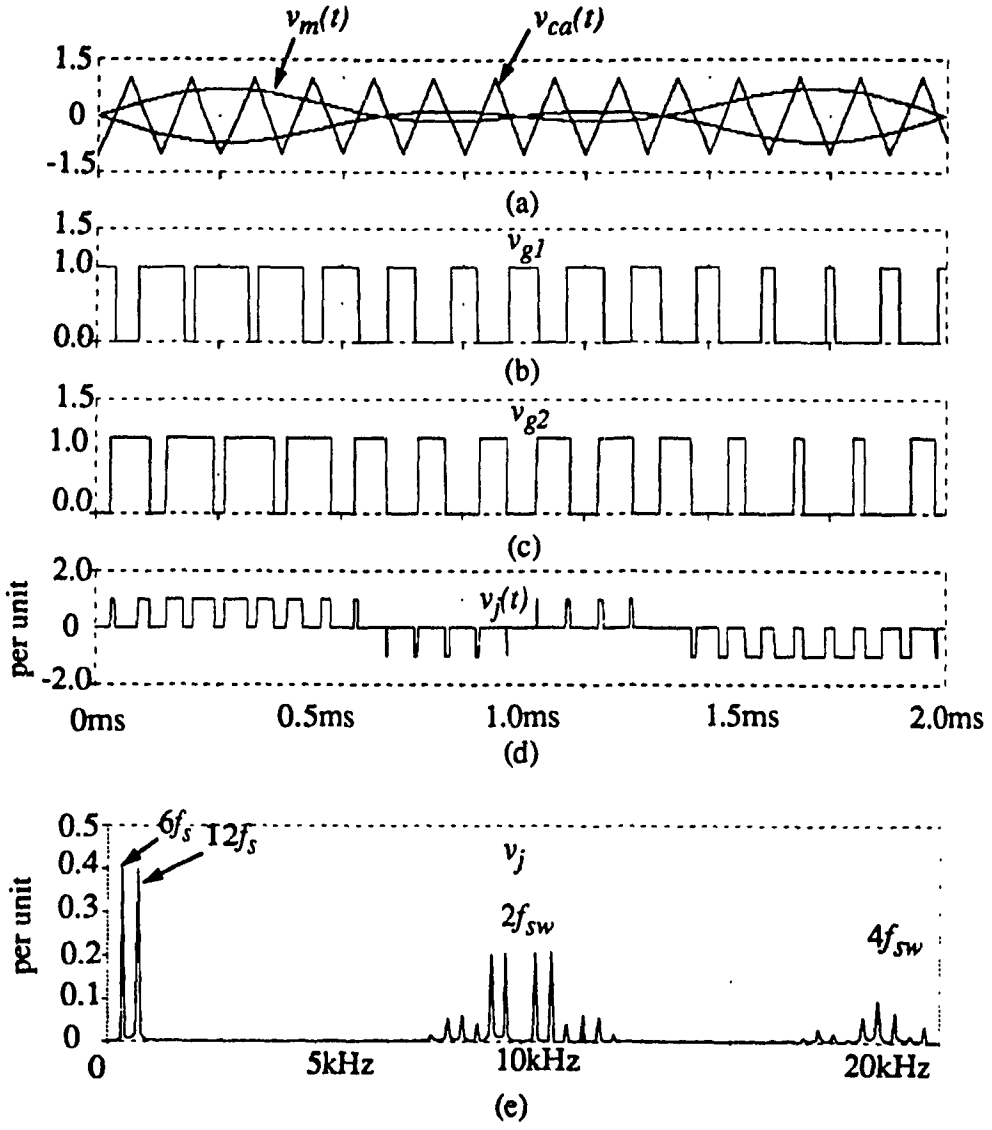

Figure 3.3: (a) Carrier waveform with two opposite modulation waveforms; (b) Gating signal for switch Q_1; (c) Gating signal for switch Q_2; (d) Output voltage waveform $v_j(t)$; (e)Harmonic spectrum of $v_j(t)$.

3.4 Control Scheme

In this section, the control scheme of the proposed magnet power supply system is designed to achieve the following features:

1) Excellent load current regulation;

2) Desired the power sharing in the hybrid structure: the main power is provided by the phase-controlled rectifier, and the PWM converter only provides a small amount of energy for compensating the harmonics and tracking errors.

The proposed control scheme is shown in Figure 3.4. There are two control sections: one for the rectifier and the other for the PWM converter.

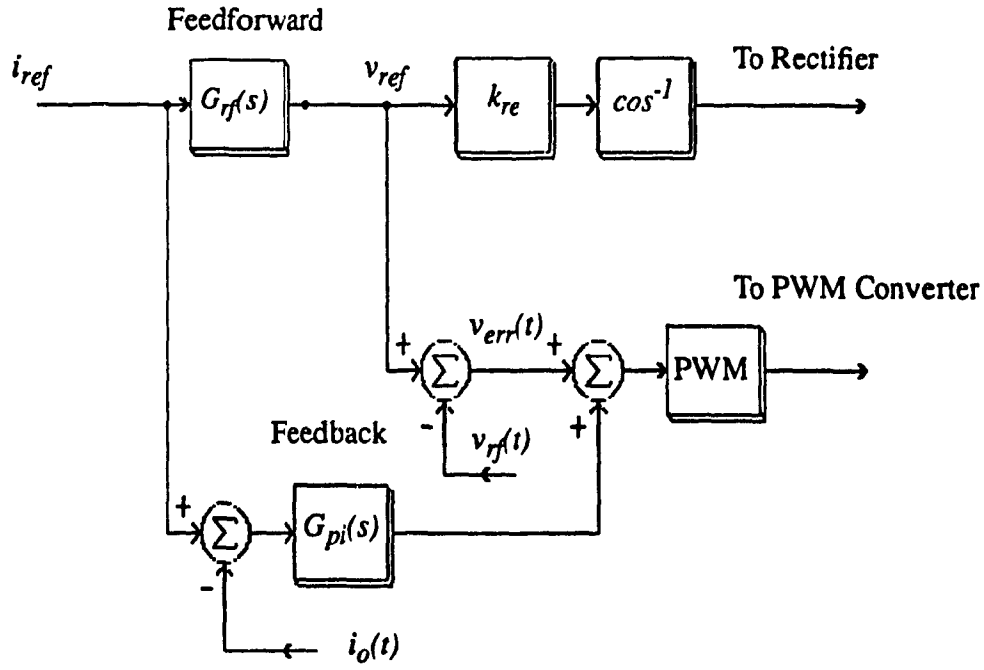

Figure 3.4: Proposed control scheme.

3.4.1 Rectifier Control

For magnet power supplies, a typical current cycle of operation includes not only the steady state operation, but also a ramp period as shown in Figure 2.5 (a). When the current is ramping up, the voltage changes rapidly shown in Figure 2.5 (b). During the ramp transient period, the PWM converter will tend to supply all the additional power required since it responds much faster than the rectifier. This problem can be solved if the rectifier is controlled, not through feedback, but in an open-loop fashion, to generate the desired output voltage profile beforehand. This is implemented in Figure 3.4 through the reference feedforward loop and the $G_{rf}(s)$ is chosen by using (2.14). Using an arc cosine function block, the rectifier loop is linearized and the output varies linearly with the input. The input comes from the feedforward branch which provides the desired voltage profile as is shown in Figure 2.5 (b).

A proportional controller K_{re} (shown in Figure 3.4) can be designed such that the rectifier output voltage equals the voltage reference required by the load:

$$K_{re} = \frac{1}{K_r} \tag{3.3}$$

then,

$$v_r(t) = K_r \cdot e^{-sT_d} \cdot \cos^{-1}(\cos(K_{re} \cdot v_{ref}))$$

$$= v_{ref} \cdot e^{-sT_d} \tag{3.4}$$

In the low frequency range, $v_r(t) = v_{ref}$.

This means that the rectifier output can follow the rapid transient of the reference without the adverse effects of a long settling time or oscillation existing in a feedback control system. Furthermore, the rectifier feedforward control loop is independent of the PWM control loop since the voltage reference is pre-determined and depends only on the load parameters and the current reference. This automatically ensures that the larger share of the output voltage is always provided by the rectifier. Moreover, this control loop is simple to design compared to that of the feedback control loop.

3.4.2 PWM Converter Control

The prime purpose of the PWM converter is to cancel rectifier harmonics and compensating for errors during steady state and transient operations. In order to achieve this goal, the control signal of the converter consists of two parts: one from the reference feedforward branch, which is a voltage loop, and another from the load current feedback as is shown in Figure 3.4. The voltage loop is mainly designed to cancel rectifier harmonics. The current feedback loop is designed to correct any offset between the actual current and the current reference.

This thesis uses a linear mode for the PWM two-quadrant chopper. According to (3.2), the transfer function of the two-quadrant chopper can be expressed as follows:

$$G_{co}(s) = \frac{V_{dc}}{V_{ca,peak}} \tag{3.5}$$

However, the relation given by (3.5) is applicable only for low frequency input (modulation) signals. As the frequency of the modulation signal, which is the control signal, increases and gets closer to the chopping frequency ω_{sw}, the switching action makes

the chopper behavior more resemble that of a discrete system.

In this thesis, the PWM converter (active compensator) is designed mainly to compensate for low-frequency harmonics and is operated with a high switching frequency, ω_{sw}. High order harmonics are easily filtered through the passive filter and magnet load. The modulation frequency, ω_m, is much lower than the switching frequency, ω_{sw}. Therefore, the linear model of the two-quadrant chopper, given by (3.5), is feasible.

3.4.2.1 Voltage Loop

The block diagram of the voltage loop is redrawn in Figure 3.5. The main function of this loop is to cancel the rectifier harmonics. Therefore, the reference of this controller should contain all of the concerning harmonics.

In order to make the load current follow the current profile, as shown in Figure 2.5 (a), the rectifier output dc voltage component V_{rd} is required to follow the voltage reference v_{ref}, i.e., $V_{rd} = v_{ref}$. By ignoring the losses in the passive filter, $V_{fd} = v_{ref}$. The error between the voltage reference v_{ref} and the filter output voltage $v_{rf}(t)$ is given by:

$$
\begin{aligned}
v_{err}(t) &= v_{ref} - v_{rf}(t) \\
&= v_{ref} - V_{fd} - \sum_{n=6,12,\ldots}^{\infty} V_{rfn} \times \sin(n\omega_s t + \theta_n) \\
&= -\sum_{n=6,12,\ldots}^{\infty} V_{rfn} \times \sin(n\omega_s t + \theta_n)
\end{aligned}
\tag{3.6}
$$

The computer simulation waveforms, which verify the above concept, are shown in Figure 3.6. The current reference in this simulation operates at 2A.

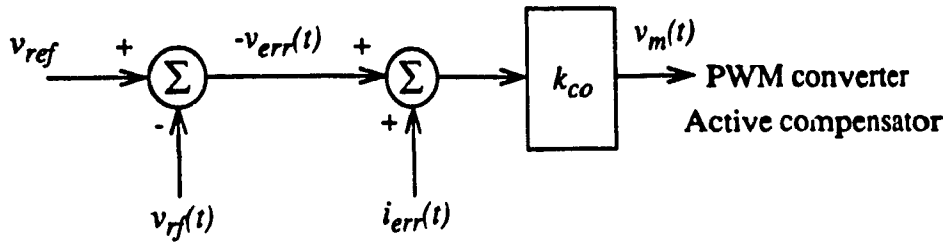

Figure 3.5: Block diagram of the voltage control to PWM converter.

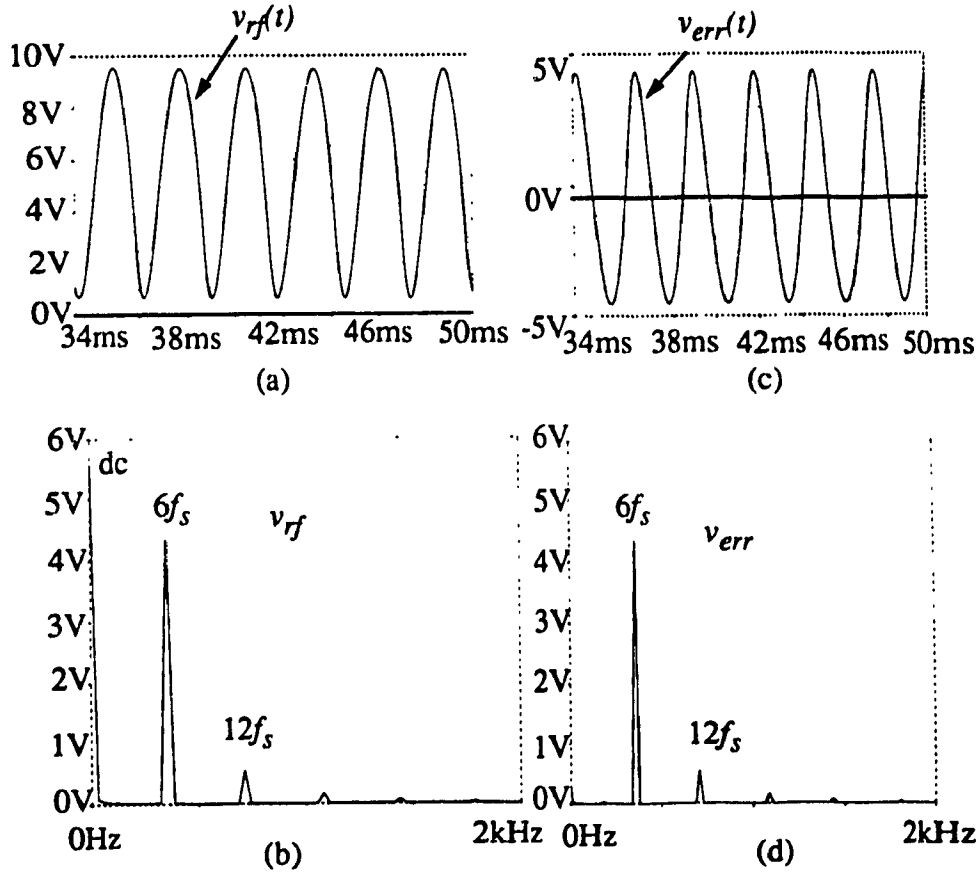

Figure 3.6: (a) and (b) Filter output voltage waveform and harmonic spectrum; (c) and (d) Error signal waveform and harmonic spectrum.

It should be noted that any errors generated during steady state and transient operations are also compensated by the PWM converter since $v_{err}(t)$ contains all of the errors between the desired and the actual rectifier output voltage. Using $v_{err}(t)$ as a part of the control signal to the PWM converter, the output voltage, $v_f(t)$, can be controlled such that it has an equal but opposite value as $v_{err}(t)$. Therefore, the harmonics appearing at the rectifier output are cancelled and the expected voltage waveform appears in the load.

This control scheme is a feedforward control technique. By measuring the input voltage (rectifier output voltage) variation, the switching gatings of the PWM converter are selected by control signals such that input harmonics and disturbances are cancelled or reduced through the modulation process of the switching modulator.

3.4.2.2 Current Feedback Loop

The feedforward control technique can significantly reduce harmonics and disturbance at the output. It is, nevertheless, still a type of open-loop control since it does not monitor the output quantity. In order to provide more accurate load current regulation, a combined feedforward/feedback control strategy is presented and the schematic form is shown in Figure 3.4. The feedback control schematic form of Figure 3.4 is redrawn in Figure 3.7.

According to Figure 3.7, the loop transfer function of this current feedback loop is given by:

$$G_c(s) = G_{pi}(s) \times G_{co}(s) \times G_o(s) \tag{3.7}$$

where $G_{pi}(s)$ is a PI controller, and $G_{co}(s)$ is the model of the PWM converter.

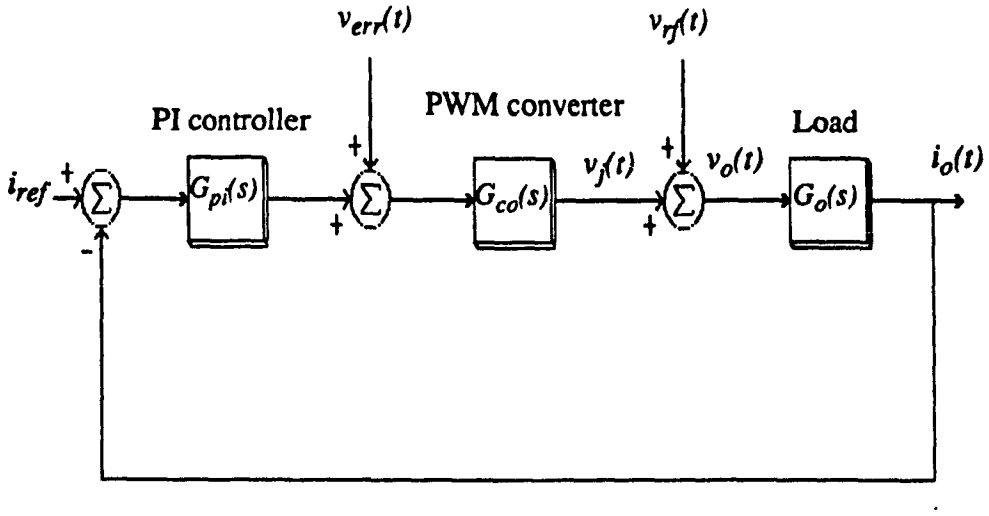

Figure 3.7: Block diagram of the PWM converter current feedback loop.

3.5 Summary

The feedforward control technique is applied to the phase-controlled rectifier and solved the power sharing problem in the hybrid structure. In the steady state operation, the two-quadrant active compensator works as an active filter for harmonic cancellation. In transient operation, it compensates for the tracking error. By using the series topology with the proposed control scheme, the larger power is handled by the phase-controlled rectifier, the PWM converter provides only a small portion of output power for harmonic cancellation and error compensation. Excellent current regulation can also be achieved. This will be verified in the next chapter through experimental results.

Chapter 4

Series Topology - Design and Implementation

4.1 Introduction

The purpose of this chapter is to design and implement the proposed magnet power supply system with a series hybrid topology using the concept discussed in the previous chapter.

In this chapter, design procedures are given and explained in details through a design example. Based on the requirements and specifications given for the system, the power circuits and the control loops, including the phase-controlled rectifier and the PWM converter, are designed by following the design procedures. The power ratings of the rectifier and PWM converter are also calculated. The design example is also implemented on a laboratory prototype and experimental results are presented.

4.2 Design Procedures

For the magnet power supply system with the series active compensator, once requirements and specifications are given, the following parameters can be determined:

1) **In the power circuit**: parameters of the rectifier, the active compensator, and the passive filter, power ratings of the rectifier and the active filter.

2) **In the control circuit**: parameters of the rectifier and the active compensator control loops.

The system design procedures consist of the following steps:

1. Determine the voltage rating of the phase-controlled rectifier.

2. Determine the parameters of the rectifier output passive filter.

3. Determine the voltage ratings of the active compensator.

4. Determine the current and power ratings of the rectifier and the compensator.

5. Design the rectifier feedforward control loop.

6. Design the PWM converter's voltage loop.

7. Design the PWM converter's current feedback loop.

A design example is given and design procedures will be explained in detail in the next section through the design example.

4.3 Design Example

The design example of this section illustrates how to follow the design procedures outlined in Section 4.2 and how to apply the information obtained in Chapters 2 and 3. The system schematic circuit, including the power and control circuits, is shown in Figure 4.1.

Due to the limitations of the laboratory equipment and devices, such as low precision and low current rating, some of the parameters in the experimental setup are not typical for magnet power supplies. The stringent requirements of bending magnet power supply may not be achieved in the experimental setup. However, the experimental system provides sufficient results for the verification of the basic concept presented in this thesis.

Parameters of the magnet power supply system are listed below:

- Configuration: a 6-pulse phase-controlled rectifier connected in series with a two-quadrant chopper;
- Input source: 3-phase, 60 Hz, 207.8 V;
- Magnet load: $P_{o,\,rated} = 200$ W, $V_{o,rated} = 25$ V and $\tau_o = 25.6$ ms;
- Load current: 2 A to 10 A; ramp period = 0.1 s;
- Switching frequency (chopper): 5kHz.

The calculation is done in the per unit system. The steady state load current at the flat-top period and the corresponding steady state load voltage are chosen as the base values, that is, $V_{base} = 25$ V and $I_{base} = I_{o,max} = 10$ A. The base value for the power is $S_{base} = V_{base}\, I_{base} = 250$ VA.

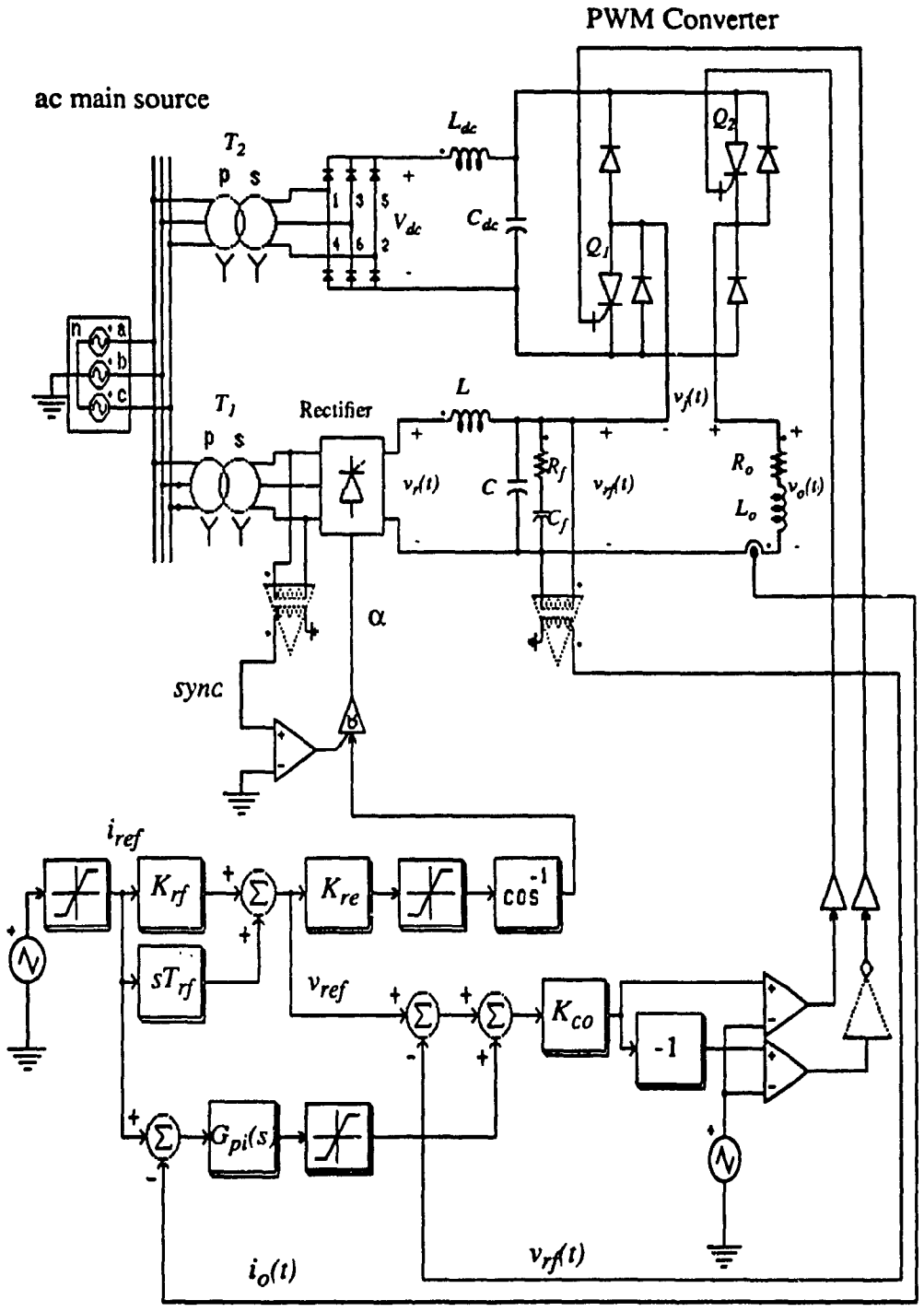

Figure 4.1: Proposed magnet power supply with hybrid structure using series topology.

4.3.1 Power Circuit Design

The power circuit, including the rectifier and the active compensator, is designed to satisfy the system's power requirements. The following parameters can be determined in details by the analysis of the design example in this section:

- Turns ratio of the rectifier input transformer: $a_{T_1} = 8.3$;
- Rectifier passive filter: $L = 8\text{mH}$, $C = 125\mu\text{F}$, $R_f = 5.7\Omega$, $C_f = 900\ \mu\text{F}$;
- Turns ratio of the PWM converter input transformer: $a_{T_2} = 35$;
- Diode filter: $L_{dc} = 8\text{mH}$, $C_{dc} = 900\mu\text{F}$.

4.3.1.1 Rectifier

According to the given system specifications, the load resistance and inductance can first be calculated as:

$$R_o = \frac{V_{o,rated}}{P_{o,rated}} = 2.5\Omega \tag{4.1}$$

and,

$$L_o = \tau_o \cdot R_o = 0.064\,(\text{mH}) \tag{4.2}$$

Based on the known parameters of the load resistance R_o, inductance L_o, and the required load current profile, the maximum voltage required by the load occurs at the top of the current ramp is:

$$V_{o,max} = R_o \times i_o + L_o \times \frac{di_o}{dt}$$

$$= 2.5 \times 10 + 0.064 \times \frac{10-2}{0.1}$$

$$= 30.12\,(\text{V}) = 1.2\text{p.u.} \tag{4.3}$$

If the effect of the rectifier output filter is neglected, $V_{o,max}$ will be the voltage required at the rectifier output, i. e.,

$$V_{rd} = V_{o,max} = 1.2\text{p.u.} \tag{4.4}$$

In order to generate such a voltage, the minimum rectifier input line voltage can be determined as:

$$V_{ll,min} = \frac{V_{rd}}{1.35} = 0.89 \text{ p.u.} \tag{4.5}$$

Considering the voltage drops due to switch commutations and possible source fluctuations, a 10% margin for the line voltage is left; that is, V_{ll} = 1 p.u., or 25 V.

The turns ratio of the rectifier input transformer can be chosen as:

$$a_{T1} = \frac{V_{s,ll}}{V_{ll}} = \frac{207.8}{25} = \frac{8.3}{1} \tag{4.6}$$

The passive filter of the output of the rectifier is designed to have a cut-off frequency of f_c = 160Hz and the system damping ratio of ξ = 0.7. By choosing the capacitor of the passive filter as C = 125 μF, the inductance of this second order filter can be calcu-

lated by using (2.6). Hence, the inductance is given by:

$$L = \frac{1}{(2\times\pi\times f_c)^2\times C} = \frac{1}{(2\times\pi\times 160)^2\times 125\times 10^{-6}} = 8\,(\text{mH}) \tag{4.7}$$

The damping resistance R_f can be calculated by using (2.7):

$$R_f = \frac{1}{2\times\xi}\sqrt{\frac{L}{C}} = \frac{1}{0.7}\sqrt{\frac{8\times 10^{-3}}{125\times 10^{-6}}} = 5.7\,(\Omega) \tag{4.8}$$

The damping capacitor C_f should be sufficiently larger than C, in this design example, C_f is chosen as:

$$C_f = 7.2\times C = 900\,(\mu\text{F}) \tag{4.9}$$

4.3.1.2 PWM Converter

In steady state operation, the PWM converter will compensate for the dominant 360-Hz harmonic. The minimum dc bus voltage should be selected such that the 360-Hz harmonic can be reproduced at the output.

The largest 360-Hz harmonic occurs when the delay angle α equals 90°. At this angle, the harmonic amplitude is calculated by using (2.4):

$$V_{r,\,6peak} = 0.45V_{ll} \tag{4.10}$$

If the rectifier output filter is designed to have a cut-off frequency of 160-Hz and a

system damping ratio of 0.7, at the filter output, the 360-Hz harmonic can be calculated by (2.11):

$$V_{rf,6peak} = V_{r,6peak} \times \left(\frac{\omega_c}{n\omega_s}\right)^2$$

$$= 0.45 \times 0.2 = 0.09 \text{ p.u.} \tag{4.11}$$

To generate such a harmonic voltage at the PWM converter output, without creating any other undesired low-order harmonics, the minimum dc bus required is:

$$V_{dc,min} = V_{rf,6peak} = 0.09 \text{ p.u.} \tag{4.12}$$

This is the minimal dc bus voltage required to cancel only the 360-Hz harmonic. Considering that there exists 720-Hz and other higher-order harmonics, and more importantly, taking into account the fact that the PWM converter should be designed to handle small amounts of dc power during transient operation, a much larger dc bus voltage needs to be selected. By considering the above fact and by running computer simulations, in this design example, an additional 0.23p.u. voltage margin is used. The dc bus voltage is:

$$V_{dc} = V_{dc,min} + 0.23 = 0.32 \text{ p.u.} \tag{4.13}$$

This dc voltage is fed by a diode rectifier through a second order L-C filter. The ac line voltage at the diode bridge input is found to be:

$$V_{ll,diode} = \frac{V_{dc}}{1.35} = 0.24 \text{ p.u.} \tag{4.14}$$

Therefore, the turns ratio of the diode input transformer can be chosen such that:

$$a_{T_2} = \frac{V_{s,ll}}{V_{ll,diode}} = \frac{35}{1} \tag{4.15}$$

If the dc input filter of the PWM converter is chosen to have a resonant frequency of f_c = 60-Hz and a capacitance of C_{dc} = 900 μF, the inductance of this L-C filter can be determined as L_{dc} = 8 mH.

4.3.2 Power Ratings

4.3.2.1 Rectifier Power Rating

Since the rectifier is connected in series with the load, it conducts the full load current. Therefore, the dc current rating of the rectifier is given by:

$$I_{r,rated} = I_{o,max} = 1 \text{ p.u.} \tag{4.16}$$

The dc voltage rating of the rectifier can be calculated based on the 1p.u. ac line voltage, that is:

$$V_{r,rated} = 1.35 V_{ll} = 1.35 \text{p.u.} \tag{4.17}$$

Finally, the dc power rating of the rectifier can be calculated as:

$$S_{r,rated} = V_{r,rated} \cdot I_{r,rated} = 1.35 \text{p.u.} \tag{4.18}$$

4.3.2.2 PWM Converter Power Rating

In the hybrid system structure, the active compensator is directly connected in series with the load. The dc current rating of the active compensator is the same as the load current rating, as well as the current rating of the rectifier; that is:

$$I_{j,\,rated} = I_{o,\,max} = 1\text{p.u.} \tag{4.19}$$

Since the maximum voltage of the PWM chopper is the dc bus voltage, the voltage rating can be selected such as:

$$V_{j,\,rated} = V_{dc} = 0.32\text{p.u.} \tag{4.20}$$

Therefore, the peak power rating of the active compensator, is given by:

$$S_{j,\,rated} = V_{j,\,rated} \cdot I_{j,\,rated} = 0.32\text{p.u.} \tag{4.21}$$

This shows that the power rating of the PWM converter is only 23.7% of that of the rectifier.

It is worthy to note that, since the PWM converter delivers only a small amount of the real power, the ratings for the diode bridge and its input transformer are also small. Therefore, the additional ratings due to the PWM converter are not significant when compared to those of the rectifier system.

4.3.3 Control Design

4.3.3.1 Rectifier Control

Feedforward control, a type of predictive control, is designed for the rectifier and it is based on the load parameters. In this design example, by using (2.14), parameters of the feedforward controller, a PD controller, can be determined as follows.

The gain of the PD controller is given by:

$$K_{rf} = R_o = 2.5 \tag{4.22}$$

The time constant of the PD controller is:

$$T_{rf} = (L_o + L) = (0.064 + 0.008) = 0.072\,(\mathrm{s}) \tag{4.23}$$

The proportional controller K_{re} can be chosen by using (3.3):

$$K_{re} = \frac{1}{K_r} = \frac{1}{1.35 \times 25} = 0.03 \tag{4.24}$$

4.3.3.2 PWM Converter Control

A combined feedforward/feedback control scheme is used to control the PWM converter. The Bode plot of the loop transfer function for the current loop, given in (3.7), is illustrated in Figure 4.2.

As mentioned in the previous chapter, the linear model of the PWM two-quadrant chopper is applicable only in low frequency modulation signals region which is below 1/3

of the switching frequency. To ensure that the PWM converter is modeled as a linear gain, the cut-off frequency of the PWM control loop is designed around 1.67 kHz, which is one-third of the switching frequency (5kHz).

To have a system phase margin of 60 degrees, and a gain-cross-over frequency of 1.67 kHz, the gain and time constant of the PI controller are found to be: K_{pi} =57.9, and T_{pi} = 16.4 ms. Figure 4.2 shows the Bode plot of the system loop transfer function with the designed PI.

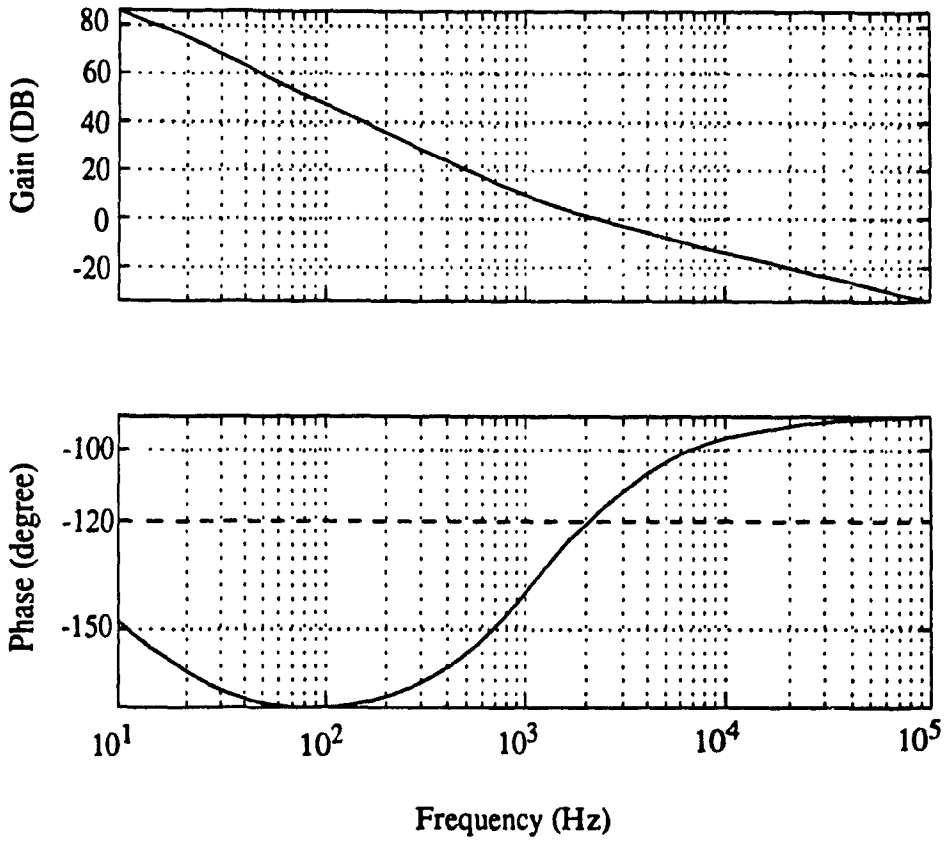

Figure 4.2: Bode plot of the PWM converter current feedback loop.

4.4 Results

To verify the concept, the system designed in the previous section is implemented on a laboratory prototype with the same system parameters.

Experimental results of the complete system, including both the rectifier and the PWM converter, are shown in Figure 4.3.

Figure 4.3 (a) shows the effect of a small PWM converter voltage riding on a large rectifier voltage. By including the PWM converter and the combined voltage/current feedback loop, the current ripples have been greatly reduced. This can be seen more clearly from the steady state waveform shown in Figure 4.3(c). In addition, Figure 4.3(d) also shows that, by using this hybrid structure, the 6^{th} order harmonic has been significantly reduced.

4.5 Summary

In this chapter, a large-power high-performance magnet power supply using series compensation topology has been proposed, designed, and implemented on a laboratory prototype. Experimental waveforms prove that the rectifier voltage harmonics and deviations are compensated by a high-frequency PWM converter. It also shows that, by using the hybrid structure, the large power rating, low current ripple and the fast response can be achieved simultaneously. Moreover, the proposed control scheme achieved that the main power is provided by the rectifier and only a small portion of output power is provided by the PWM converter for error compensation. Overall, excellent load current regulation is given by the proposed magnet power supply with the series topology.

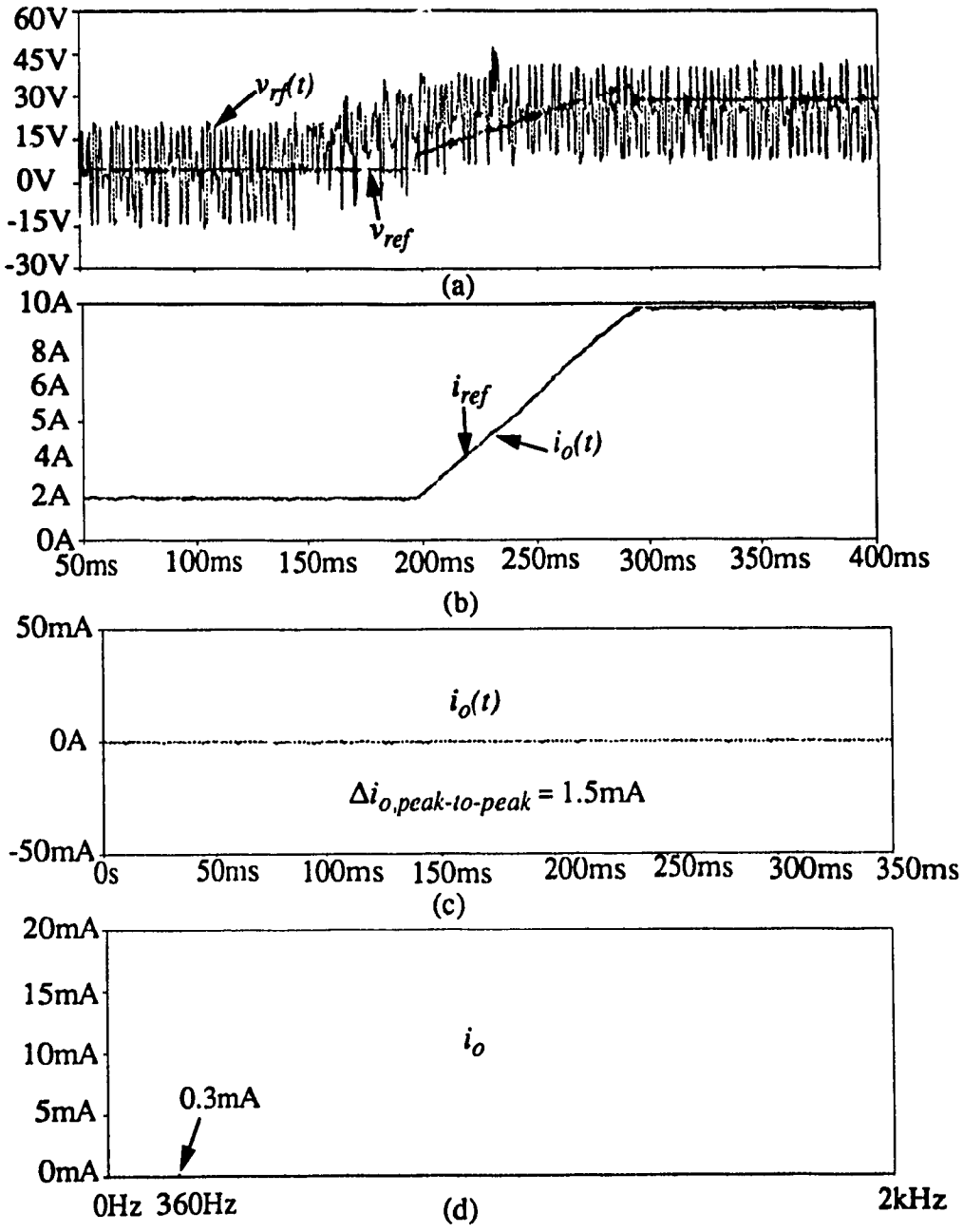

Figure 4.3: Experimental results. (a) Load voltage and voltage reference; (b) Load current and current reference; (c) Expanded load current at 2A; (d) Harmonic spectrum of the load current at 2A.

Chapter 5

Shunt Topology - Principle

5.1 Introduction

In the previous chapter, the operating principle of a magnet power supply system based on the series topology was discussed. Experimental results proved that excellent current regulation can be achieved by using the hybrid structure with the series topology. However, one of the disadvantages is that the high-frequency switches have to conduct the full load current (large current). In addition, in other types of applications such as HVDC stations, series topology may be impractical because of its infeasibility due to the factors such as cost, unreliability and difficult fault protection [20].

In this chapter, the shunt topology proposed in Section 1.3, Chapter 1, is discussed. The principle of harmonics cancellation by means of a shunt topology is explained through the equivalent circuit concept. The power circuit configuration, including the rectifier and the PWM converter, is described. System components and their basic functions are explained. A simple control scheme which achieves the desired power sharing for the hybrid structure, both in steady state and transient periods, is also proposed. Harmonics and current errors are compensated by the active compensator with high-frequency

switchmode PWM converters. Furthermore, the power rating of this active compensator is only a fraction of the overall rating and high-frequency switches only conduct small ripple currents.

5.2 Principle of Harmonic Cancellation

To explain the basic concept of harmonic cancellation of the proposed magnet power supply system, the power circuit is presented in Figure 5.1 (a), and the equivalent circuit is drawn in Figure 5.1 (b).

In Figure 5.1, V_{rd} and $v_{rn}(t)$ are the equivalent dc and harmonic voltage components at the rectifier output, L_s is the smoothing reactor, $i_j(t)$ is the harmonic current injected by the active compensator, and R_o and L_o represent the magnet load.

Based on the KCL at node 1, the load current $i_o(t)$ is given by:

$$i_o(t) = i_r(t) + i_j(t) = i_{rn}(t) + I_{rd} + i_j(t) \tag{5.1}$$

From the principle of superposition, the harmonic current due to the voltage harmonic $v_{rn}(t)$ is expressed as:

$$i_{rn}(t) = \frac{v_{rn}(t)}{R_o + j \cdot 2\pi n f_s (L_o + L_s)} \tag{5.2}$$

If a current $i_j(t)$ is controlled such that it equals the harmonic current generated by the rectifier, e.g. $i_j(t) = - i_{rn}(t)$, then the harmonic current produced by the rectifier can theoretically be completely cancelled. Moreover, any errors due to ac unbalances and load parameter variances can also be compensated by the compensator.

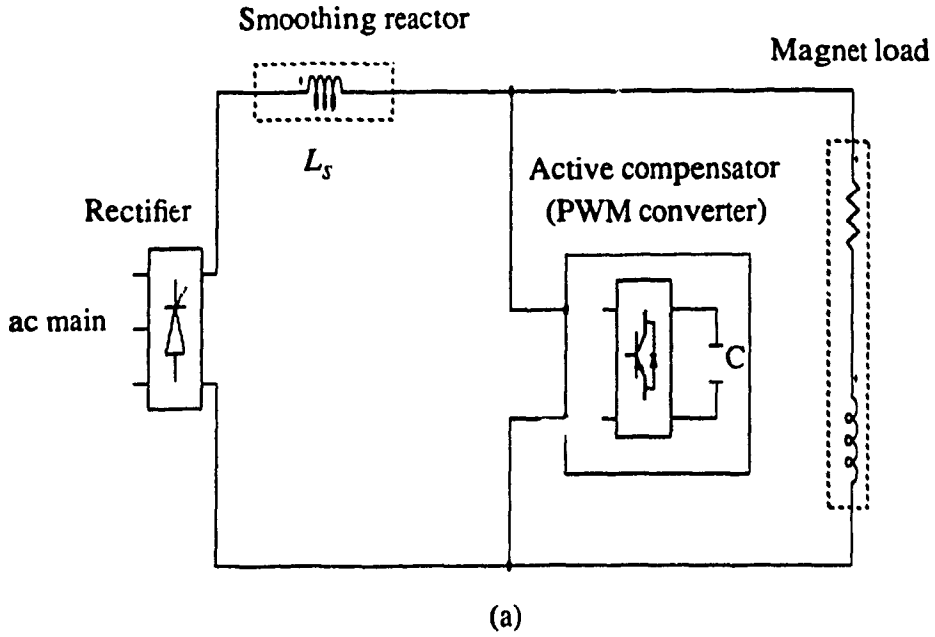

(a)

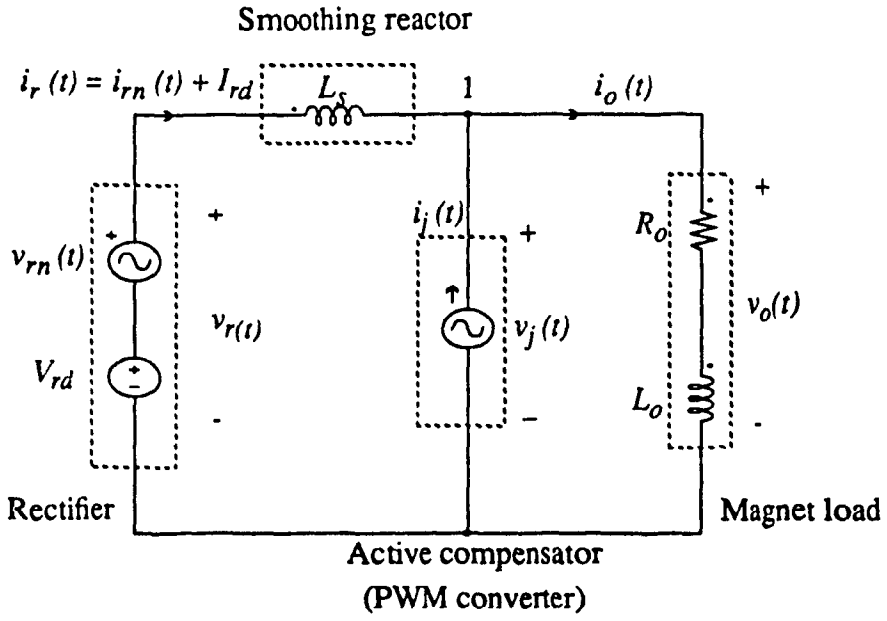

(b)

Figure 5.1: Shunt topology. (a) Power circuit; (b) Equivalent circuit.

5.3 System Configuration

In this section, the power circuit configuration with a hybrid structure is proposed as is shown in Figure 5.2. It consists of a phase-controlled rectifier and a single phase bridge PWM inverter. In this hybrid structure, the rectifier is designed to handle the bulk of the output power, whereas the PWM bridge inverter is only used for harmonic cancellation and current error compensation under transient operation. In the following sections, the power circuit structures of the rectifier and the PWM converter are described.

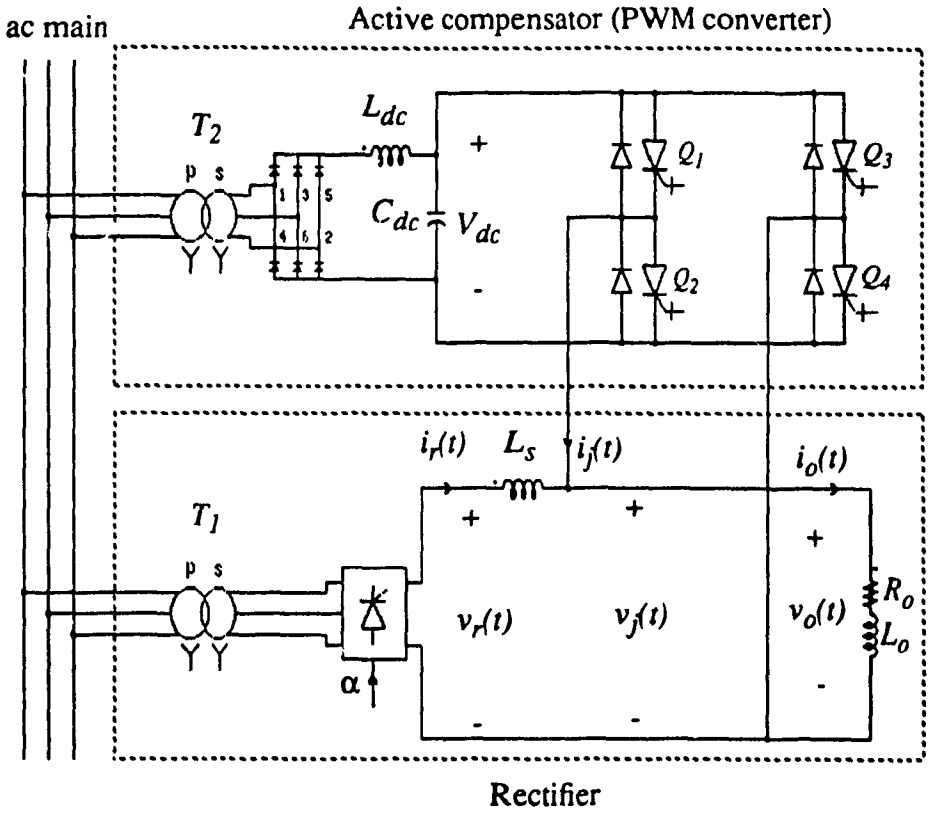

Figure 5.2: Proposed power circuit configuration.

5.3.1 Rectifier Power Circuit

The rectifier power circuit consists of a six-pulse phase-controlled rectifier and a smoothing reactor which acts as a first-order low pass filter. In this configuration, the smoothing reactor plays an important role for the following reasons:

1) Without this smoothing reactor, there is a conflict in the control of the load voltage, since the phase-controlled rectifier and the active compensator are both of the voltage type devices.

2) The smoothing reactor absorbs or attenuates the harmonic current at the rectifier output, thereby reducing the current rating of the active compensator.

In the series topology, the rectifier output filter is optional. In the shunt topology, however, the smoothing inductor is essential for the system operation.

The size of the smoothing reactor will affect the power rating of the PWM compensator. In steady state operation, only harmonic current passes through the PWM compensator. The larger the smoothing reactor, the smaller the compensator, thus the more bulky and expensive the passive filter. There is, therefore, a trade-off between the size of the smoothing inductor and the rating of the compensator. The selection of the smoothing inductor value is discussed in more details in Chapter 6.

5.3.2 PWM Converter Power Circuit

In the proposed magnet power supply system shown in Figure 5.2, the PWM converter is directly connected in parallel with the magnet load. The output voltage of the converter equals the load voltage. The dc bus voltage of the PWM converter is supplied by a 3-phase bridge diode rectifier through a second order low-pass filter. The diode rectifier

is fed from the ac main through an isolation transformer.

The direction of the compensator output voltage may vary from positive to negative, if a complete repeat current cycle is considered, as is shown in Figure 1.1. This means that during the energy recovery period, which corresponds to the current ramp-down stage, the load voltage, as well as the output voltage of the converter, may become negative. This can be shown in (5.3):

$$v_j(t) = R_o \cdot i_o(t) + L_o \cdot \frac{di_o(t)}{dt} \tag{5.3}$$

Equation (5.3) shows that $v_j(t)$ may become negative during the ramp-down period because of the large load inductance and the large falling slope $(di_o(t)/dt)$.

In addition, since the PWM converter is designed to compensate for the harmonics and current errors, the current passing through the active compensator is bidirectional. Thus, a full bridge PWM current-controlled voltage source inverter is chosen as an active compensator in the shunt compensation topology.

In this structure, the current of the PWM inverter is controlled by using a PWM technique operating in a high switching frequency. The objective of the PWM inverter is to eliminate low frequency current harmonics at the rectifier output. The gating signal method used for the PWM inverter is triangular-carrier-wave modulation. And the PWM scheme uses unipolar pulse-width modulation.

5.4 Control Scheme

Figure 5.3 shows the diagram of the control scheme for the proposed shunt struc-

ture. There are two control schemes: one for the rectifier and the other for the PWM converter.

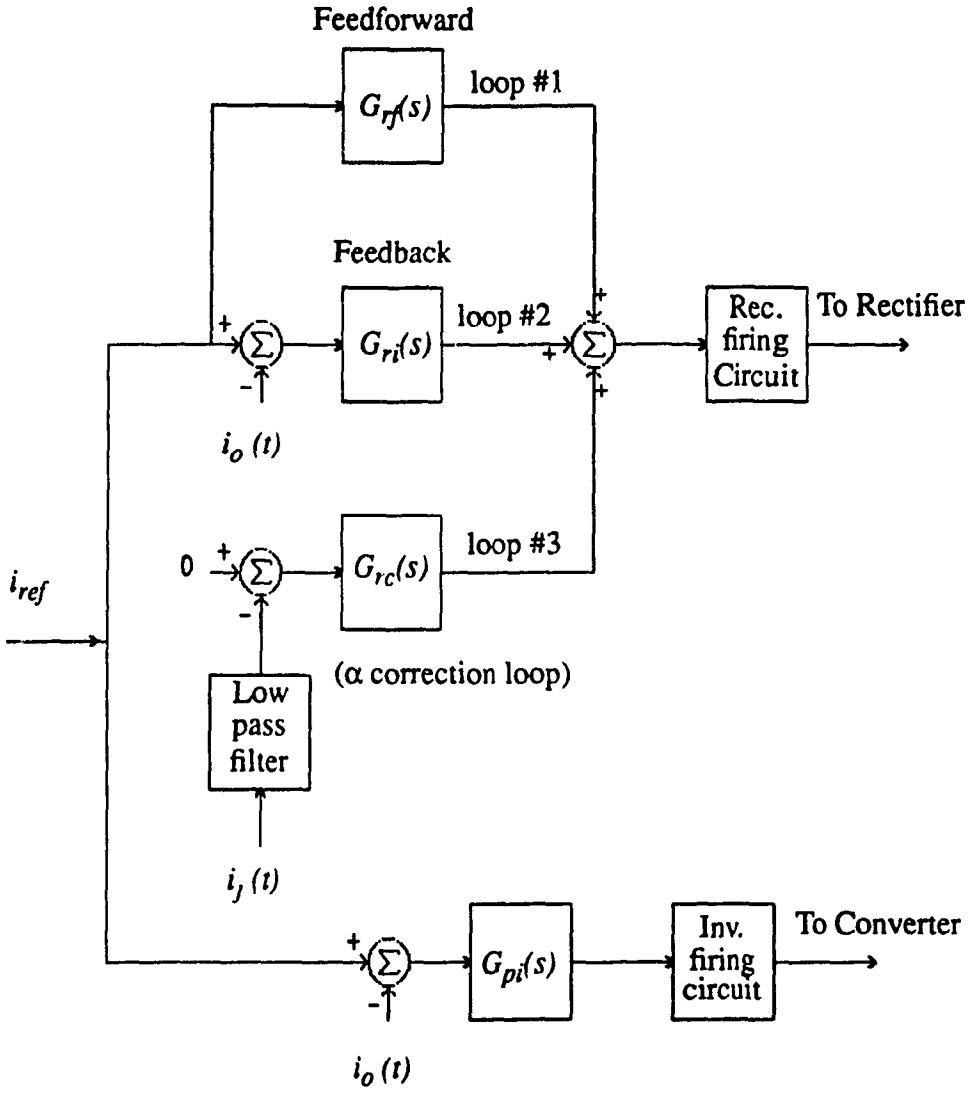

Figure 5.3: Block diagram of the proposed control scheme.

5.4.1 Rectifier Control

A major feature of the hybrid structure is the power sharing between the phase-controlled rectifier and the PWM converter during the ramp operation. This is due to the special load current requirement from the application (shown in Figure 1.1). The PWM converter tends to supply a fair portion of the current change during ramp operation, due to the large difference in the response speeds of the rectifier and the PWM converter. This problem can be solved by ensuring that the rectifier is forced to supply all of the load current in the steady state, and to provide a fair portion of the load current change during ramp operation. This can be done by using the control approach shown in Figure 5.4, with multiple loops: (a) a feedforward loop (loop #1); (b) current feedback loop (loop #2); and (c) an α correction loop (loop #3).

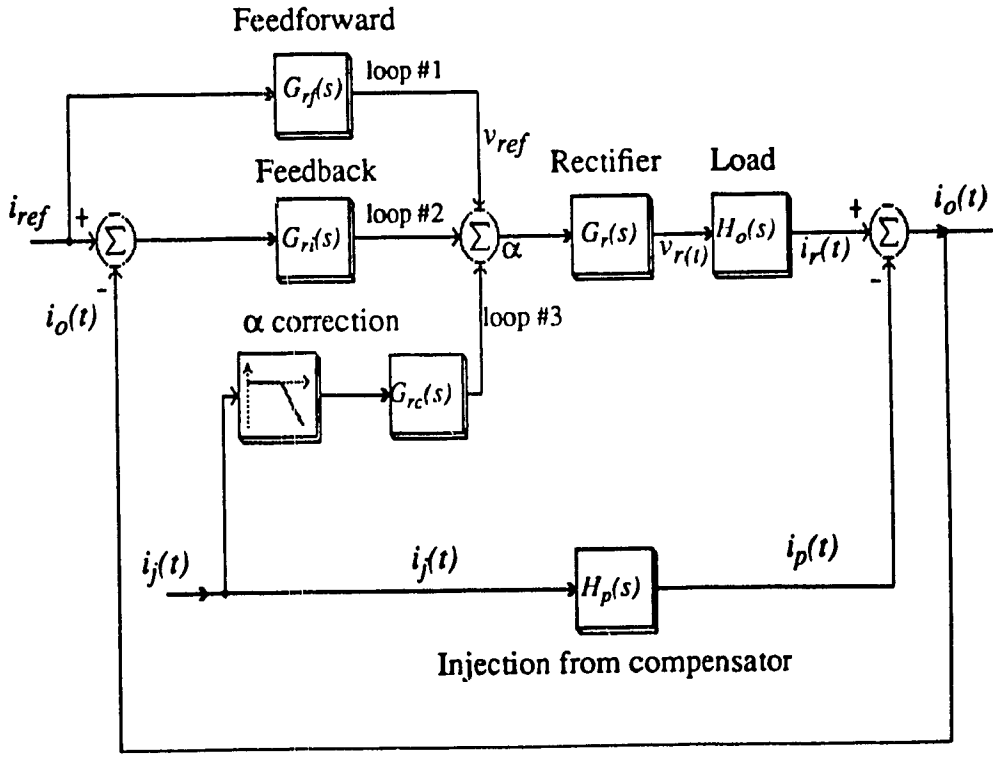

Figure 5.4: Small-signal block diagram of the rectifier control scheme.

In Figure 5.4, $G_{rf}(s)$ and $G_{ri}(s)$ are the rectifier feedforward and feedback controllers, $G_r(s)$ is the modeling of the rectifier, $H_o(s)$ is the load transfer function including a smoothing inductor, and $H_p(s)$ is the injected distortion from the PWM inverter.

5.4.1.1 Feedforward/Feedback Control

The feedforward loop sets instantaneously a pre-calculated value of α satisfying the load current requirement. According to the current profile and the load parameters, the desired rectifier output voltage can be calculated as:

$$v_{ref}(t) = R_o \times i_{ref}(t) + (L_o + L_s) \times \frac{di_{ref}(t)}{dt} \tag{5.4}$$

Similar to series topology, shunt topology demonstrates only the system performance from the flat bottom and the ramping slope to the flat top. The current profile is shown in Figure 2.5 (a). Knowing the desired rectifier output voltage as shown in Equation (5.4), the delay angle of the phase-controlled rectifier can be pre-calculated exactly such that the output voltage follows the reference given in (5.4). This is implemented as the feedforward controller $G_{rf}(s)$ shown in Figure 5.4 (loop #1). This loop enhances the dynamic response and there is no delay as exists when using only a feedback loop.

The experimental waveforms presented in Figure 2.7, Chapter 2, show that with the rectifier alone, which only uses feedforward control, the load current closely tracks the current reference. However, there is a steady state error in the flat bottom and flat top, because the feedforward control is an open loop control. This error becomes larger if system characteristics such as input voltage or load parameters change. By using only feedforward control, the PWM converter needs to provide additional dc power in order to

compensate for this steady state error during steady state operation. Therefore, the feedback loop (Figure 5.4, loop #2) needs to be included in the rectifier control loop and will compensate for the small discrepancies introduced by load parameter deviations and input voltage fluctuations. For this purpose, the main control loop for the rectifier is a combined feedforward/feedback controller (Figure 5.4, loop #1 and loop #2).

5.4.1.2 α Correction Loop

A α correction loop is introduced (loop #3, Figure 5.4) to the rectifier control system for the following reasons:

- to ensure that the PWM inverter supplies only the ripple current required for harmonic cancellation and no dc current under steady state operating conditions; and

- to ensure that the dc current of the PWM inverter is minimal, as required to compensate for the current error during transient operation.

This is done by transferring part of transient current from the PWM converter to the rectifier by correcting the rectifier firing angle. To avoid having the rectifier loop overproduce additional power which is required during the ramp, the α correction loop (loop #3, Figure 5.4) has to be designed slower than the combined feedforward/feedback loop (loop #1 and loop #2, Figure 5.4).

5.4.2 PWM Converter Control

A current feedback loop is used to control the PWM converter. The objective of this loop is to cancel harmonics and offsets between the load current and the current reference. A PI controller is used in this loop.

Since PWM control loop is operated in high frequency ranges, the effect of the rectifier loop can be ignored when this loop is designed. The PWM inverter is modeled by a linear block with a constant gain, K_j. A small-signal block diagram of the PWM converter feedback loop is shown in Figure 5.5 and the loop transfer function is given by:

$$G_{pl}(s) = G_{pi}(s) \times K_j \times \frac{1}{R_c + sL_o} \tag{5.5}$$

The current regulator $G_{pi}(s)$, which uses a PI controller, can, therefore, be designed using the frequency domain approach and conventional design techniques.

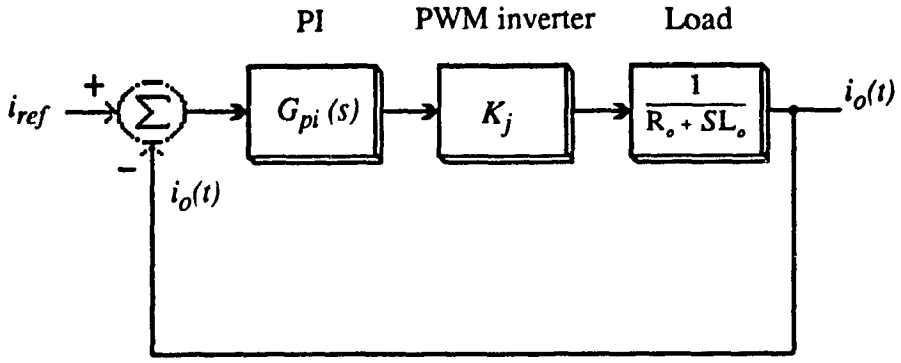

Figure 5.5: Small-signal block of the inverter current feedback loop.

5.5 Summary

In this chapter, a multi-converter system with appropriate control loops for large-power high-performance magnet power supplies, featuring fast transient response and low harmonic currents, has been presented. It uses a combined feedforward/feedback loop to

control the rectifier and to generate the desired output profile. Moreover, an α correction loop is designed to minimize the dc current of the inverter during transient operation by adjustment of the rectifier delay angle. The PWM converter operates only as a compensator for harmonic cancellations and error compensations, and is controlled by using a current feedback loop. The power rating is, therefore, only a fraction of that of the rectifier. This will be verified in the next chapter through theoretical calculations and experimental results.

Chapter 6

Shunt Topology - Design and Implementation

6.1 Introduction

Studies in the previous chapter provide basic information for designing magnet power supply systems using shunt topologies. The purpose of this chapter is to apply this information to design the proposed magnet power supply system.

To illustrate the design procedures, a design example is given and is implemented on a laboratory prototype. Based on the requirements and specifications given for the system, the magnet power supply system, including the power and control circuits, is designed by following the design procedures.

The power ratings of the rectifier and the active compensator are calculated. In addition, the relationship between the smoothing reactor and the active compensator is discussed in this chapter and the smoothing reactor is designed. Experimental results are also presented for verification of the theoretical concept.

6.2 Design Procedures

To design a magnet power supply system with a shunt topology, and given the input ac source, the components and parameters of the system, and the system requirements, the following parameters can be determined:

1) **In the power circuit**: the turns ratio of the transformers, passive filter parameters, parameters and power ratings of the rectifier and the active compensator,

2) **In the control circuit**: parameters of the rectifier and the active compensator control loops.

In order to determine the above parameters, the system design procedures consist of the following steps:

1. Design the rectifier output passive filter.

2. Determine the current, voltage and power ratings of the rectifier.

3. Determine the current, voltage and power ratings of the PWM converter.

4. Design the dc input filter of the PWM converter.

5. Design the rectifier feedforward and feedback loop.

6. Design the rectifier α correction loop.

7. Design the PWM inverter's current feedback loop.

A design example illustrating each step of the design procedure is given in the following sections.

6.3 Design Example

A design example is presented in the following description to illustrate the design procedures. The system schematic circuit, including power and control circuits, is shown in Figure 6.1.

Similar to the series topology, the stringent requirements of the bending magnet power supply may not be achieved on the experimental setup, due to limitations of the laboratory equipment and devices. However, this experimental system provides sufficient results for verification of the basic concept presented in this thesis.

To validate the proposed structure, a 1kVA laboratory prototype having the following parameters, is used:

- Configuration: a 6-pulse phase-controlled rectifier connected in parallel with a signal phase PWM inverter through a smoothing reactor;
- Input source: 3-phase, 60 Hz, 207.8 V;
- Magnet load: $P_{o,\,rated}$ = 200 W, $V_{o,rated}$ = 25 V and τ_o = 25.6 ms;
- Load current: 2 A to 10 A; ramp period = 0.1 s;
- Switching frequency (chopper): 5kHz.

Calculation of the power circuit parameters of the rectifier and PWM inverter are done on a per unit basis. The base values are V_{base} = 25 V, I_{base} = 10 A and S_{base} = 250 VA.

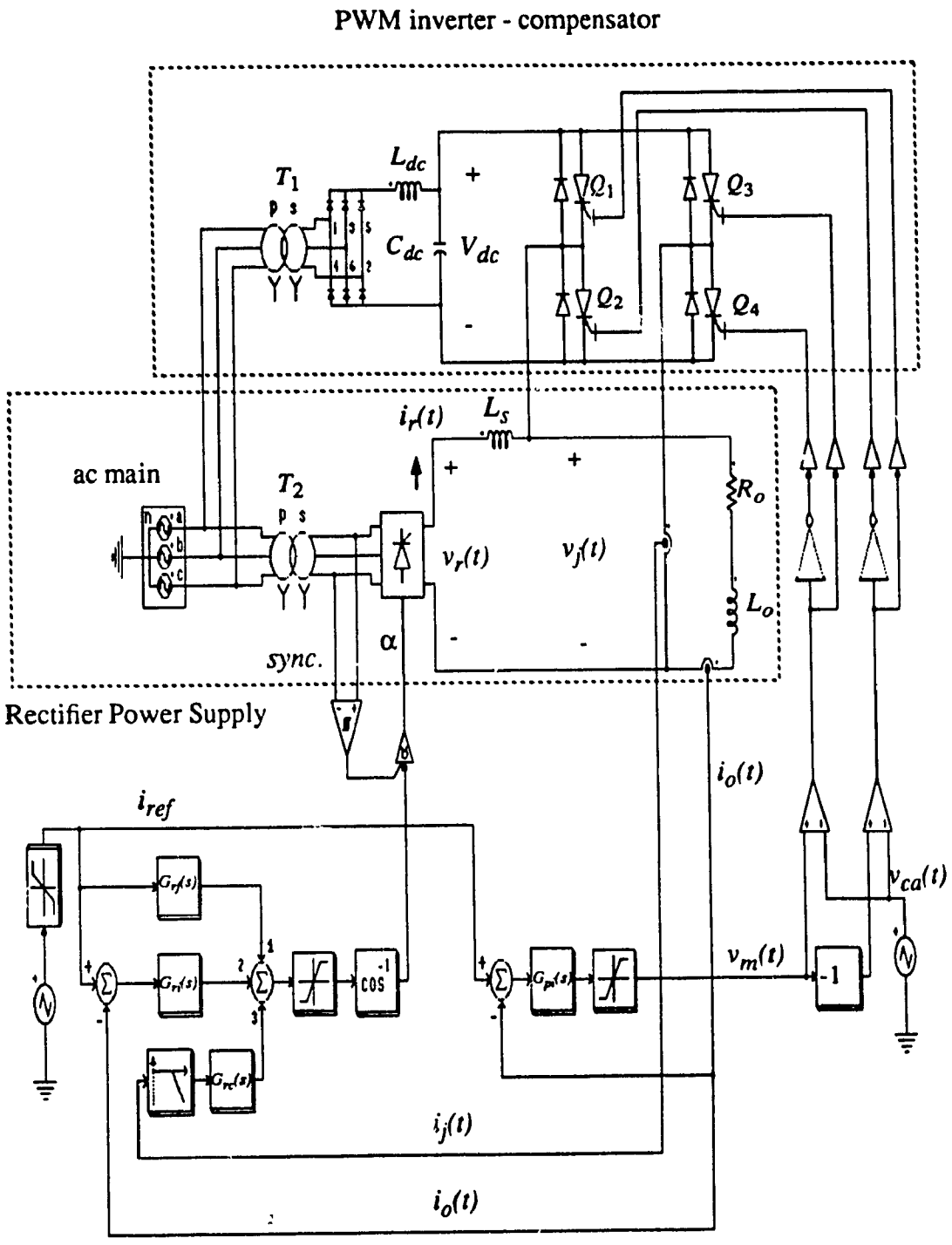

Figure 6.1: Proposed magnet power supply using shunt topology.

6.3.1 Power Circuits Design

6.3.1.1 Smoothing Reactor

The size of the smoothing reactor will affect the costs and transient response of the designed system. In the steady state, the larger the smoothing reactor, the smaller the current rating of the PWM inverter, and the more bulky and expensive the passive filter. During transient operation, the larger the smoothing reactor, the larger the current rating of the compensator, since slow rectifier system response due to the smoothing reactor demands that the PWM inverter provides more of the load current. However, this fact can be ignored as long as the rectifier output voltage is large enough to compensate for the voltage drop caused by the increasing of the smoothing reactor.

In this chapter, the smoothing reactor is designed based on steady state operating conditions under the above assumption. In addition, the load current is also assumed to be ripple free, which means that all of harmonics produced by the rectifier are compensated by the PWM inverter. The harmonic equivalent circuit can be drawn in Figure 6.2.

Figure 6.2 also shows that the rectifier harmonic current, $i_{rn}(t)$, as well as the current of the compensator, $i_j(t)$, can be calculated as:

$$i_{rn}(t) = \frac{v_{rn}(t)}{j\omega_n L_s} = \frac{v_{rn}(t)}{X_{sn}} = i_{sn}(t) = i_{jn}(t) \qquad (6.1)$$

where n is the n^{th} order harmonic, $\omega_n = 2\pi n f_s$, $i_{rn}(t)$ is the harmonic current produced by the rectifier, $v_{rn}(t)$ is the harmonic voltage at the rectifier output, $i_{sn}(t)$ is the harmonic current of the smoothing inductor, and $i_{jn}(t)$ is the injected harmonic current by the PWM inverter.

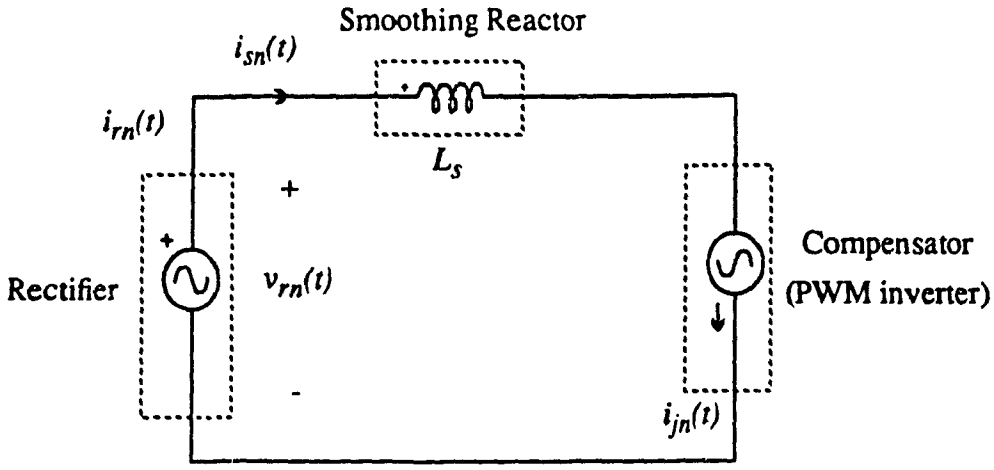

Figure 6.2: Equivalent power circuit for harmonic calculation.

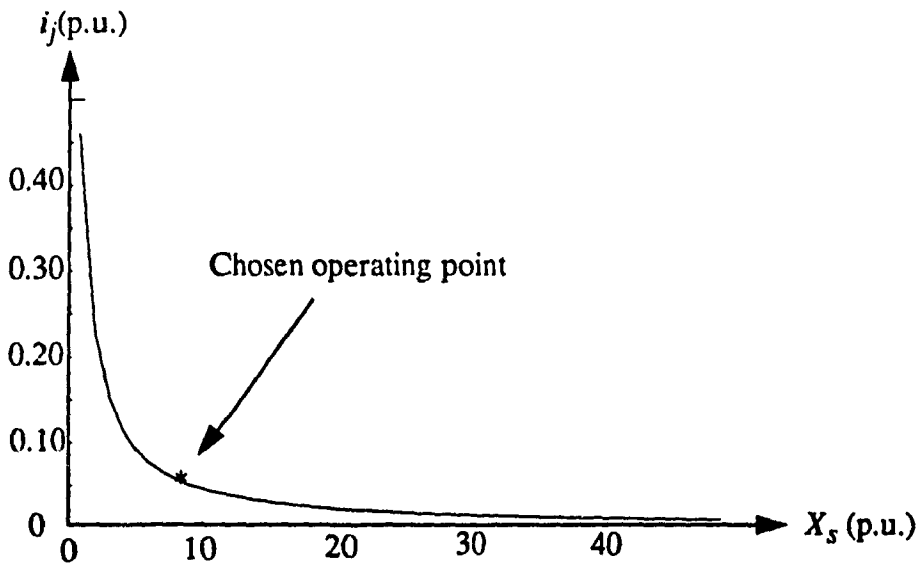

Figure 6.3: Harmonic current of the active compensator vs. impedance of the smoothing inductor ("*" is the selected operating point).

The smoothing inductance can be chosen by using (6.1) which is illustrated in Figure 6.3. In this design example, by choosing the operation point "*", as shown in Figure 6.3, the smoothing reactor can be chosen as L_s = 10 mH.

6.3.1.2 Rectifier

The rectifier is designed for the total load power requirement. Under steady state operation and rated current, the required voltage is defined as V_{ro} = 1 p.u.. During the ramping operation, the voltage across the load has to be boosted to meet the tracking requirements. If the ramp period is defined as 0.1s, the voltage across the magnet inductor during the ramp, Δv_{lo}, can be calculated as:

$$\Delta v_{lo} = L_o \times \frac{di_o}{dt} = 0.064 \times \frac{10-2}{0.1} = 0.2\text{p.u.} \tag{6.2}$$

A 10-mH smoothing inductor L_s, during the ramp, will also contribute to the voltage boost requirement. The new voltage required for the ramp can be calculated as:

$$\Delta v_l = (L_o + L_s) \times \frac{di_o}{dt} = (0.01 + 0.064) \times \frac{10-2}{0.1} = 0.23\text{p.u.} \tag{6.3}$$

The maximum voltage required by the load is found at the top of the current ramp and can be calculated as:

$$V_{r,max} = V_{rc} + \Delta v_l = 1.23\text{p.u.} \tag{6.4}$$

Considering the voltage drops due to the switches and possible source voltage fluctuations, a 10% voltage margin for the rectifier output voltage is used, that is:

$$V_{r,max} = 1.1 \times 1.23 = 1.36\text{p.u.} \tag{6.5}$$

In order to generate such a voltage in Equation (6.20), the minimum rectifier input line voltage should be:

$$V_{ll} = \frac{V_{r,max}}{1.35} = 1\text{p.u.} \tag{6.6}$$

The turn ratio of the rectifier input transformer T_1 is given by:

$$a_{T1} = \frac{V_{s,ll}}{V_{ll}} = \frac{207.8}{25} = 8.3 \tag{6.7}$$

6.3.1.3 PWM Converter

Because the compensator is connected in parallel with the magnet load, the maximum dc bus voltage of the PWM inverter is chosen such that it equals the maximum voltage of the magnet load. Therefore:

$$V_{dc} = V_{j,rated} = \Delta v_{lo} + V_{ro} = 1.2\text{p.u.} \tag{6.8}$$

The minimum input line voltage of the diode rectifier can be calculated as:

$$V_{diode,ll} = \frac{V_{dc}}{1.35} = 0.89\text{p.u.} \tag{6.9}$$

Then, the turns ratio of the diode input transformer T_2 is given by:

$$a_{T_2} = \frac{v_{s,ll}}{v_{diode,ll}} = 9.33 \tag{6.10}$$

6.3.2 Power Ratings of the Rectifier and the Compensator

6.3.2.1 Rectifier Power Rating

Since the rectifier supplies the main power to the load, the maximum current passing through the rectifier is the maximum load current required, that is:

$$I_{r,rated} = I_{o,rated} = 1\text{p.u.} \tag{6.11}$$

The power rating is defined as:

$$S_{rated} = V_{rated} \times I_{rated} \tag{6.12}$$

The voltage rating of the rectifier is chosen as its maximum output voltage, that is:

$$V_{r,rated} = V_{r,max} = 1.36\text{p.u.} \tag{6.13}$$

Then, the power rating for the rectifier can be calculated as:

$$S_{r,rated} = V_{r,rated} \cdot I_{r,rated} = 1.36\text{p.u.} \tag{6.14}$$

6.3.2.2 PWM Converter Power Rating

In steady state operation, the PWM converter will essentially compensate for the dominant 360-Hz harmonic. The largest 360-Hz harmonic occurs when the delay angle α equals 90^{o}. At this angle, the harmonic amplitude is calculated as:

$$V_{r,\,6peak} = 0.46V_{ll} = 0.46 \times 1\text{p.u.} = 0.46\text{p.u.} \tag{6.15}$$

The dominant 360 Hz harmonic current which passes through the PWM inverter can be calculated as:

$$I_{j,\,6} = \frac{V_{r,\,6peak}}{X_{s,\,6}} = \frac{0.46\text{p.u.}}{9.05\text{p.u.}} = 0.05\text{p.u.} \tag{6.16}$$

with,

$$X_{s,\,6} = \frac{6\omega_s L_s}{Z_{base}} = 9.05\text{p.u.} \tag{6.17}$$

The above calculation is based on the following assumptions:

1) All of the harmonic currents generated by the phase-controlled rectifier are compensated by the PWM inverter; and

2) The rectifier output contains a 10-mH smoothing reactor.

Taking into account the existence of higher order harmonics and the requirement to provide a small amount of dc power during transient operation, in this design example, an additional 0.1p.u. current margin is used. The current rating of the PWM inverter is chosen

as $I_{j,rated} = 0.1 + I_{j,6} = 0.15$ p.u.. This can be obtained by running simulations and can also be verified from experimental results shown in Figure 6.9 (a). Under different operating conditions, the maximum current supplied by the PWM converter is about 0.1 p.u. during the ramp operation, this value depends on the design of the rectifier control loops and the response time of the rectifier and the PWM converter.

The voltage rating of the PWM converter is chosen the same as the load voltage rating as well as the dc bus voltage of the converter, that is:

$$V_{j,rated} = V_{dc} = 1.2\text{p.u} \tag{6.18}$$

Hence, the power rating of the PWM converter is given by:

$$S_{j,rated} = V_{j,rated} \cdot I_{j,rated} = 0.18\text{p.u.} \tag{6.19}$$

This result shows that the power rating of the PWM converter is only 13% of that of the rectifier.

6.3.3 Relationship of the Passive Filter and the Compensator

The previous discussion shows that the power rating of the PWM converter depends on the ramping period (di_o/dt), the time constant (τ_o) of the magnet load, and the smoothing inductor (L_s). The relationship between these quantities is examined below.

Equations (6.20) and (6.20) show that the larger the magnet inductor or the larger the current ramp rate, the higher the voltage rating the rectifier and the compensator. This is further illustrated in Figure 6.4. Figure 6.4 (a) shows that during the current ramp

period, the required load voltage is directly proportional to the load inductance and the current ramp rate. As a result, the PWM converter voltage, $v_j(t)$, increases linearly, as is shown in Figure 6.4 (b).

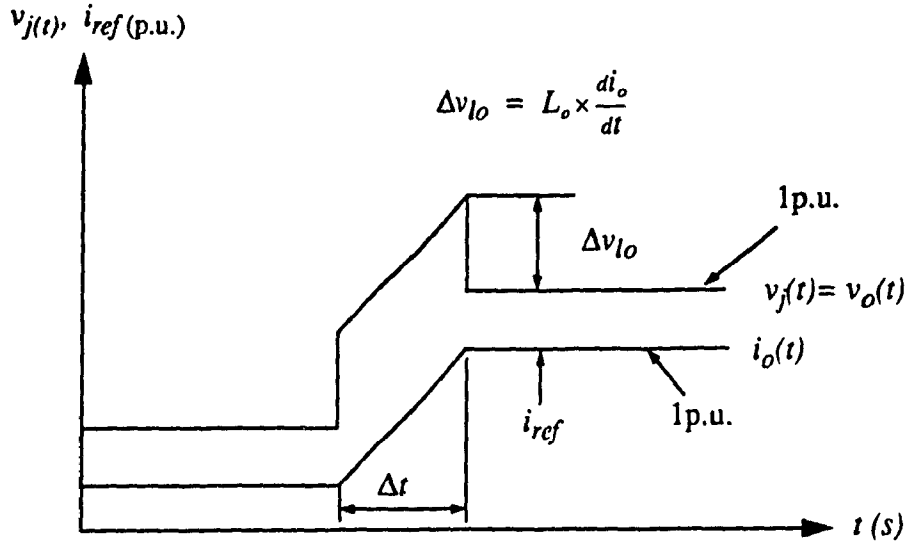

(a)

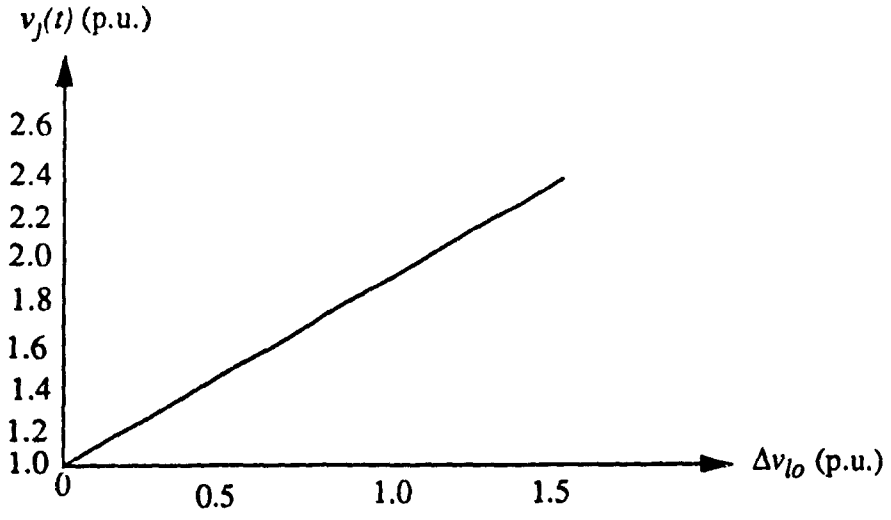

(b)

Figure 6.4: Peak voltage rating of the PWM converter.

The relationship between the current rating of the compensator and the size of the passive filter is investigated under steady state operation conditions using (6.1) which is illustrated in Figure 6.3.

The above presentations show that the voltage rating of the compensator is determined by the load and the required current profile. The current rating of the compensator on the other hand, is dictated by the passive filter (smoothing inductor). In other words, once the system specifications are given, the voltage rating of the compensator is fixed. Therefore, the power rating of the compensator depends mainly only on its current rating.

Figure 6.3 also reflects the active filter portion of the compensator power rating versus the size of the passive filter. Hence, the smoothing reactor can be chosen such that the costs of the passive filter and the PWM inverter are minimum.

6.3.4 Control Circuit Design

6.3.4.1 Rectifier Control

Rectifier control contains three parts as shown in Figure 5.3: 1) feedforward control; 2) current feedback control; 3) α correction loop.

6.3.4.1.1 Feedforward/Feedback Control

As discussed in the previous chapter, a combined feedforward and feedback control is mainly used to control the rectifier. A PD controller is implemented in the feedforward control loop and a PI controller is implemented in the feedback control loop.

Ignoring the effect of the α correction loop and the $i_p(t)$, the rectifier feedback/ feedforward loop is designed based on the small-signal block diagram shown in Figure

6.5. This can be simplified as Figure 6.6.

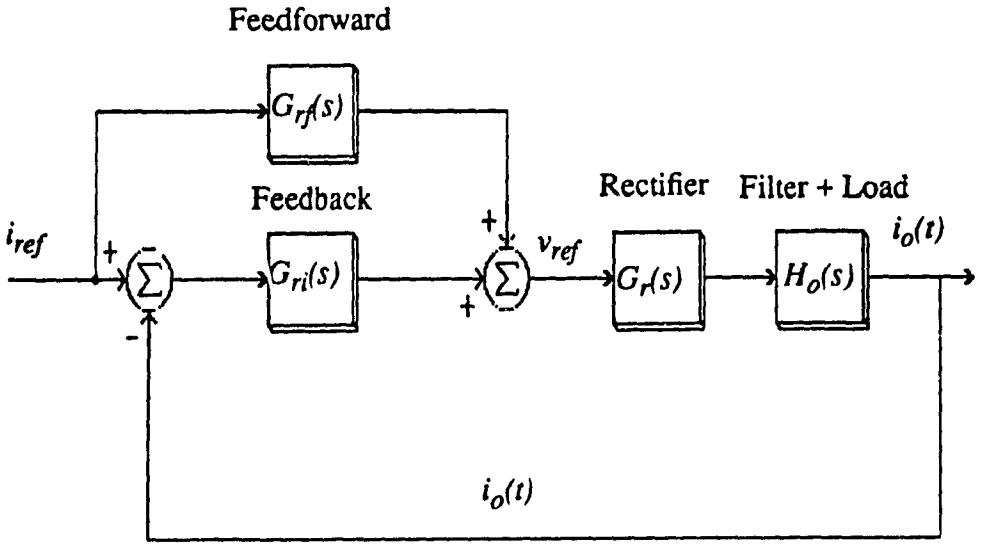

Figure 6.5: Simplified small-signal block diagram of Figure 5.4.

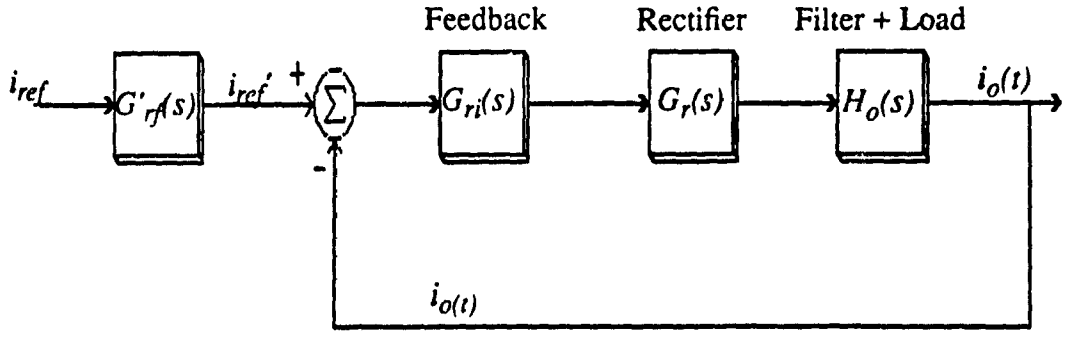

Figure 6.6: Simplified block diagram of the phase-controlled rectifier of Figure 6.5.

Thus, the closed-loop transfer function of the rectifier loop is given by:

$$\frac{i_o(s)}{i_{ref}} = \frac{G_{ri}(s) \times G_r(s) \times H_o(s)}{1 + G_{ri}(s) \times G_r(s) \times H_o(s)} \cdot G'_{rf}(s) \tag{6.20}$$

$$G'_{rf}(s) = \frac{G_{ri}(s) + G_{rf}(s)}{G_{ri}(s)} \tag{6.21}$$

If the feedforward controller is designed to compensate for the rectifier (including passive filter) and the magnet load, that is:

$$G_{rf}(s) = \frac{1}{G_r(s) \times H_o(s)} \tag{6.22}$$

Substitute (6.21) into (6.20), yields:

$$\frac{i_o(s)}{i_{ref}} = \frac{1 + G_{ri}(s) \times G_r(s) \times H_o(s)}{G_{ri}(s) \times G_r(s) \times H_o(s)} \times \frac{G_{ri}(s) \times G_r(s) \times H_o(s)}{1 + G_{ri}(s) \times G_r(s) \times H_o(s)}$$

$$= 1 \tag{6.23}$$

Therefore:

$$i_o(t) = i_{ref} \tag{6.24}$$

This means that, in theory, the load current can exactly follow the current reference by operating the rectifier alone with the combined feedback/feedforward control. However, in practice, it is not easy to implement a feedforward controller to complete compensate for the rectifier and load by using (6.22) due to the nonlinear effect of the rectifier. The

implementation on the laboratory prototype in this thesis is done by using the approximation formula as is shown in (6.25):

$$G_{rf}(s) = \frac{1}{K_r \cdot H_o(s)} \tag{6.25}$$

where,

$$G_r(s) = K_r e^{-sT_d} \tag{6.26}$$

$$H_o(s) = \frac{1}{R_o + s(L_o + L_s)} \tag{6.27}$$

$$H_p(s) = \frac{sL_s}{R_o + s(L_o + L_s)} \tag{6.28}$$

$$G_{ri}(s) = K_{ri} \times \frac{sT_{ri} + 1}{sT_{ri}} \tag{6.29}$$

Based on the above discussion, by using (6.25), the gain and the time constant of the feedforward controller are given by:

$$K_{rf} = \frac{R_o}{K_r} = \frac{2.5}{1.35 \times 25} = 0.074 \tag{6.30}$$

$$T_{rf} = \frac{L_s + L_o}{K_r} = \frac{0.074}{1.35 \times 25} = 2.19 \times 10^{-3}(s) \tag{6.31}$$

To design the rectifier current feedback loop shown in the Figure 6.6, the loop

transfer function of the rectifier system can be expressed as:

$$G_{rl}(s) = G_{ri}(s) \times G_r(s) \times H_o(s) \tag{6.32}$$

In order to obtain the optimum damping of the loop, the time constant of the PI controller $G_{ri}(s)$ can be chosen by using a "symmetrical optimum" method [28], yields:

$$T_{ri} = 2T_d(1+2\xi)^2 = 0.016\,(s) \tag{6.33}$$

where the damping ratio ξ of the system is chosen as 0.707. To obtain the system phase margin around 60 degrees, the gain of the PI controller can be chosen by using the conventional Bode plot approach which is shown in Figure 6.7, that is:

$$K_{ri} = 2 \tag{6.34}$$

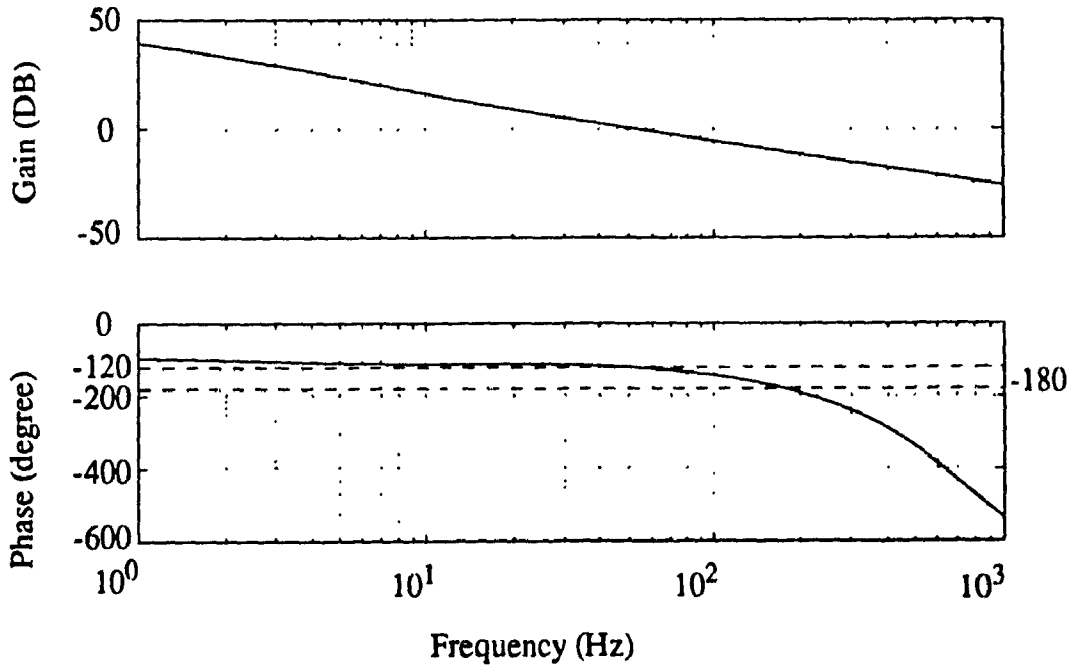

Figure 6.7: Bode plot of the rectifier current feedback loop transfer function.

In this design example, K_r is the gain of the phase-controlled rectifier and it equals 33.75, T_d is the average dead-time delay of the controlled rectifier and it equals 1.38ms, and $H_o(s)$ is the transfer function including the load and the smoothing reactor.

6.3.4.1.2 α Correction Control

The α correction loop (loop #3, Figure 5.4) can be designed such that the rectifier is forced to take over (more or less) the dc power generated by the PWM inverter during transient operation through the adjustment of the rectifier delay angle α. Equation (5.1) shows that the same load current can be achieved by combining the current of the rectifier and PWM inverter. This means that the additional rectifier output voltage can be accurately calculated by knowing the dc current passing through the PWM inverter, that is:

$$\Delta V_{rd} = \Delta I_{rd} \times (R_o + s(L_o + L_s)) \tag{6.35}$$

where ΔI_{rd} is the additional PWM converter's dc current needed to be compensated by the rectifier, and ΔV_{rd} is the desired additional rectifier output voltage due to ΔI_{rd}. Behind this ideal, the α correction loop can be designed such that:

$$G_{cr}(s) = \frac{R_o + s(L_o + L_s)}{K_r} \tag{6.36}$$

The gain and time constant of this controller are given by using (6.20), that is:

$$K_{cr} = \frac{R_o}{K_r} = 0.074 \tag{6.37}$$

$$T_{cr} = \frac{L_o + L_s}{K_r} = 2.19 \times 10^{-3}\,(s) \tag{6.38}$$

To attract the dc current of the PWM inverter, the cut-off frequency of the low pass filter is chosen as 10-Hz which is slower than the rectifier current feedback loop.

6.3.4.2 PWM Converter Control

The inverter current feedback loop uses a PI controller. The loop transfer function was presented in (5.5) and is illustrated in Figure 6.8.

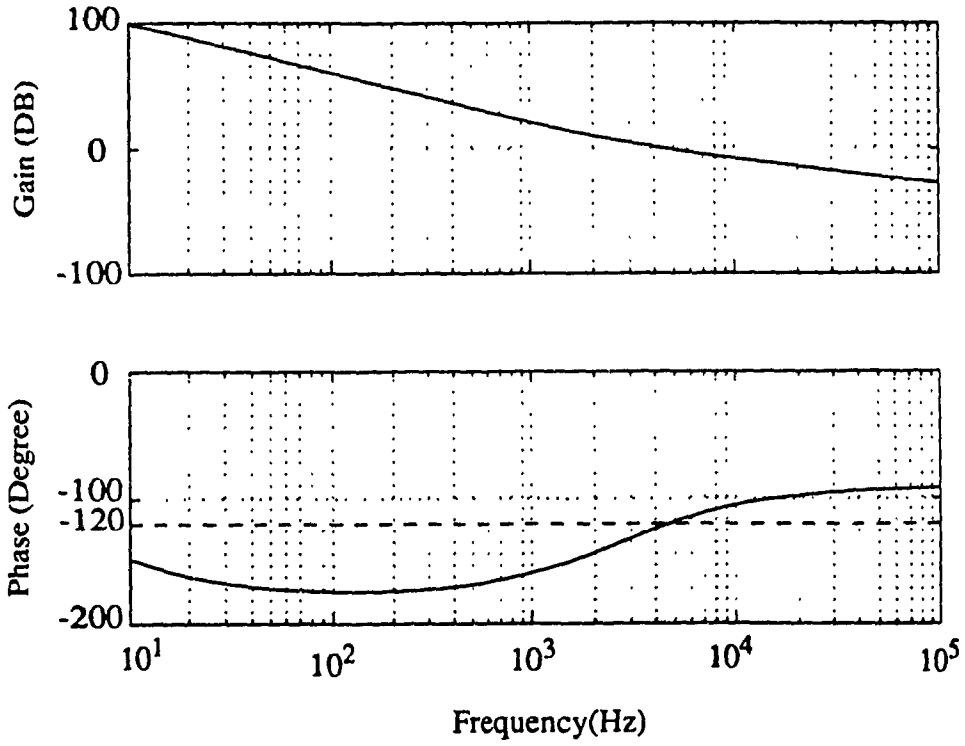

Figure 6.8: Bode plot of the converter current loop transfer function.

To ensure that the linear model of the PWM inverter is suitable for this purpose, the system cut-off frequency is chosen to be around one-third of the switching frequency, that is 1.67kHz. By using the conventional Bode plot approach, the gain and the time constant of the PI controller, $G_{pi}(s)$, can be chosen as:

$$K_{pi} = 16.55 \tag{6.39}$$

$$T_{pi} = 16.4\,(\text{ms}) \tag{6.40}$$

Figure 6.8 also shows that by choosing the above controller parameters, the system phase margin is around 60 degrees. This shows that the system dynamic response is greatly improved when compared with the rectifier current feedback control loop.

6.4 Results

The system has been implemented on a laboratory prototype with the design parameters. Experimental results are discussed in the following.

Figure 6.9 shows the experimental load current waveforms with only the phase-controlled rectifier. Figure 6.9 (a) shows that, even without the PWM inverter feedback loop, the load current is able to track the reference command closely due to the rectifier feedforward/feedback control loop. As expected, using only a combined feedforward/feedback loop (loop #1, Figure 5.4), the steady state error during the flat bottom/top periods are smaller when compared with the feedforward control alone, as shown in Figure 2.7. Also, the load current still contains a large amount of current ripples, as can be seen in Figure 6.9 (b). Figure 6.9 (c) shows the harmonic spectrum of the load current at the flat bottom, as can be seen there is a larger portion of 360Hz harmonic in the load current. In

addition, the tracking error still exists because there is a certain degree of error between the designed and implemented parameters, it can be seen in Figure 6.9 (a).

Figure 6.10 gives experimental results of the complete system, which includes both the rectifier and the PWM converter and is shown in Figure 6.1. Figure 6.10 (a) shows that, by including the PWM converter and its current feedback loop, the load current can track the current reference and the ripple has been greatly reduced. This can be seen more clearly from the steady state waveform in Figure 6.10 (b). It also shows that by using the active compensator, the peak-to-peak ripple at 2A is attenuated by more than 100 times. Compared with Figure 6.9(c), Figure 6.10(c) show that the 360Hz harmonic has been reduced 100 times by using the proposed shunt compensation approach. These waveforms show that this system provides an excellent current regulation under various operating conditions.

To verify the operation of the α correction loop (loop #3, Figure 5.4), the current waveforms of the PWM converter are recorded in Figure 6.11. Without the α correction loop, the PWM inverter is required to generate the large current during the ramp period and a sustained dc current during the flat top region. When the α correction loop is included, the PWM converter dc current is forced back to the minimum (ideally zero) under the new steady state conditions.

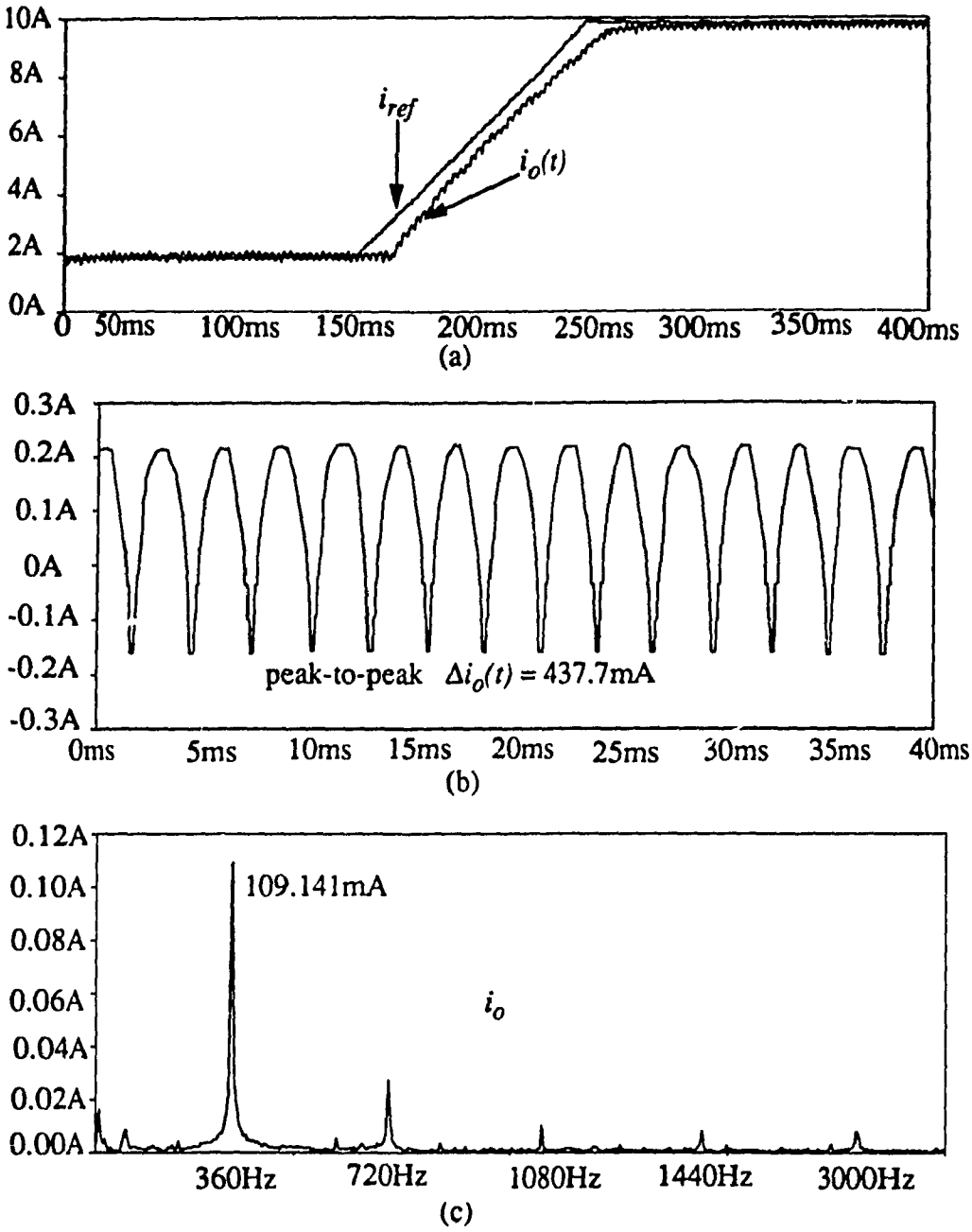

Figure 6.9: Experimental waveforms of the system with only the rectifier. (a) Load current and current reference; (b) Expanded ac portion of the load current at 2A; (c) Harmonic spectrum of the load current at $\alpha = 80^0$ (i_o=2A).

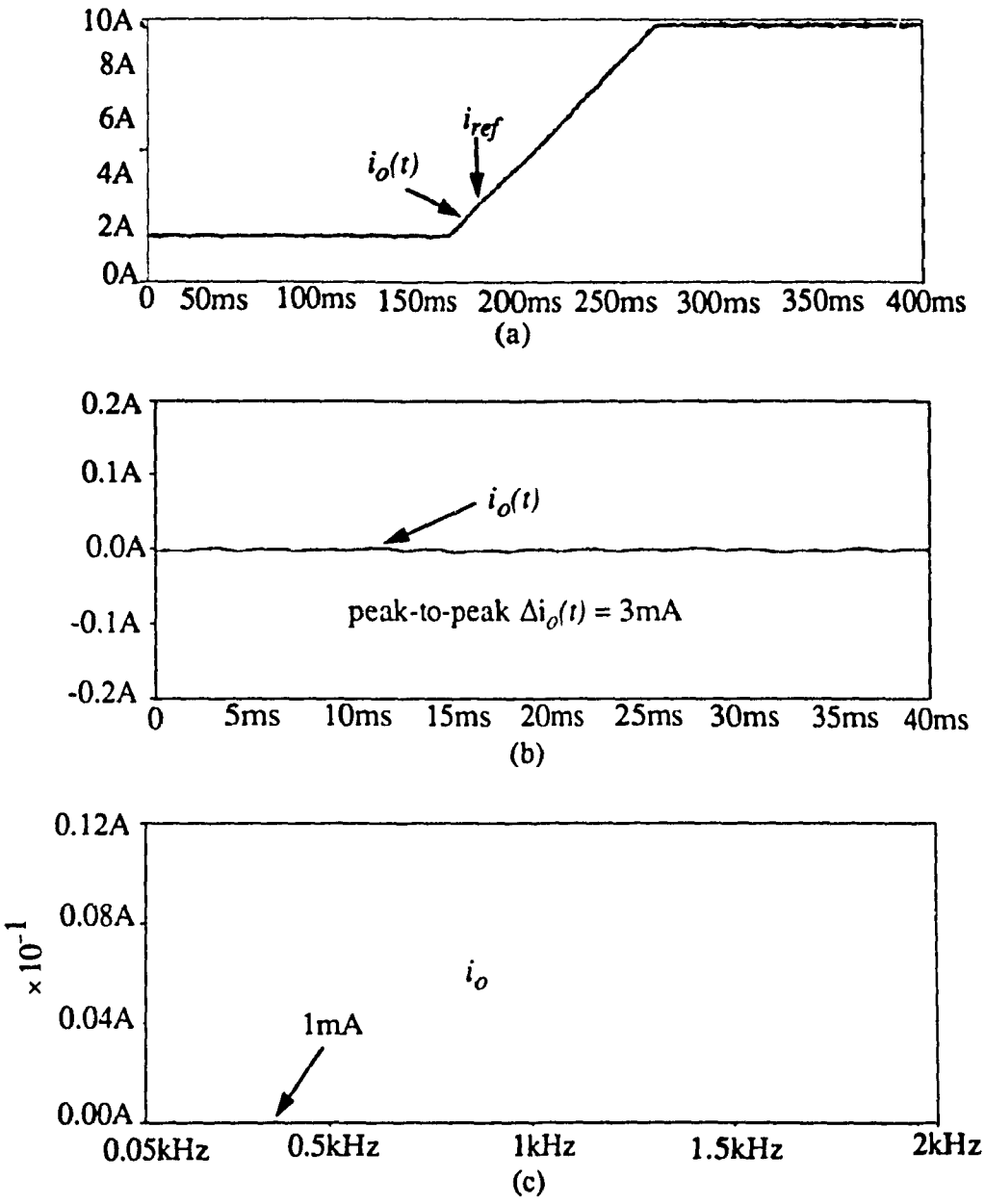

Figure 6.10: Experimental waveforms of the proposed system.
(a) Load current and current reference;
(b) Expanded ac portion of load current at 2A;
(c) Harmonic spectrum of load current at $\alpha = 80^0$.

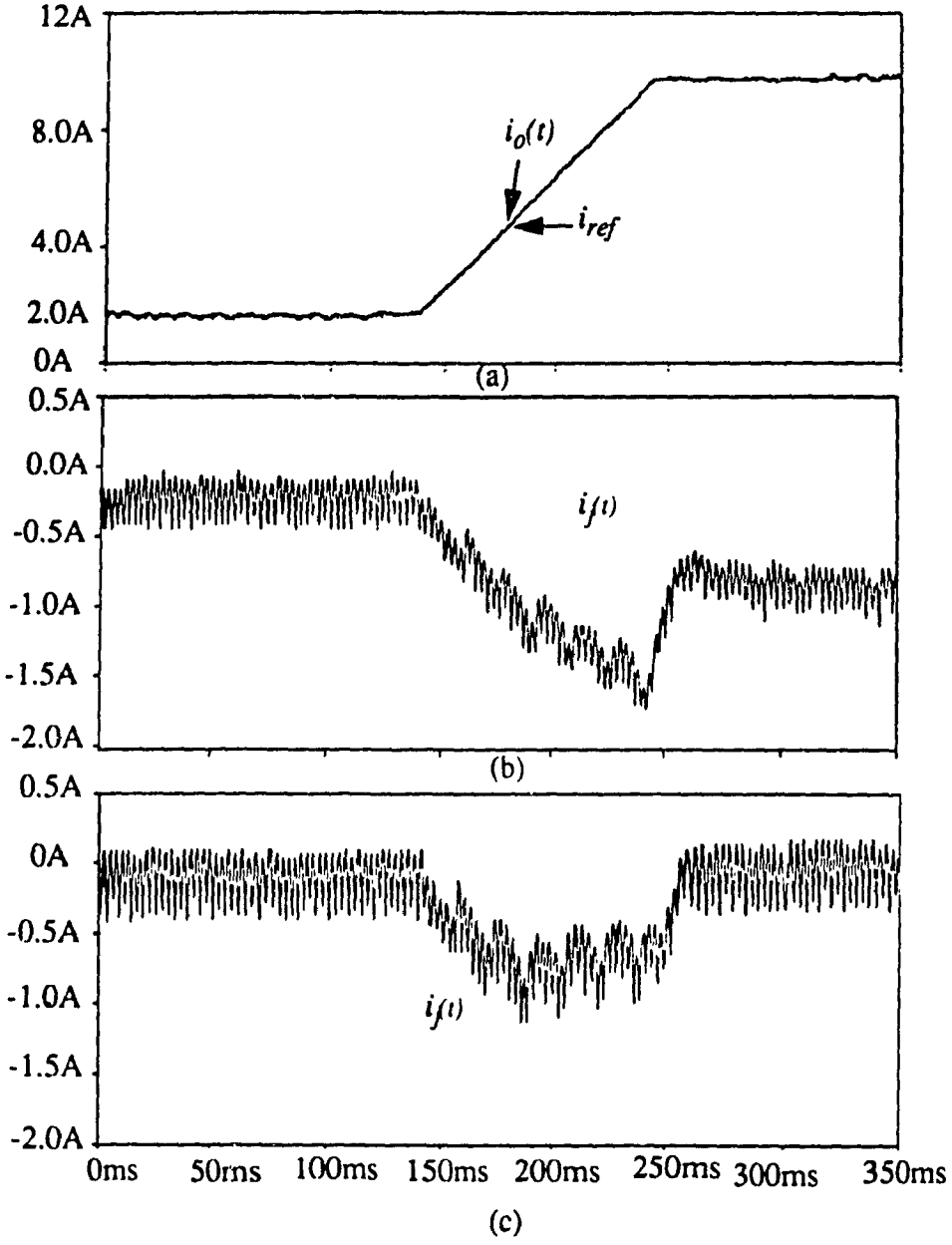

Figure 6.11: Experimental inverter current waveforms. (a) Current reference; (b) Without α correction loop (Figure 5.3, loop #3); (c) Including α correction loop.

6.5 Summary

In this chapter, a large-power high-performance magnet power supply using shunt compensation topology has been designed and implemented on a laboratory prototype. Experimental waveforms show that the rectifier voltage harmonics and tracking errors are compensated by the high-frequency PWM converter. Large power rating and fast response can, therefore, be achieved simultaneously. Moreover, the power rating of the compensator is only a portion (13%) of that of the rectifier. Overall, excellent load current regulation is achieved with the proposed magnet power supply.

Chapter 7

Conclusion

7.1 Summary

The work presented in this thesis contributes to improving the performance of high current bending magnet power supplies based on thyristor rectifiers. Two of the stringent requirements of this application, low current ripple and fast system dynamic response, are achieved by proposed hybrid structure using either series or shunt compensation topologies.

The presented magnet power supplies are studied under both steady state and transient operations. Components of the power circuits, including the passive filters, are chosen and the functions of each component are explained. The proper control schemes are designed so as to meet the two stringent requirements and to ensure proper power sharing between the rectifier and the PWM converter. The phase-controlled rectifier is designed to handle the bulk of the power required by the magnet load and the active compensator, using a high-frequency PWM converter provides only for harmonic cancellation and error compensation. The power rating of the PWM compensator is only a fraction of the total power.

Excellent load current regulation is demonstrated with both the series and shunt hybrid topologies under steady state and transient operations. The results of computer simulations and experimental setups provided in this thesis validate the theoretical concept.

7.2 Contributions and Conclusions

In conventional active filter topologies, high-frequency PWM converters are ac-coupled and compensated only for harmonics. The major contribution of this thesis is to use directly dc-coupled high frequency PWM converters for both harmonic current cancellation and tracking error compensation.

The direct coupling active filter results in added complexity in the design of the magnet power supply control loops. This is caused by the difficulty in controlling the load sharing between high power rectifiers and high frequency converters during transient operation.

Control issues related to the solution of the above problem are addressed in the following manner:

1) In series topology, a simple control scheme with feedforward (predicative) control is applied to the phase-controlled rectifier to solve the power sharing problem. The series connected compensator is a high-frequency PWM two-quadrant chopper.

To compensate for the current errors due to sudden changes in the current reference, the directly dc-coupled compensator is used to provide a small portion of output power during transient operation. Moreover, a combined current feedback and voltage feedforward control scheme is designed to control the PWM two-quadrant converter for harmonic cancellation and error compensation. A suitable control scheme guarantees that

the rectifier provides the bulk of the power required by the magnet and that the power rating of the PWM compensator is only a fraction portion of the system power rating.

Excellent performance, which results in low current ripple and fast system dynamic response both in steady state and transient operations is achieved by using this topology. The steady state performance can be seen from Table 7.1.

Table 7.1: Steady state performance of using the series topology ($I_{base} = i_o(t) = 2A$).

Components	Peak-to-peak ripple (Load current) $\times 10^{-3}$(per unit)	*THD* (Load current) (%)
Rectifier + Passive filter	40	1.72
Rectifier + Passive filter + Active Compensator	0.75	0.02

2) In shunt structure, a simple control scheme with a combined feedforward/feedback control loop is added to the phase-controlled rectifier to solve the power sharing problem between the rectifier and the PWM converter. It also compensates for the small discrepancies which arise due to the load parameter deviations and input voltage fluctuations. An α correction loop helps this respect by transferring part of the transient current to the rectifier (shown in Figure 6.11) and to ensure that under steady state operation the high frequency converter reverts to its strict role as an active filter. The shunt connected compensator is a high-frequency PWM four-quadrant chopper (inverter).

To compensate for the current errors due to sudden changes in the current reference, the directly dc-coupled PWM compensator is made to provide the additional output power required during transient operation. This compensator is controlled by using con-

ventional current feedback scheme.

Excellent performance, which results in low current ripple and fast system dynamic response both in steady state and transient operations, is achieved by using shunt topology. The steady state performance is shown in Table 7.2.

Table 7.2: Steady state performance of using the shunt topology ($I_{base} = i_o(t) = 2A$).

Components	Peak-to-peak ripple (Load current) $\times 10^{-3}$(per unit)	*THD* (Load current) (%)
Rectifier + Passive filter	220	5.45
Rectifier + Passive filter + Active Compensator	1.5	0.05

Since the dominant harmonic current is the 6^{th}, in Table 7.1 and Table 7.2, the *THD* (total current distortion) is calculated by using the following equation:

$$THD = \frac{I_{r,6peak}}{I_o} \tag{7.1}$$

Additional issues related to power rating minimization and performance can be summarized as follows:

1) In order to minimize the power rating of the high-frequency PWM converters, passive filters are proposed.

In series structure, a second order L-C filter with an R-C damping branch is chosen. It reduces the amount of harmonics in the first step, hence, the power rating of the active filter is also reduced.

In shunt topology, a first order filter, such as a smoothing reactor, is used. This passive filter is used not only to reduce the harmonics at the rectifier output, but also to make load voltage controllable. The design of the smoothing reactor is discussed by comparing the costs of the passive filter and the active compensator.

2) The power rating of the PWM converter is calculated for both topologies. In series topology, a 23.7% power rating is required that of the rectifier to have a passive filter with a cut-off frequency of $3\omega_0$ at the rectifier output. In shunt topology, a 13% power rating is required that of the rectifier for an 0.032 p.u. smoothing reactor based on a 0.2p.u. load inductor. Table 7.3 and Table 7.3 show the detail results of using the series and shunt topologies, respectively.

Table 7.3: Series topology (Base: Load rated quantity).

Components			Actual	per unit
Steady state ripple			1.5 mA	0.15×10^{-3}
Rectifier (main power supply)		V (Voltage rating)	33.75V	1.35
		I (Current rating)	10A	1.0
		S (Power rating)	330.75 VA	1.35
Compensators	Passive	L	8mH	7.24
		C	125μF	1.4
	Active	Quadrant	2	2
		V (Voltage rating)	8V	0.32
		I (Current rating)	10A	1
		S (Power rating)	80VA	0.32

Table 7.4: Shunt topology (Base: Load rated quantity)

Components			Actual	per unit
Steady state ripple			3mA	0.3×10^{-3}
Rectifier (main power supply)		*V* (Voltage rating)	34V	1.36
		I (Current rating)	10A	1
		S (Power rating)	340 VA	1.36
Compensators	Passive	*L*	10 mH	9.05
		C	-	-
	Active	Quadrant	4	4
		V (Voltage rating)	30V	1.2
		I (Current rating)	1.5A	0.15
		S (Power rating)	45VA	0.18

It should be noted that, in the series topology, a large compensator power rating is required comparing with that of the shunt compensation topology. This is due to the following reasons:

- The comparison of the two topologies was not under the same rating of the passive filters.

- Two topologies did not use the same control scheme. In the series topology, the rectifier uses only the feedforward control, which requires the PWM converter to provide more power to compensate for the steady state error during the steady state and transient operations comparing with the shunt topology.

3) The advantages/disadvantages of using series and shunt topologies are as follows:

- In series topology, the high-frequency switches conduct the high currents, but

only see low reverse voltages (harmonic voltages). On the other hand, in shunt topology, the high-frequency switches conduct low currents (harmonic currents), but with a high reverse voltage (maximum load voltage).

The final choice depends upon the voltage and current ratings of the magnet. If voltage limitation of standard switches is not exceeded (typically 1500V for IGBT's), then it might be advantageous to use the lower current shunt topology.

7.3 Future Work

The following suggestions for research can be carried out in the future.

1) Scheme refinements:

In this thesis, 1kVA experimental systems have been set up in both of series and shunt topologies. Due to the limitations of the laboratory equipment, such as the lack of precision instruments (less than 0.01%) and the low prototype current ratings, the experimental setups can not be utilized to verify the typically large magnet power supply performance particularly regarding to accuracy and bandwidth. Applying the system to a large power magnet would allow further refinements of the proposed schemes.

2) Investigations of current source PWM converter topologies rather than of voltage source PWM converter topologies used in this thesis.

3) Study of the effects on hybrid structures under ac unbalanced operating conditions.

At last, it is worth to mention that some results of this research have already been published [29][30], where the hybrid structure with both the series and shunt topologies are presented.

REFERENCES

[1] R. Liang, "A low ripple power supply system for high current magnet load", Ph. D Thesis, University of Toronto, 1993

[2] J. Lisser and K. Bouwknegt, "High-speed high-precision programmable magnet power supply for a wide range of magnet time constants", *IEEE Trans. on Nuclear Science*, Vol. NS-28, No.3, June 1981, pp. 2859-2861

[3] T. Kitayama et al, "High-speed high-accuracy magnet power supply using FET chopper for synchrotron facility", *IEEE PAC Prod.*, 1989

[4] E. A. Knapp, "New applications of particle accelerators in medicine, materials science, and industry", *IEEE Trans. on Nuclear Science*, Vol. NS-28, No.3, June 1981

[5] G. Karady and H. A. Thiessen, "Accelerator magnet power supply using storage generator", *IEEE PAC Prod.*, 1987

[6] P. Proudlock, H. W. Isch and J. G. Pett, "The use of switch-mode power converters for the LEP main ring power converter system", *IEEE PAC Prod.*, 1987

[7] W. P. Sims et al, "The neutrino horn 300 kiloampere pulsed power supply at Brookhaven National Laboratory", *IEEE PAC Prod.*, 1987

[8] H. Sato and et al, "High accuracy magnet power supply for proton synchrotron by repetitive control", *IEEE PESC'91 Prod.*, 1991

[9] N. Mohan, T. M. Undeland and W. P. Robbins, "Power electronics: converter, applications and design", John Wiley & Sons, Inc., New York, 1989

[10] H. W. Isch and et al, "Switch mode power converter; present and future", *IEEE PAC Prod.*, 1989

[11] H. Jin, "Low ripple ac/dc one-quadrant switch-mode magnet power supply", Ph. D Thesis, University of Toronto, 1991

[12] R. J. Yarema, "A four quadrant magnet power supply for superconducting and conventional accelerator applications", *IEEE Trans. on Nuclear Science*, Vol. NS-28, No. 3, June 1981

[13] T. Jackson, "Design and performance of PEP dc power systems", *IEEE Trans. on Nuclear Science*, Vol. NS-28, No. 3, June 1981

[14] R. Liang and S. B. Dewan, "A low ripple supply for high current magnet load", *IEEE IAS Conf. Prod.*, 1992, pp. 888-893

[15] R. Liang and S. B. Dewan, "Modeling and control of magnet power supply system with switch mode ripple regulator", *IEEE IAS Conf. Prod.*, 1993, pp.1152-1159

[16] R. Liang, "A switch-mode ripple regulator for high-current magnet power supplies", *IEEE APEC'94 Prod.*, 1994, pp. 989-923

[17] W. M. Grady, M. J. Samotyj and A. H. Noyola, "Survey of active power line conditioning methodologies", *IEEE Trans. on Power Delivery*, Vol. 5, No. 3, July 1990, pp 1536-1542

[18] L. Gyngyi and E. C. Strycula, "Active ac power filters", *IEEE IAS' 76 Annual meeting*, 1976, pp. 529-535

[19] F. A. Peng et al, "A new approach to harmonic compensation in power systems - a combined system of shunt passive and series active filters", *IEEE Trans. on Nuclear Science*, Vol. IA-26, No. 6, Nov. /Dec. 1990

[20] C. Wong et al, "Feasibility study of ac- and dc-side active filter for HVDC converter terminals", *IEEE Trans. on Power Delivery*, Vol. 4, Oct. 1989, pp. 2064-2075

[21] W. Zhang, A. Aberg, V. Jonsson and O. Loof, "Active DC filter for HVDC system - a test installation in the Konti-Skan DC link at Lindome converter station", *IEEE Trans. on Power Delivery*, Vol. 8, No. 3, July 1993, pp. 1599-1606

[22] H. Fujita and H. Akage, "A practical approach to harmonic compensation in power systems - series connection of passive and active filters", *IEEE Trans. on Nuclear Science*, Vol. IA-27, No. 6, Nov. / Dec. 1991

[23] R. J. Yarema, "A four quadrant magnet power supply for superconducting and conventional accelerator applications", *IEEE Trans. on Nuclear Science*, NS-28, No.3, June 1981

[24] F. F. Cliyo et al, "Active filter for high current dc magnets", *IEEE Trans. on Nuclear Science*, Vol. NS-28, No. 3, June 1981, pp. 3014-3016

[25] J. A. Pomolio, D. Wisnivesky, and A. C. Lira, "A novel topology for the bending magnets power supply at LNLS", *IEEE Trans. on Nuclear Science*, Vol. NS-39, No.5, Oct. 1992, pp. 1506-1511

[26] H. Sato et al, "Performance of the main ring magnet power supply of the LEL 12 GeV Proton synchrotron", *IEEE Trans. on Nuclear Science*, Vol. NS-39, No.5, Oct., 1992, pp. 1490-1495

[27] B. H. Kwon, J. H. Suh, and S. H. Han, "Novel transformer active filters", *IEEE*

Trans. on Industrial Electronics, Vol. 40, No. 3, June 1993, pp. 385-388

[28] W. Leonhard, "Control of electrical drivers", Springer-Verlag, Berlin, 1985

[29] Y. Wang, G. Joos, and H. Jin, "DC-Side Shunt Active Power Filter for Phase-Controlled Magnet-Load Power Supplies", *IEEE PESC'94 Conf. Proc.*, Vol.1, pp. 183-188

[30] H. Jin, Y. Wang and G. Joos, "A Combined Approach Using Phase-Controlled Rectifiers and High-Frequency Converters for Magnet-Load Power Supplies", *IEEE APEC'94 Conf. Proc.*, Vol. 1, pp. 135-139